

**UNIVERSIDADE DE LISBOA
FACULDADE DE FARMÁCIA**



**Intracellularly-Targeted Nanoplatfom to
Target Dendritic Cells and for
Immunomodulation**

Carina Sofia Gonçalves Peres

Orientadores: Professora Doutora Helena F. Florindo
Professor Doutor Luís Graça
Professora Doutora Véronique Préat

Tese especialmente elaborada para obtenção do grau de Doutor
em Farmácia, especialidade em Tecnologia Farmacêutica

2020

**UNIVERSIDADE DE LISBOA
FACULDADE DE FARMÁCIA**



**Intracellularly-Targeted Nanoplatfom to Target Dendritic Cells
and for Immunomodulation**

Carina Sofia Gonçalves Peres

Orientadores: Professora Doutora Helena F. Florindo
Professor Doutor Luís Graça
Professora Doutora Véronique Préat

Tese especialmente elaborada para obtenção do grau de Doutor em Farmácia,
especialidade em Tecnologia Farmacêutica

Júri

Presidente:

Doutora Dora Maria Tuna de Oliveira Brites, Investigadora Coordenadora e membro do Conselho Científico da Faculdade de Farmácia da Universidade de Lisboa.

Vogais:

Doutor João Nuno Sereno Almeida Moreira, Professor Auxiliar com Agregação da Faculdade de Farmácia da Universidade de Coimbra;

Doutor José Carlos Lemos Machado, Professor Associado da Faculdade de Medicina da Universidade do Porto;

Doutor Duarte Custal Ferreira Barral, Investigador Principal da Faculdade de Ciências Médicas da Universidade Nova de Lisboa;

Doutor António José Leitão das Neves Almeida, Professor Catedrático da Faculdade de Farmácia da Universidade de Lisboa;

Doutora Helena Isabel Fialho Florindo Roque Ferreira, Professora Auxiliar com Agregação da Faculdade de Farmácia da Universidade de Lisboa, Orientadora.

This work was financially supported by Fundação para a Ciência e a Tecnologia (FCT), Ministério da Ciência e da Tecnologia, Portugal (PhD Grant: SFRH/BD/ 87591 /2012; and the research projects: PTDC/SAU-FAR/119389/2010; UTAP-ICDT/DTP-FTO/0016/2014), iMed.Ulissboa grants (Pest-OE/SAU/UI4013/2011 and UID/DTP/04138/2013), and research projects ENMed/0003/2015 under the framework of EuroNanoMed-I and ENMed/0051/2016 under the framework of EuroNanoMed-II, as well as by the European Structural & Investment Funds through the COMPETE Programme and from National Funds through FCT under the Programme grant SAICTPAC/0019/2015.

Abstract

Triple-negative breast cancer (TNBC) is the most aggressive subtype of breast cancer. Immunotherapy, notably cancer vaccines and immune checkpoint modulators, has emerged as a promising alternative therapy. However, limited efficacy has been obtained for cancer vaccines and severe immune-mediated side effects have been related to immune checkpoint inhibitors under clinical development. Thus, to overcome the main disadvantages presented by these two therapeutic options when used individually, and considering the heterogeneity of TNBC, combination therapies are under clinical development to treat this specific breast cancer subtype.

We hypothesized that the development of a multifunctional nanovaccine could reshape the tumour microenvironment (TME), sensitizing TNBC to the agonist immune checkpoint OX40, and thus, improving the overall anti-tumour immune response.

For this purpose, a poly(lactic acid) (PLA) nanoparticle (NP)-based nanovaccine was designed and synthesized to target dendritic cells (DC) and the TME by incorporating TNBC-associated antigens, toll-like receptor ligands CpG and Poly(I:C), and siRNA to downregulate the potent immunosuppressive cytokine transforming growth factor- β (TGF- β). NP surface was modified by hyaluronic acid to promote DC activation, but also to potentiate their delivery to the TME by targeting CD44 receptor, overexpressed in TNBC cells.

NPs presented a spherical-shape with an average diameter close to 200 nm, displaying narrow polydispersity index, near-neutral surface charge, and entrapment efficiencies (EE) superior to 85%. NPs were extensively taken up by both DC and TNBC cells, without affecting their viability. In addition, NPs induced DC activation and maturation, increasing significantly the expression of the surface markers. 4T1 tumour-bearing animals treated with the multifunctional nanovaccine combined with α OX40 showed a noteworthy tumour remission, with a higher overall survival and a tumour volume 4-fold lower than those obtained for α OX40-treated mice. The nanovaccine reshaped the immune profiling within the TME, which correlated with the overall anti-tumour effect obtained in this combinatorial scheme. This study revealed the synergy between a multi-targeting nanovaccine and α OX40 in TNBC, providing important insights for the establishment of novel combination regimens against this tumour.

Keywords: vaccine, triple-negative breast cancer, nanomedicine, tumour microenvironment, immune checkpoints

Resumo

De acordo com a Organização Mundial de Saúde (OMS), o cancro da mama é o tipo de cancro mais frequente nas mulheres e apresenta a maior taxa de mortalidade relacionada com cancro nas mulheres a nível mundial. Anualmente, estima-se que mais de 2,1 milhões de mulheres são diagnosticadas e que mais de 627'000 mulheres morrem desta doença. Além disso, a OMS estima que até 2020 uma em cada oito mulheres será afetada por esta doença.

O cancro da mama é uma doença complexa e com um elevado grau de heterogeneidade. Esta heterogeneidade dá origem a tumores com comportamentos distintos, e diferentes características clínicas, patológicas e moleculares, com prognósticos distintos e implicações terapêuticas distintas. Atualmente, o cancro da mama pode ser classificado em diferentes subtipos moleculares, tendo por base a expressão de três biomarcadores, determinados por imunohistoquímica: o recetor de estrogénio, o recetor de progesterona e a proteína transmembranária HER2.

O cancro da mama triplo negativo (CMTN) é um subtipo molecular de cancro da mama caracterizado pela ausência de expressão dos recetores de estrogénio e de progesterona e a ausência de sobre-expressão de HER2. Estima-se que a prevalência do CMTN seja de cerca de 15 a 20% de todos os casos metastáticos de cancro da mama, sendo tipicamente observado em mulheres com menos de 40 anos, especialmente em mulheres de raça negra, e/ou portadoras de mutações germinais no gene BRCA1. Os pacientes diagnosticados com esta doença apresentam um mau prognóstico e falecem rapidamente quando comparado com outros subtipos de cancro da mama, o que se pode dever ao seu comportamento agressivo, mas também à falta de terapia direcionada. O CMTN caracteriza-se por um tumor maior no diagnóstico, maior grau histológico, metastização precoce (1 a 3 anos após o diagnóstico) e mais agressiva.

Contrariamente aos outros subtipos de cancro da mama, os pacientes diagnosticados com o CMTN não beneficiam das terapias endócrinas nem das terapias direcionadas para o HER2 devido à ausência destes mesmos biomarcadores, o que limita fortemente as opções terapêuticas disponíveis para esta doença. Tradicionalmente, a quimioterapia tem sido a principal opção para o tratamento desta doença, tanto em estadios inicial como avançado. No entanto, esta abordagem terapêutica está associada a uma resposta fraca por parte da maioria dos pacientes, toxicidade e eventual desenvolvimento de resistência aos agentes quimioterapêuticos.

Resumo

Por estas razões, considera-se urgente o desenvolvimento de terapêuticas direcionadas para o CMTN.

A imunoterapia tem surgido como uma opção terapêutica promissora para o tratamento desta doença. Nas últimas décadas, a imunoterapia passou de uma “terapia promissora” para uma realidade clínica já bem comprovada. Diversas opções imunoterapêuticas foram já aprovadas pelas agências reguladoras do medicamento norte-americana (FDA) e europeia (EMA), e muitos outros estão em ensaios clínicos, como monoterapia ou combinado com tratamentos convencionais ou outros agentes direcionados. Estas terapêuticas inovadoras, baseiam-se em respostas anti-tumorais desencadeadas pelo próprio sistema imunitário do doente, através da ativação de uma complexa rede de células imunitárias, tais como os linfócitos T efetores CD8⁺ e os linfócitos T auxiliares CD4⁺, mas também em respostas de memória que impeçam a formação de metástases e a disseminação da doença. Contrariamente aos outros subtipos de cancro da mama, o microambiente tumoral do CMTN apresenta uma grande infiltração de linfócitos T, o que aumenta a suscetibilidade dos pacientes com esta patologia para a imunoterapia.

Dois tipos de imunoterapia que têm sido aplicados em doentes com CMTN em ensaios clínicos são os moduladores dos *immune checkpoints* e as vacinas anti-tumorais. Os *immune checkpoints* são um conjunto de moléculas co-estimuladoras e co-inibitórias envolvidas na ativação de complexas vias de sinalização que previnem a ativação excessiva dos linfócitos T em condições normais. No ambiente tumoral, a expressão dos *immune checkpoints* está alterada, evitando a resposta imunitária anti-tumoral pelos linfócitos T. Os anticorpos monoclonais (mAb) direcionados contra estas moléculas permite reverter a inibição da imunidade adquirida e, assim, contribuir para a sobrevivência dos pacientes. Um dos mAb em estudo em ensaios clínicos para o tratamento do CMTN é direcionado contra o OX40. O OX40 é um recetor co-estimulador expresso pelos linfócitos T, cuja ativação, induz a expansão e sobrevivência dos linfócitos T efetores e bloqueia a ação inibitória dos linfócitos T reguladores no microambiente tumoral.

Apesar dos resultados promissores, os moduladores dos *immune checkpoints*, em particular quando usados em regimes de monoterapia, têm sido associados a efeitos adversos graves e a baixas taxas de respostas prolongadas e perduráveis em doentes de cancro metastático. As vacinas anti-tumorais têm vindo a ser desenvolvidas ao longo destes últimos 100 anos e é possível identificar vários casos de remissão completa em diversos tipos de cancro. No entanto, a maioria dos ensaios clínicos envolvendo vacinas anti-tumorais falharam em demonstrar qualquer melhoria clínica nos pacientes.

Assim sendo, de forma a ultrapassar as principais desvantagens apresentadas por estas duas opções imunoterapêuticas quando usadas individualmente, deve-se ter em consideração a terapêutica combinatória para tratar este subtipo específico de cancro de mama. A terapêutica combinatória tem sido um tópico importante no desenvolvimento clínico de abordagens mais eficazes contra diferentes tipos de cancro, incluindo no campo da imunoterapia. Ao combinar dois ou mais agentes terapêuticos que possuem mecanismos de ação diferentes, mais células cancerígenas devem ser destruídas, melhorando assim a resposta geral do paciente à terapêutica.

Por conseguinte, este trabalho consistiu no desenvolvimento de uma nanovacina multifuncional com o objetivo de remodelar o microambiente tumoral sensibilizando-o para o agonista dos *immune checkpoints* OX40, e assim melhorar a resposta imunitária anti-tumoral. Com esse objetivo foram desenvolvidas nano-vacinas anti-tumorais baseadas em nanopartículas (NPs) biodegradáveis constituídas por uma matriz de ácido polilático (PLA), direcionadas para as células dendríticas (DCs) e para o microambiente tumoral. Para a indução de uma resposta anti-tumoral específica, este nanossistema incorporou o antígeno α -Lactalbumina cuja expressão está aumentada no CMTN, ligandos dos recetores *toll-like*, nomeadamente CpG-ODN e Poly(I:C) para potenciar a resposta imunitária, juntamente com o siRNA direcionado contra o TGF- β , uma importante citocina imunossupressora. A superfície das NPs foi modificada com ácido hialurónico de forma a promover a ativação das DCs, mas também direcionar as NPs para o microambiente tumoral ao reconhecerem o recetor CD44, sobre-expresso nas células de CMTN.

As NPs apresentaram forma esférica com um diâmetro hidrodinâmico médio de cerca de 200 nm, com um índice de polidispersão baixo, carga à superfície da NP próxima da neutralidade, e eficiência de encapsulação superior a 85%. As NPs foram extensivamente internalizadas pelas DCs e células de CMTN, sem afetar as suas viabilidades. Além disso, as NPs induziram a ativação e maturação das DCs, aumentando significativamente a expressão de diferentes marcadores de superfície, e permitiram reduzir significativamente a expressão do TGF- β *in vivo*. Os murganhos inoculados com células de CMTN 4T1 e tratados com a nanovacina combinada com o mAb anti-OX40 demonstraram uma notável remissão do tumor, com um aumento de sobrevivência geral, apresentando um volume de tumor 4 vezes menor que o obtido pelos murganhos tratados com o mAb anti-OX40. A nanovacina permitiu remodelar o perfil imunológico dentro do microambiente tumoral, o que se correlacionou com o efeito antitumoral geral obtido neste esquema combinatório. Este estudo revelou a sinergia entre uma nano-vacina multi-direcionada e o mAb anti-OX40 no CMTN, fornecendo

Resumo

informações importantes para o estabelecimento de novos regimes de combinação contra este tumor.

Palavras-chave: vacina, cancro de mama triplo negativo, nanomedicina, microambiente tumoral, *immune checkpoints*

Acknowledgments/Agradecimentos

“Ninguém escapa ao sonho de voar, de ultrapassar os limites do espaço onde nasceu, de ver novos lugares e novas gentes. Mas saber ver em cada coisa, em cada pessoa, aquele algo que a define como especial, um objeto singular, um amigo, é fundamental. Navegar é preciso, reconhecer o valor das coisas e das pessoas, é mais preciso ainda.”

Antoine de Saint-Exupéry

Quando iniciei o meu projeto de doutoramento, achava que iria ter pela frente uma longa jornada, e em grande medida individual e solitária, mas estava errada. Longa, lá isso ela foi, mas na verdade nunca me senti só. Ao longo destes quase sete anos, tive a oportunidade de conhecer pessoas fantásticas, sem as quais não seria possível chegar onde cheguei hoje e a quem não poderia deixar de agradecer.

Em primeiro lugar, quero agradecer à minha orientadora e amiga Prof. Doutora Helena F. Florindo pela orientação, mas sobretudo pelo apoio incondicional que me demonstrou ao longo destes anos. Obrigada pela compreensão, pelas palavras amigas e de encorajamento sempre que precisei, e por tudo o que me ensinou. Vou recordar para sempre com carinho e saudade estes anos de trabalho, amizade e convívio. Obrigada por esta oportunidade. Foi um privilégio tê-la como orientadora, e é um privilégio tê-la como amiga!

Agradeço ao meu co-orientador, Professor Doutor Luís Graça, por me receber tão bem no seu laboratório no Instituto de Medicina Molecular, colocando à minha disposição todos os recursos necessários para a realização de parte do meu trabalho experimental. Agradeço também a disponibilidade demonstrada e o interesse no meu trabalho pelos elementos do seu grupo, em particular à Doutora Sílvia Almeida, à Doutora Raquel Freitas e ao Doutor Afonso Basto, por me ajudarem sempre que precisei e por todo o conhecimento que me transmitiram.

I am grateful to my co-supervisor Prof. Véronique Prétat for her support and encouragements through the years.

Agradeço à Fundação para a Ciência e a Tecnologia (FCT) pelo financiamento dos trabalhos de investigação desenvolvidos no âmbito desta tese de doutoramento.

I would like also to acknowledge Prof. Ronit Satchi-Fainaro from the University of Tel-Aviv in Israel for her wised advices and guidance.

Agradeço também a todos os investigadores que me ajudaram e possibilitaram a realização deste projeto. Agradeço à Doutora Liana Silva da Faculdade de Farmácia

Acknowledgments/Agradecimentos

pelos seus conselhos e ajuda na realização dos ensaios de microscopia confocal. Agradeço à Prof. Doutora Ana Viana da Faculdade de Ciências, pela sua disponibilidade e ajuda no microscópio de força atómica. Ao Prof. Doutor Carlos Afonso e à Doutora Catarina Rodrigues da Faculdade de Farmácia, pela colaboração com o nosso grupo e pela síntese dos polímeros de PLGA marcado com rodamina e Cy5. Agradeço às antigas técnicas da Unidade de Citometria de Fluxo do Instituto de Medicina Molecular, Ana Viana, Andreia, Bárbara e Rute pela ajuda, disponibilidade, e acima de tudo, por me transmitirem o seu conhecimento em imunologia e citometria de fluxo. Agradeço à Ana Nascimento e ao José Rino da Unidade de Bioimaging e à Iolanda da Unidade de Roedores do Instituto de Medicina Molecular pela simpatia, disponibilidade e ajuda na realização dos ensaios de biodistribuição. Agradeço ao Doutor João Nuno Moreira e à Doutora Ana Gregório do Centro de Neurociências e Biologia Celular (CNC) em Coimbra pela ajuda no desenvolvimento do modelo animal de cancro de mama ortotópico. Agradeço à Ana Salgado pelos bons momentos que passámos juntas, o seu apoio constante e a sua ajuda para a realização dos ensaios de quantificação de proteínas por HPLC. Agradeço à Prof. Doutora Cecília Rodrigues e à Doutora Marta Afonso da Faculdade de Farmácia pela sua colaboração com o nosso grupo e ajuda na realização dos ensaios de biologia molecular. Um obrigado muito especial às investigadoras do nosso polo do Lumiar, Doutora Manuela Gaspar, Doutora Manuela Colla, Prof. Doutora Luísa Corvo, e Doutora Sandra Simões, pela vossa simpatia, prontidão em ajudar sempre que necessitei, mas também pelos nossos diversos momentos de convívio que recordarei com carinho. I would like to acknowledge Lea Eisenbach from Weizmann Institute in Rehovot, Israel for providing us the metastatic B16 melanoma cell line transfected with OVA gene (B16.MO5).

Não poderia deixar de agradecer aos meus colegas de grupo (BioNanoSciences – Drug delivery & Immunotherapy), em especial à Ana Matos, Liane, Bárbara e João. Vocês não são meros colegas, são meus amigos de verdade. Obrigada pela vossa amizade, por estarem sempre disponíveis para me ajudar, pelas gargalhadas e pelos abraços nos momentos menos bons. Acreditem, vocês fizeram com que esta jornada fosse muito mais fácil! Agradeço ainda à Ana Ester, Tânia e Rita Acúrcio, e aos meus antigos colegas de grupo, Vanessa, Ana Carreira, Melissa, Eva e Nuno pelos bons momentos, que vou recordar com carinho. Um obrigado muito especial à Joana Silva, pela forma como me recebeu quando me juntei ao grupo, por me ter acompanhado nos meus primeiros passos no laboratório e por tudo o que me ensinou.

Quero igualmente agradecer aos professores e colegas do antigo NanoDDS, em especial ao Professor Doutor António Almeida, Professor Doutor Rogério Gaspar,

Professora Doutora Helena Marques, Joana Marto, Diana, Inês, Paulo, Maria, pela simpatia e por me terem recebido tão bem nesta casa.

Deixo ainda um agradecimento muito especial à D. Fernanda e à Carla pelo apoio constante e disponibilidade que sempre demonstraram em me ajudar no que fosse preciso.

Não poderia deixar de agradecer a todos os meus amigos, em particular à Raquel Varela, Nélio Drummond, André Sá Couto, Mariana Dalagnol, Joana Varge, Andreia Ramos, Carlos Gaspar, Daniel Rodrigues e Inês Gomes. Obrigada pela vossa amizade e por estarem a meu lado nos bons e maus momentos.

Deixei para o fim as pessoas mais importantes da minha vida, a minha família. Um sincero obrigada aos meus pais e à minha irmã pelo apoio incondicional e incansável que foi fundamental, não só durante etapa, mas ao longo de toda a minha vida. Papy, mamy e mana, não tenho como vos agradecer por tudo o que fizeram por mim, por todo o amor, carinho e compreensão. Se hoje consegui terminar esta etapa, em grande parte o devo a vocês. Quero também agradecer aos meus avós, tios, primos, sogros e cunhados. Sei que para eles não é fácil entenderem o meu dia-a-dia, mas nunca deixaram de acreditar em mim, de celebrar comigo as minhas vitórias e de deixar as melhores palavras de conforto nos momentos mais difíceis. Por fim, um obrigado muito especial aos meus amores, ao meu marido Bruno e à nossa filha Sofia. Bruno, não tenho palavras para exprimir o quanto te quero agradecer por estares sempre ao meu lado e me apoiares incondicionalmente nas minhas decisões. Obrigada por rires comigo nos bons momentos, e pelos abraços apertados nos momentos mais difíceis. Obrigada pelo teu amor, carinho, dedicação, compreensão e paciência, mesmo nos dias em que estou mais “chata”. Sofia, meu amor pequenino, desculpa se a mamã não esteve tão disponível para brincar contigo e te encher de mimos e beijinhos nos últimos tempos, mas prometo que vamos recuperar cada segundinho. Obrigada meus amores por tornarem a minha vida ainda mais bela.

Obrigada a todos!!!

List of abbreviations

aa	Amino acids
ACK	Ammonium-chloride-potassium
AFM	Atomic force microscopy
ALDH1	Aldehyde dehydrogenase 1
APC	Antigen-presenting cell or Allophycocyanin
APS	Ammonium persulfate
BCT	Breast-conserving therapy
BMDC	Bone marrow-derived dendritic cell
Breg	Regulatory B-cell
BSA	Bovine serum albumin
BTK	Bruton's tyrosine kinase
CAF	Cancer-associated fibroblast
CBR	Clinical benefit rate
CD	Cluster of differentiation
cDC	Conventional/classical DC
cDNA	Complementary DNA
CEA	Carcinoembryonic antigen
CK	Cytokeratin
CpG	Cytosine phosphorothioate-guanine motifs
Cs	Chitosan
CTA	Cancer testis antigens
CTL	Cytotoxic T lymphocyte
CTLA-4	Cytotoxic T-lymphocyte antigen 4
DAMP	Danger-associated molecular pattern
DC	Dendritic cell
DCM	Dichloromethane
DGAV	Direção-Geral de Alimentação e Veterinária
DLS	Dynamic light scattering
DMEM	Dulbecco's Modified Eagle Medium
DMSO	Dimethylsulfoxide
DNA	Deoxyribonucleic acid
dsDNA	Double-stranded DNA
EC	Endothelial cell
EDTA	Ethylenediamine tetraacetic acid

List of abbreviations

EE	Entrapment efficiency
EGFR	Epidermal growth factor receptor
EMA	European Medicines Agency
EMSA	Electrophoretic mobility shift assay
EPR	Enhanced permeability and retention
ER	Oestrogen receptor
FBS	Fetal bovine serum
FcR	Fc receptors
FDA	Food and Drug Administration
FFPE	Formalin-fixed paraffin embedded
FITC	Fluorescein isothiocyanate
FoxP3	Forkhead box P3
GCs	Glycol chitosan
GlutCs	Glutamate chitosan
GM-CSF	Granulocyte macrophage colony-stimulating factor
G-SCF	Granulocyte-colony stimulating factor
GSH	Glutathione
GST	Glutathione-S-transferase
H&E	Haematoxylin and eosin
HA	Hyaluronic acid
HBV	Hepatitis B virus
HCCs	Hydrochloride chitosan
HCl	Hydrochloric acid
HEPES	4-(2-hydroxyethyl)-1-piperazineethanesulfonic acid
HER2	Human epidermal growth factor receptor 2
HPLC	High-performance liquid chromatography
HPV	Human papillomavirus
hTERT	Human telomerase reverse transcriptase
iDC	Immature DC
IFN	Interferon
IHC	Immunohistochemistry
IL	Interleukin
IP	Intraperitoneal
IT	Intratumoural
LC	Loading capacity
LDV	Doppler velocimetry

LN	Lymph node
LPS	Lipopolysaccharide
mAb	Monoclonal antibody
MAC	Membrane attack complex
M-CSF	Macrophage colony-stimulating factor
mDC	Mature DC
MDSC	Myeloid-derived suppressor cell
MEM	Minimum essential medium
MHC	Major histocompatibility complex
moDC	Monocyte-derived DC
MP	Microparticle
MPLA	Monophosphoryl lipid A
MPS	Mononuclear phagocyte system
mRNA	Messenger RNA
mTOR	Mammalian target of rapamycin
MUC1	Mucin 1
Mw	Molecular weight
NaCl	Sodium chloride
NEAA	Non-essential amino acids
NIH	National Institutes of Health
NK	Natural killer
NKT	Natural killer T
NP	Nanoparticle
NSCLC	Non-small cell lung cancer
ODN	Oligodeoxynucleotides
OS	Overall survival
OVA	Albumin from chicken egg white
PALS	Phase analysis light scattering
PAM	PI3K-Akt-mTOR
PAMP	Pathogen-associated molecular pattern
PAP	Prostatic acid phosphatase
PARP1	Poly (ADP-ribose) polymerase 1
PAT	Process analytical technologies
PBS	Phosphate-buffered saline
PCL	Poly(ϵ -caprolactone)
PCR	Polymerase Chain Reaction

List of abbreviations

pCR	Pathologic complete response
PD-1	Programmed death-1 receptor
pDC	Plasmacytoid DC
PdI	Polydispersity index
PD-L1	Programmed death ligand-1
PDX	Patient-derived xenograft
PE	Phycoerythrin
PEG	Poly(ethylene glycol)
PerCP	Peridinin-Chlorophyll-protein
PEST	Penicillin-streptomycin
PF127	Pluronic® F-127
PFA	Paraformaldehyde
PFS	Progression-free survival
PGA	Poly(glycolic acid)
PI3K	Phosphoinositide 3-kinase
PLA	Poly lactide/polylactic acid
PLGA	Poly(lactic-co-glycolide) or poly(lactic-co-glycolic) acid
PLGA-Cy5	Cyanine 5 carboxylic acid-grafted PLGA
PMMA	Poly(methyl methacrylate)
Poly(I:C)	Polyinosinic:polycytidylic acid
PR	Progesterone receptor
PRR	Pattern-recognition receptors
PSA	Prostate-specific antigen
PVA	Polyvinyl alcohol
qRT-PCR	Quantitative real-time reverse transcription-PCR
rDC	Regulatory DC
RNA	Ribonucleic acid
SC	Subcutaneous
SD	Standard deviation
sDC	Stimulatory DC
SDS	Sodium dodecyl sulfate
SEM	Standard error of the mean
siRNA	Small interfering RNA
siTGF-β1	Small interfering RNA anti-TGF- β 1
ssDNA	Single-stranded DNA
TAA	Tumour-associated antigen

TAE	Tris-acetate-EDTA
TAM	Tumour-associated macrophage
TAN	Tumour-associated neutrophil
TCGA	The Cancer Genome Atlas
TCR	T-cell receptor
TEMED	N,N,N',N'-tetramethylethylenediamine
TGF	Transforming growth factor
Th	T helper
TIL	Tumour-infiltrating lymphocyte
TIM-3	T-cell immunoglobulin and mucin domain 3
TKI	Tyrosine kinase inhibitor
TLR	Toll-like receptors
TME	Tumour microenvironment
TNBC	Triple-negative breast cancer
TNF	Tumour necrosis factor
Treg	T regulatory cell
w/o/w	Double emulsion solvent evaporation
WGA	Wheat germ agglutinin
WHO	World Health Organization
Z-Ave	Z-average hydrodynamic diameter
ZP	Zeta potential or surface charge
α-Lac	α -lactalbumin
αOX40	Monoclonal antibody against OX40 receptor
αPD-1	Monoclonal antibody against programmed death-1 receptor

List of figures

Chapter I

- Figure 1** Overview of signalling pathways involved with identified potential inhibitors in TNBC. The network of multiple signalling cascades with downstream effectors help in the maintenance of growth, proliferation, survival and metastasis of triple-negative breast cancer (TNBC) cells. The signalling pathways like NF- κ B, PI3/AKT/mTOR (PAM), JAK/STAT and RTKs (receptor tyrosine kinases) are implicated in the pathogenesis of TNBC cells. The developmental pathways like Wnt/ β -Catenin, Notch, Hh (Hedgehog) are associated with invasion, migration, and metastatic potential. Most of the potential inhibitors directly induced apoptosis in TNBC by up-regulation of Bad, Caspase 3 and down-regulation of BCL-2, BCL-XL and surviving. **10**
- Figure 2.** The innate and adaptive immune response. The innate immune response functions as the first line of defence against infection. It consists of soluble factors, such as complement proteins, and diverse cellular components including granulocytes (basophils, eosinophils and neutrophils), mast cells, monocytes/macrophages, dendritic cells and natural killer cells (NK). The adaptive immune response is slower to develop, but manifests as increased antigenic specificity and memory. It consists of antibodies, B-cells, and CD4⁺ and CD8⁺ T lymphocytes. NKT cells and $\gamma\delta$ T-cells are cytotoxic lymphocytes that straddle the interface of innate and adaptive immunity. **14**
- Figure 3.** The three phases of cancer immunoediting process. In the elimination phase, tumour cells are recognized by innate and adaptive immune cells and are destroyed before they can become a clinical malignancy. If not destroyed, the tumour enters into the equilibrium phase and suffers genetic changes and/or becomes resistant to immune detection. In the escape phase, the tumour microenvironment becomes immunosuppressive, promoting the tumour development. **18**

List of figures

- Figure 4.** TGF- β signalling affects all populations of leukocytes in a stimulatory or inhibitory manner. Positive or negative effects of transforming growth factor- β (TGF- β) signalling on the indicated aspects of leukocyte biology are marked by arrows pointing up or down. Only cellular processes with a well-documented role for TGF- β are indicated in this figure. **23**
- Figure 5.** Desired immune response elicited by a therapeutic cancer vaccine. **36**
- Figure 6.** Schematic representation of polymeric, lipid, metal and inorganic nanocarriers. **37**
- Figure 7.** Schematic representation of PLA chemical structure **42**
- Chapter III**
- Figure 8.** Electrophoretic mobility of chitosan-siRNA polyplexes formed with different chitosan derivatives (glycol chitosan (GCs), glutamate chitosan (GlutCs) and hydro-chloride chitosan (HCCs)) with siTGF- β 1 at two different Cs-siRNA ratios (5:1 and 15:1). Free siRNA was used as control. **71**
- Figure 9.** Physical properties of nanoparticles (NPs) and stability. a, Schematic representation of nanoparticles (NP). b, AFM images of empty NPs showing spherical shape, slight roughness on the surface and a narrow size polydispersity ($N = 3$). c-e, Empty NP physicochemical stability in PBS (pH 7.4) at 25 °C. **72**
- Figure 10.** a, SDS-PAGE of α -Lac protein (14 kDa) in solution (positive control) or entrapped into NPs ($N = 3$). b, Release profile of OVA-Alexa 647[®] entrapped in the nanovaccine over 28 days ($N = 3$; $n = 3$). **73**
- Figure 11.** a, Cell viability of DC (JAWSII ATCC[®] CRL-11904TM and BMDC) and breast tumour cells (4T1 ATCC[®] CRL-2539TM) after incubation of NPs for 48 hours. Mean \pm SD ($N = 3$ independent **76**

experiments, $n = 6$ replicate measurements). b, Rho-labelled NP internalisation by murine immature DCs (JAWSII and BMDCs), and by murine 4T1 breast tumour cells, determined by FACS. Non-treated cells and non-labelled NPs were used as negative controls. Data are presented as mean \pm SD, $N = 4$ independent samples, with 3 technical replicates ($n = 3$). One-way ANOVA followed by Tukey Post-Hoc test. *** $P = 0.0001$. c, Confocal images (Z-stack and maximum projection) of murine immature DC (JAWSII) after 4, 12 and 24 hours of incubation with Cy5-labelled NPs ($N = 3$; $n = 3$). Scales bar: 25 μ m.

- Figure 12.** Median fluorescence intensity (MFI) of activated DCs that internalised NP1, present in the lymph nodes, 17 hours after immunisation. Mean \pm SD; $N = 3$, $n = 3$, where N denotes the number of independent experiments and n denotes the number of measurements per experiment. One-way ANOVA followed by Tukey Post-Hoc test. *** $P < 0.001$. **77**
- Figure 13.** Non-invasive intravital fluorescence imaging 24 hours following hock immunisation with NP (left) and PBS (right) of a, BALB/c mouse 24 hours following hock immunisation with NP (left) and PBS (right). b, Organ biodistribution. ($N = 3$ animals). LN: lymph nodes. **78**
- Figure 14.** Nanovaccines synergize with α OX40 immune checkpoint against TNBC. a, Timeline (days) of tumour inoculation in BALB/c mice, immunisation scheme, and immune checkpoint therapy. b, Body weight change, expressed as percent change from the day of treatment initiation. Data are presented as mean \pm SEM ($N = 5$ animals per group). c, Kaplan-Meier overall survival over time graph for mice inoculated with 7×10^5 4T1 cells (two independent assays were performed with $N = 8$ animals for NP1+NP2+ α OX40 group and $N = 5$ animals for the remaining groups). Log-Rank test, for the combination NP1+NP2+ α OX40 compared to all other treatment groups. d, Tumour growth curve. Data are presented as mean \pm SEM ($N = 5$ animals). P values correspond to tumour **79**

volume at day 22 after tumour inoculation relative to PBS-treated group and **P* values are relative to the nanovaccine + α OX40 group. One-way ANOVA followed by Tukey Post-Hoc test. e, Individual tumour volume at day 22 (*N* = 5 animals) with mean \pm SEM. *P* values correspond to tumour volume at day 22 after tumour inoculation relative to PBS-treated group and **P* values are relative to the nanovaccine + α OX40 group. One-way ANOVA followed by Tukey Post-Hoc test. f, Tumour mass and spleen weight recovered after mice sacrifice. *N* = 3, Mean \pm SD. One-way ANOVA followed by Tukey Post-Hoc test. *P* values relative to the PBS-treated group and **P* values relative to the nanovaccine + α OX40 group.

Figure 15. Tumour-infiltrating immune cell populations after the combination of nanovaccines with α OX40. a-n, Tumour-infiltrating immune cell populations for CD3⁺ (a), CD3⁺CD8⁺ (b), CD3⁺CD8⁺CD107b⁺ (c), CD3⁺CD8⁺PD-1⁺ (d), CD3⁺CD4⁺ (e), CD3⁺CD4⁺CD25⁺FoxP3⁺ (f), CD3⁺CD8⁺TNF- α ⁺ (g), CD3⁺CD8⁺IFN- γ ⁺ (h), CD3⁺CD8⁺IL-2⁺ (i), CD11c⁺MHCII⁺CD11b⁺ (j), CD11c⁺MHCII⁺CD11b^{hi} (k), CD11c⁺MHCII⁺CD11b⁺ (l), CD11b⁺Gr-1⁺ (m), CD11c⁺MHCII⁺CD11b^{dim}CD8⁺CD103⁺ (n). Tumours were isolated on day 19 after tumour cell inoculation. Quantification was performed by flow cytometric analysis. Data are presented as mean \pm SD, *N* = 3 animals, *n* = 3 measurements per experiment. One-way ANOVA followed by Tukey Post-Hoc test. *P* values relative to PBS-treated group. **81**

Figure 16. Ibrutinib did not improve the antitumour effect of the dual therapy. a, Timeline (days) of tumour inoculation in BALB/c mice, immunisation scheme, and treatments. b, Body weight change, expressed as percent change from the day of treatment initiation. Data are presented as mean \pm SEM (*N* = 5 animals per group). c, Tumour growth curve. Data are presented as mean \pm SEM (*N* = 5 animals). *P* values correspond to tumour volume at day 22 after tumour inoculation relative to PBS-treated group. **P* value correspond to tumour volume at day 22 after tumour inoculation **83**

relative to the nanovaccine + α OX40 group. One-way ANOVA followed by Tukey Post-Hoc test. d, Kaplan-Meier overall survival over time graph for mice inoculated with 7×10^5 4T1 cells (two independent assays were performed for groups nanovaccine + α OX40 and nanovaccines + α OX40 + Ib with $N = 8$ animals for nanovaccine + α OX40 group and $N = 5$ animals for the remaining groups). Log-Rank test, $P = 0.0006$ for the combination nanovaccine + α OX40 compared to all other treatment groups. e, Individual tumour volume at day 22 ($N = 5$ animals) with mean \pm SEM. P values correspond to tumour volume at day 22 after tumour inoculation relative to PBS-treated group and * P values are relative to the nanovaccine + α OX40 group. One-way ANOVA followed by Tukey Post-Hoc test. f, Tumour mass and spleen weight recovered after mice sacrifice. $N = 3$, Mean \pm SD. One-way ANOVA followed by Tukey Post-Hoc test. P values relative to PBS-treated group and * P values relative to the nanovaccine + α OX40.

Figure 17. Tumour-infiltrating immune cell populations after the combination of nanovaccines + α OX40 with Ibrutinib showed a decrease on the MDSCs, besides not improving the antitumour effect of the dual therapy. a-n, Tumour-infiltrating immune cell populations for CD3⁺ (a), CD3⁺CD8⁺ (b), CD3⁺CD8⁺CD107b⁺ (c), CD3⁺CD8⁺PD-1⁺ (d), CD3⁺CD4⁺ (e), CD3⁺CD4⁺CD25⁺FoxP3⁺ (f), CD3⁺CD8⁺TNF- α ⁺ (g), CD3⁺CD8⁺IFN- γ ⁺ (h), CD3⁺CD8⁺IL-2⁺ (i), CD11c⁺MHCII⁺CD11b⁺ (j), CD11c⁺MHCII⁺CD11b^{hi} (k), CD11c⁻MHCII⁺CD11b⁺ (l), CD11b⁺Gr-1⁺ (m), CD11c⁻MHCII⁺CD11b^{dim}CD8⁺CD103⁺ (n). Tumours were isolated on day 19 after tumour cell inoculation. Quantification was performed by flow cytometric analysis. Data are presented as mean \pm SD, $N = 3$ animals, $n = 3$ measurements per experiment. One-way ANOVA followed by Tukey Post-Hoc test. P values relative to PBS-treated group. **84**

Figure 18. PD-1 blockade did not improve the antitumour effect of the dual therapy. a, Timeline (days) of tumour inoculation in BALB/c mice, **85**

immunisation scheme, and immune checkpoint therapy. b, Body weight change, expressed as percent change from the day of treatment initiation. Data are presented as mean \pm SEM ($N = 5$ animals per group). c, Tumour growth curve. Data are presented as mean \pm SEM ($N = 5$ animals). One-way ANOVA followed by Tukey Post-Hoc test. P values correspond to tumour volume at day 22 after tumour inoculation relative to PBS-treated group. d, Tumour mass and spleen weight recovered after mice sacrifice. $N = 3$, Mean \pm SD. One-way ANOVA followed by Tukey Post-Hoc test. P values relative to PBS-treated group.

Figure 19. Tumour-infiltrating immune cell populations after the combination of nanovaccines + α OX40 with α PD-1 monoclonal antibody decreased the PD-1 expression on CD8⁺ T-cells, besides not improving the antitumour effect of the dual therapy. a-n, Tumour-infiltrating immune cell populations for CD3⁺ (a), CD3⁺CD8⁺ (b), CD3⁺CD8⁺CD107b⁺ (c), CD3⁺CD8⁺PD-1⁺ (d), CD3⁺CD4⁺ (e), CD3⁺CD4⁺CD25⁺FoxP3⁺ (f), CD3⁺CD8⁺TNF- α ⁺ (g), CD3⁺CD8⁺IFN- γ ⁺ (h), CD3⁺CD8⁺IL-2⁺ (i), CD11c⁺MHCII⁺CD11b⁺ (j), CD11c⁺MHCII⁺CD11b^{hi} (k), CD11c⁺MHCII⁺CD11b⁺ (l), CD11b⁺Gr-1⁺ (m), CD11c⁺MHCII⁺CD11b^{dim}CD8⁺CD103⁺ (n). Tumours were isolated on day 19 after tumour cell inoculation. Quantification was performed by flow cytometry. Data are presented as mean \pm SD, $N = 3$ animals, $n = 3$ measurements per experiment. One-way ANOVA followed by Tukey Post-Hoc test. P values relative to PBS-treated group. **86**

Figure 20. a, qRT-PCR analysis of TGF- β 1 in tumours. Data are shown as mean \pm SD fold change of 3 individual animals ($N = 3$). Unpaired two-tailed t test. b, Immunoblotting and densitometry of TGF- β 1. Blots were normalised to the endogenous β -actin. Representative immunoblots are shown. Results are expressed as mean \pm SD fold change of 3 individual animals ($N = 3$). Unpaired two-tailed t test. c-e, Flow cytometric analysis of T-cell specificity. Spleens from animals treated with NP1+NP2 were recovered on day 23 (after tumour inoculation) and co-cultured in medium, medium **87**

with gp100 or medium with α -Lac. Data are presented as mean \pm SD of 3 individual animals ($N = 3$)

Figure 21. T cell induced response by nanovaccine on B16.MO5 model is specific for OVA antigen. a, Timeline (days) of B16.MO5 inoculation in C57BL/6J mice, immunisation scheme, and immune checkpoint therapy. b, Body weight change, expressed as percent change from the day of treatment initiation. Data are presented as mean \pm SEM ($N = 5$ animals per group). c, Tumour growth curve. Data are presented as mean \pm SEM ($N = 5$ animals). P values correspond to tumour volume at day 22 after tumour inoculation. One-way ANOVA followed by Tukey Post-Hoc test. d, Frequency of SIINFEKL (OVA)-specific CD8⁺ T-cells (in live CD3⁺CD19⁻ cell population) in spleen. Data are presented as mean \pm SD ($N = 5$ animals per group, $n = 3$ measurements per experiment). One-way ANOVA followed by Tukey Post-Hoc test. P values relative to PBS. **88**

List of tables

Chapter I

Table 1.	Breast cancer molecular subtypes: standard classification, correlation with biomarker staining on immunohistochemistry, outcome and prevalence.	6
Table 2.	Some clinical trials using FDA and EMA approved immune checkpoint agents, alone or in combination with other agents, under investigation in triple-negative breast cancer	25
Table 3.	Example of ongoing clinical studies involving cancer vaccines	34

Chapter II

Table 4.	Biomolecules co-entrapped in the nanovaccine formulations	51
Table 5.	Treatment groups and the respective route(s) of administration in the three combination assays	58
Table 6.	Treatment groups and the respective route(s) of administration for the functional assessment of T-cell	62

Chapter III

Table 7.	Size, polydispersity index, ζ potential, and entrapment efficiency and loading capacity of the different biomolecules within nanovaccines	74
-----------------	---	-----------

Aims and outline

The main goal of the research described in this thesis was to evaluate whether the combination of a multifunctional nanovaccine could re-shape the tumour microenvironment, sensitizing triple-negative breast cancer to the immune checkpoint OX40 agonist, and thus, improving the overall anti-tumour immune response.

For this purpose, several questions were addressed:

1. Can biodegradable polymeric nanoparticles entrapping a tumour-associated antigen, immune potentiators and regulators of potent immune suppressor molecules within the TME be produced with optimal physicochemical characteristics for antigen-presenting cell and tumour cell targeting?
2. Can antigen-presenting cells and tumour cells extensively internalize these nanoparticles without affecting their viability?
3. Can these nanoparticles knockdown the expression of immune suppressor molecules within the TME?
4. Can nanoparticles induce a cytotoxic antitumour immune response *in vivo*?
5. Can we induce a synergistic antitumour immune response by combining DC-targeted nanoparticles with OX40 stimulation?
6. Which populations of tumour-infiltrated immune cells are driving the therapeutic response?

The results of the research are presented in chapter III, which is preceded by chapter I, a general introduction where several aspects of the field are addressed. Chapter II presents detailed information regarding materials and methods used to prepare nano-vaccine and the evaluation of their efficacy under both *in vitro* and *in vivo* studies. In chapter IV, the results are subject to discussion and in chapter V, concluding remarks and future perspectives are presented.

Table of contents

Abstract	v
Resumo	vii
Acknowledgments/Agradecimientos	xi
List of abbreviations	xv
List of figures	xxi
List of tables	xxix
Aims and outline	xxxii
Chapter I – General introduction	5
1. Breast cancer – A brief discussion of the disease	5
1.1. Incidence and mortality	5
1.2. Distinct subtypes	5
1.2.1. Triple-negative breast cancer	7
1.2.1.1. Conventional therapies.....	8
1.2.1.2. Targeted therapies	10
2. The immune system.....	13
2.1. Cancer immunoediting.....	17
2.2. Tumour microenvironment	19
2.3. Cancer immunotherapy.....	22
2.3.1. Immune checkpoint modulation	23
2.3.2. Cancer vaccines	28
2.3.2.1. Essential elements of cancer vaccines.....	29
2.3.2.2. Applications in TNBC	33
2.3.2.3. Dendritic cells as targets for cancer vaccines.....	34
3. Nanodelivery systems for DC-based vaccines.....	37
3.1. Polymeric nanoparticles	38
3.1.1. Polymeric NPs as nanodelivery systems for vaccines.....	39
3.1.1.1. Influence of NP properties in cellular uptake by dendritic cells	40
3.1.1.2. Polylactic acid-based particulate systems for vaccine delivery	42
Chapter II - Materials and Methods	49
1. Materials	49
2. Methods	50
2.1. Preparation of nanovaccines	50
2.1.1. Preparation of chitosan-siRNA polyplexes	50
2.1.2. Synthesis of multifunctional biodegradable NPs	51
2.1.3. Gel retardation assay.....	52
2.1.4. Physicochemical characterisation of NP	52

Table of contents

2.1.4.1.	Size distribution and ζ potential measurements.....	52
2.1.4.2.	Particle morphology	52
2.1.5.	NP physical stability assay.....	52
2.1.6.	Entrapment efficiency and loading capacity of antigens and immune potentiators.....	53
2.1.7.	Integrity of α -Lac entrapped in NP	54
2.1.8.	NP antigen release	54
2.2.	Cell line culture conditions.....	54
2.3.	Animal studies.....	55
2.4.	Isolation of murine hematopoietic stem cells from bone marrow and differentiation into BMDC	55
2.5.	<i>In vitro</i> and <i>ex vivo</i> cell viability in the presence of NP.....	55
2.6.	<i>In vitro</i> and <i>ex vivo</i> NP internalisation by targeted cells by flow cytometric analysis.....	56
2.7.	<i>In vitro</i> NP internalisation by DCs by confocal microscopy	56
2.8.	<i>Ex vivo</i> analysis of NP effect on DC activation and maturation.....	56
2.9.	NP <i>in vivo</i> biodistribution	57
2.10.	Intervention combination therapies in triple-negative breast carcinoma	57
2.10.1.	Characterization of tumour-infiltrating immune cells by flow cytometry	58
2.10.2.	Assessment of TGF- β 1 expression in tumours.....	60
2.10.2.1.	Quantitative RT-PCR.....	60
2.10.2.2.	Protein extraction and immunoblotting	60
2.10.3.	Functional assessment of T-cells	61
2.11.	Intervention combination therapies in B16.MO5 murine model	61
2.12.	Functional assessment of T-cells.....	62
2.13.	Statistical Methods.....	63
Chapter III – Results		71
1.	Multifunctional nanoparticles as antigen delivery systems and regulators of TGF- β levels	71
2.	Multifunctional nanovaccines activate and improve the maturation of DCs.....	75
3.	Combination of therapeutic multifunctional nanovaccines with α OX40 immune checkpoint therapy restricts tumour growth and prolongs survival.....	75
4.	Ibrutinib does not improve the antitumour effect of the therapeutic multifunctional nanovaccines with α OX40	80
5.	PD-1 blockade does not improve the antitumour effect of the therapeutic multifunctional nanovaccines with α OX40.....	82
6.	Nanovaccines knockdown TGF- β expression and induce systemic CD8 ⁺ T-cell-mediated immune response.....	87
7.	Nanovaccines induce CD8 ⁺ T-cell-mediated immune response within the tumour microenvironment	88

Chapter IV – Discussion	97
1. Multifunctional nanoparticles as antigen delivery systems and regulators of TGF- β levels	97
2. Multifunctional nanovaccines activate and improve the maturation of DCs.....	99
3. Nanovaccines knockdown the expression of TGF- β , induce systemic CD8 ⁺ T-cell-mediated immune response, and, when combined with α OX40 immune checkpoint therapy, restrict tumour growth and prolongs survival	100
4. Ibrutinib does not improve the antitumour effect of the therapeutic multifunctional nanovaccines with α OX40	102
5. PD-1 blockade does not improve the antitumour effect of the therapeutic multifunctional nanovaccines with α OX40.....	103
Chapter V – Conclusions and Future Perspectives	109

CHAPTER I

Chapter I – General introduction

Part of this chapter is adapted from the following published manuscripts:

Scientific publications in peer review international journals:

1. **Peres C**, Matos AI, Conniot J, Sainz V, *et al.* Poly(lactic acid)-based particulate systems are promising tools for immune modulation. *Acta Biomaterialia*, 2017, 48: 41-57. DOI: 10.1016/j.actbio.2016.11.012;
2. Silva AS*, **Peres C***, Conniot J*, Matos AI, *et al.* Nanoparticle impact on innate immune cell pattern-recognition receptors and inflammasomes activation. *Seminars in Immunology*, 2017, 34: 3-24. DOI: 10.1016/j.smim.2017.09.003. *equally contributing authors;
3. Silva AL, Moura L, Carreira B, Conniot J, Matos AI, **Peres C**, Sainz V, Silva LC, Gaspar RS, Florindo HF. Functional moieties for intracellular traffic of nanomaterials. In: *Biomedical Applications of Functionalized Nanomaterials – Concepts, development and Clinical Translational* (Sarmiento and das Neves, Ed., Elsevier, 2018, pp. 399-448). DOI: 10.1016/B978-0-323-50878-0.00014-8;
4. Matos AI, Carreira B, **Peres C**, Moura LI, *et al.* Nanotechnology as a key strategy for combinational innovative chemo-immunotherapies against colorectal cancer. *Journal of Controlled Release*, 2019, 307: 108-138. DOI: 10.1016/j.jconrel.2019.06.017.

Chapter I – General introduction

1. Breast cancer – A brief discussion of the disease

1.1. Incidence and mortality

Although early detection and current improving treatments have been associated with a reduction in breast cancer mortality rate, over the last decade, in most developed countries (1, 2), breast cancer is still one of the most devastating diseases. According to the World Health Organization (WHO), breast cancer is the most frequent cancer in women and has the highest rate of cancer-related mortality among women worldwide, both in the developed and developing countries. In 2018, it was estimated that over 2.1 million women were newly diagnosed and over 627,000 died from this disease (3), being metastasis the leading cause of death (4). Additionally, WHO estimates that by 2020 one in every eight women will develop breast cancer (5). The 5-year survival for breast cancer is 98% for localised disease, 84% for regional disease, but only 23% for distant disease. Moreover, 25% of patients with early breast cancer will relapse and 50% of the women with axillary lymph node (LN) involvement will relapse (6).

1.2. Distinct subtypes

Breast cancer is frequently described as a heterogeneous cancer group, which differs greatly among patients (intertumour heterogeneity), and even within each individual tumour (intratumour heterogeneity) (7, 8). This heterogeneity gives rise to tumours with distinct behaviours, namely in terms of clinical presentations, treatment responses, and clinical outcomes (9). In an attempt to treat patients more efficiently, extensive research at molecular and genetic level has been conducted in order to classify these distinct breast cancers (10-12). In 2000, Perou *et al.* proposed that the phenotypical diversity of breast tumours could be associated with specific gene expression patterns. To evaluate this, Perou *et al.* used complementary DNA (cDNA) microarrays to analyse genetic profiles and grouped genes based on their similar patterns of expression (10). Subsequently, Sørlie *et al.* demonstrated that breast tumours could be divided into, at least, four distinct molecular subtypes: (i) luminal A, (ii) luminal B, (iii) human epidermal growth factor receptor 2 (HER2)-type, and (iv) basal-like, based on the expression of three biomarkers (assessed by immunohistochemistry (IHC)): oestrogen receptors (ER), progesterone receptors (PR) and the HER2 (**Table 1**) (11-14). These subtypes have diverse natural history and present different clinical, pathologic and molecular features with distinct prognostic and therapeutic implications (9).

General introduction

Luminal A breast cancer is the most common subtype, accounting for 30 - 40% of all invasive breast cancer (13). The luminal A IHC profile is characterized by ER-positive and/or PR-positive, an absence of HER2 expression, a low rate of cell proliferation measured by Ki-67 and a low histological grade (13, 15). Patients with luminal A early-stage breast cancer have the best prognosis and relatively low rates of local and regional relapses (16, 17), although they frequently have bone as the first site of metastatic disease (18). This subtype also tends to have a more indolent course with a slower evolution over time (19).

Table 1. Breast cancer molecular subtypes: standard classification, correlation with biomarker staining on immunohistochemistry, outcome and prevalence. Adapted from Fragomeni SM *et al.* (2018) *Surg Oncol Clin N Am.* 27(1):95-120. and Dai X *et al.* (2015) *Am J Cancer Res.* 15;5(10):2929-43.

Breast cancer subtype	IHC staining				Outcome	Prevalence**
	ER	PR	HER2	Grade*		
Luminal A	Either ER or PR +	-	-	1 2	Good	30 - 40%
Luminal B	(HER2 ⁻)	Either ER or PR +	-	2 3	Intermediate	20 - 30%
	(HER2 ⁺)	Either ER or PR +	+	2 3	Poor	
HER2-enriched	-	-	+	2 3	Poor	12 - 20%
Basal-like/TNBC	-	-	-	3	Poor	15 - 20%

Abbreviations: ER: oestrogen receptor; HER2: human epidermal growth factor receptor 2; IHC: immunohistochemistry; PR: progesterone receptor; TNBC: triple-negative breast cancer. *Histological grade. **Prevalence is based on all invasive breast cancer cases.

Luminal B tumours represent 20% to 30% of all invasive breast cancers (13). The luminal B IHC profile is characterized by ER-positive, with negative and/or positive expression of PR and HER2 markers, and higher level of Ki-67 labelling index, compared to luminal A (20). This subtype is more aggressive, has higher histological grade and proliferative index, and is associated with a more intermediate prognosis than luminal A subtype (13, 14, 21). Although bone is the most common site of recurrence, there is a higher recurrence rate in visceral sites in this subtype (22). Additionally, the survival from time of relapse is lower (1.6 years) compared to luminal A (2.2 years) (23).

HER2-enriched breast cancers accounts for 12 - 20% of all invasive breast cancers (13). At molecular level, HER2-positive breast cancers are characterized by the overexpression of the HER2 gene and genes related to cellular proliferation (24). These tumours are highly proliferative with a higher histological grade than the previous

subtypes (14). In addition, patients with HER2-enriched breast cancer have a higher frequency of developing brain metastases (25, 26), and a higher rate of metastases to the liver and lung (23, 25).

Basal-like breast cancer represents approximately 15% of all breast cancer cases and is defined as a tumour that lack the expression of ER, PR and HER2, although the strong expression of basal epithelial markers, such as cytokeratins (CK: CK5/6, CK14 and CK17), and low expression of luminal genes (10). Patients diagnosed with this subtype have a poor prognosis and a short-term disease-free and overall survival (OS) (27), owing to the aggressiveness of the tumour and the recurrent lesions (28).

Basal-like breast cancer and triple-negative breast cancer (TNBC) are often considered as synonymous, since most of basal-like breast cancers are also triple-negative breast cancers (77%) and the majority of TNBCs (71%) are also basal-like breast cancers (29), however the analysis of morphologic and molecular features and immunohistochemical expression has shown that these are not the same entity, and equating them is misleading (30-32). Indeed, they express different molecular markers, TNBC have a higher histologic grade, and have a worse prognosis than basal-like breast cancer (33). TNBC are of particular interest because they follow very aggressive clinical course and currently lack any form of standard targeted systemic therapy.

1.2.1. Triple-negative breast cancer

TNBC is clinically defined by a lack of ER and PR expression, and the absence of HER2 protein overexpression and HER2-gene amplification (31). It accounts for 15 - 20% of all invasive breast cancer (13, 34, 35) and is typically observed in young women (below the age of 40 years), especially in African-American women, and Hispanic women who carry BRCA1 mutations. Risk factors associated with the diagnosis of TNBC include positive BRCA mutation status, race (since African-American women have a higher risk of TNBC than non-African American women), premenopausal status, obesity and some maternal-related factors (35-38).

Patients diagnosed with TNBC have an extremely poor prognosis and die quickly (median OS of 13.3 months with treatment), when compared to the previous breast cancer subtypes (39), owing to an inherently aggressive clinical behaviour and a lack of recognized molecular targets for therapy (42). Additionally, TNBC is characterized by larger tumour at diagnosis, higher histological grade (40), an early peak of recurrence (1 to 3 years after diagnosis) (19, 41), and higher rates of distant recurrences, with more aggressive metastasis, which are more likely to occur in viscera, particularly in the lungs (40%) and brain (30%), and less likely to spread to the liver (20%) and the bone (10%) (31, 32).

1.2.1.1. Conventional therapies

In contrast to the other breast cancer subtypes, patients diagnosed with TNBC do not benefit from endocrine therapies, such as Tamoxifen and aromatase inhibitors, or HER2-directed therapies, such as Trastuzumab and Lapatinib, due to the loss of the target receptors ER, PR, and HER2 (42, 43), which limits greatly the therapeutic options available for this disease. Hence, surgery, for the excision of the lesions, radiation therapy and chemotherapy, individually or in combination, appear to be the only available modalities. However, these approaches are unspecific and are characterized by severe side effects (44).

The best method for locally controlling TNBC is surgical excision, similar to other types of breast cancer, being the breast-conserving therapy (BCT) the most applied in TNBC patients (45). However, many studies have reported local and regional recurrence after BCT, which forces clinicians to consider other therapies to be used in combination with BCT, namely radiotherapy and chemotherapy (46-48). However, the use of radiotherapy for patients with TNBC has been controversial. Indeed, radiotherapy has not been constantly associated with an OS benefit in TNBC (49). Nevertheless, recently, Yao and collaborators conducted a retrospective study to clarify the influence of radiotherapy on the survival of TNBC patients after surgery based on a large population analysis, where they showed significant survival benefits for the TNBC patients receiving radiation therapy after surgery (50).

Chemotherapy has been traditionally the primary established treatment option for patients with early- and advanced-stage TNBC (43). Over the past two decades, many studies have shown a significant benefit of chemotherapy in the treatment of patients diagnosed with TNBC (51). Despite its aggressive behaviour, a subset of early TNBC patients present a good initial response and high sensitivity to chemotherapy, specially to anthracyclines and taxanes (33). However, patients with advanced disease typically respond poorly to current chemotherapeutic agents. Even in cases in which patients respond to this standard chemotherapy regimens, rapid disease progression is observed later (33), which can be explained by the development of resistance to chemotherapy, a key player in metastasis and recurrence of cancer in TNBC patients (52, 53).

Clinically, it has been particularly challenging to find the optimal chemotherapy regimen that would improve the metastasis free and OS for these patients. Nowadays, and besides the specific regimens that may be most effective for TNBC remains incompletely defined for both early stage and advanced disease, third-generation chemotherapy regimens like those offered to other high-risk patients are among the most effective tools presently available (54). Anthracyclines (doxorubicin, epirubicin) and/or

taxanes (paclitaxel, docetaxel) are the two most active classes of cytotoxic agents for both early and advanced stage breast cancer (55), and are considered as the current standard of care for early TNBC patients (56), achieving pathologic complete response (pCR) rates of approximately 40% (57, 58). Capecitabine is often used as second-line monotherapy in patients whose disease is resistant to anthracycline, taxane, or both (59). When added to the standard chemotherapy regimen, this chemotherapeutic drug has shown a potential survival benefit in early TNBC patients. Despite a substantial toxic effect, the addition of capecitabine to the standard chemotherapy regimen has been considered as a reasonable option for patients with TNBC carrying a higher risk of relapse (59). There has also been a renewed interest in platinum compounds for the treatment of TNBC, specially for patients harbouring BRCA mutations. Although many preclinical and clinical studies have shown a significant increase in the pCR rates after the addition of platinum agents to the standard chemotherapy regimen (60, 61), platinum agents failed to demonstrate improved benefit in the context of advanced breast cancer (62). Currently, platinum-based chemotherapy is currently recommended only for patients with known BRCA mutation (63).

Several other combination chemotherapy regimens have been studied and assessed in preclinical and clinical trials in an attempt to improve the outcomes of these patients (56). Although some combination therapies have improved the response rates compared with single agents, they were also associated with an increased toxicity and did not provide any benefit in patient OS (64).

Additionally, conventional chemotherapeutic agents present several drawbacks: i) non-specific distribution in the body, where they affect both normal and malignant cells, thereby limiting the dose achievable within the tumour and thus resulting in suboptimal treatment (65); ii) high clearance rate of anticancer drugs from the blood stream requires larger doses for an effective treatment, which can be responsible for several side effects due to the excessive toxicity (65); iii) poor solubility of most conventional, thus requiring solvents that can lead to severe adverse effects, including acute hypersensitivity reactions, fluid retention, and peripheral neuropathy (66); and iv) development of multi-drug resistance, an effect that has been associated to at least six mechanisms in TNBC, namely i) ATP-binding cassette transporters; ii) overexpression of β -tubulin III subunit; iii) mutations in DNA repair enzymes such as topoisomerase II and DNA mismatch repair enzymes; iv) alterations in genes involved in apoptosis (p53, caspase-3 s, bcl-2, bcl-x); v) aldehyde dehydrogenase 1 (ALDH1) and glutathione (GSH)/ glutathione-S-transferase (GST); and vi) NF- κ B signalling pathways (67).

1.2.1.2. Targeted therapies

Considering the heterogeneity of TNBC, personalized treatment strategies targeting molecular tumour-specific alterations have been considered as the most appropriate to effectively treat the 60–70% of patients with TNBC who do not fully respond to chemotherapy (43). There are many drugs in phase I, II and III clinical trials, investigating novel molecules either alone or in combination with other novel agents or standard chemotherapeutics that are promising for improved clinical outcomes of TNBC patients. Many of them have already been approved by the US Food and Drug Administration (FDA) and the European Medicines Agency (EMA) for the treatment of other cancers. These agents target some component(s) of the signalling pathways indispensable for the growth, survival, invasion and progression of TNBC (**Figure 1**), which are altered in 90% of TNBCs that persist after chemotherapy (68).

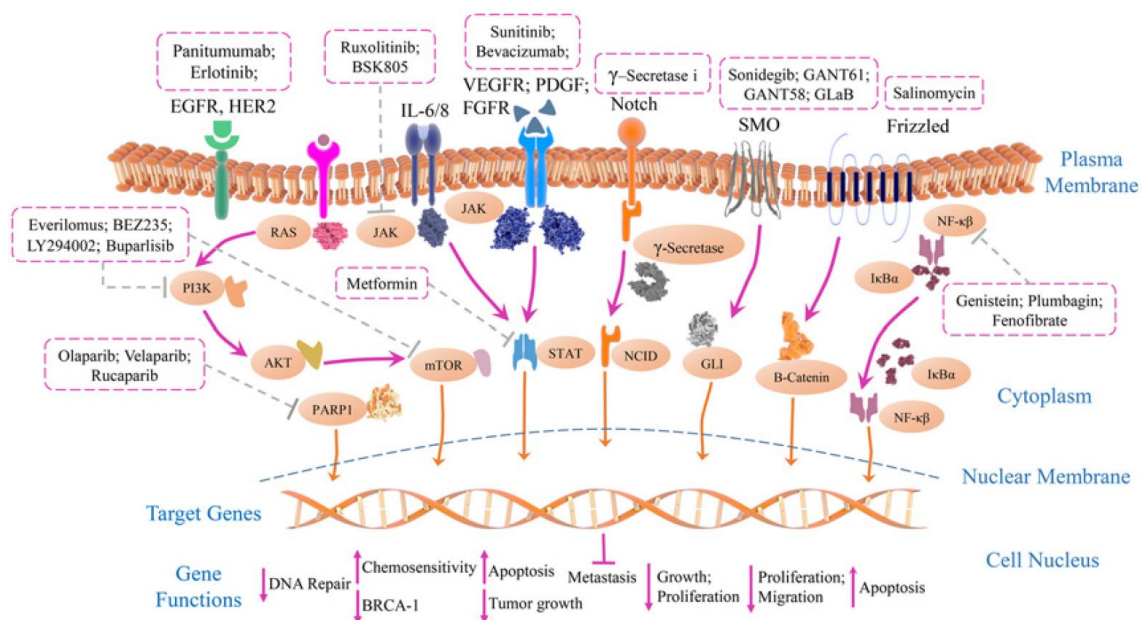


Figure 1. Overview of signalling pathways involved with identified potential inhibitors in TNBC. The network of multiple signalling cascades with downstream effectors help in the maintenance of growth, proliferation, survival and metastasis of triple-negative breast cancer (TNBC) cells. The signalling pathways like NF-κB, PI3/AKT/mTOR (PAM), JAK/STAT and RTKs (receptor tyrosine kinases) are implicated in the pathogenesis of TNBC cells. The developmental pathways like Wnt/β-Catenin, Notch, Hh (Hedgehog) are associated with invasion, migration, and metastatic potential. Most of the potential inhibitors directly induced apoptosis in TNBC by up-regulation of Bad, Caspase 3 and down-regulation of BCL-2, BCL-XL and surviving. From Chalukur-Ramireddy NKR and Pakala SB (2018) *Biosci Rep* 38(1):BSR20171357.

Although, many pathways have been targeted, only a few of them are found to be sensitive and, therefore, considered as effective targets for the treatment of TNBC. While several agents showed therapeutic response through the control of tumour growth and antiproliferative effect on TNBC cells, some of them increased their chemosensitivity (69). These targets encompass poly (ADP-ribose) polymerase 1 (PARP1), epidermal growth factor receptor (EGFR), and the PI3K-Akt-mTOR (PAM) pathway (70, 71), among many others as intensively reviewed elsewhere (72-76).

PARP1 is an abundant and constitutively expressed nuclear enzyme involved in the repair of DNA damage. Its inhibition has gained special interest for TNBC patients harbouring BRCA mutations (77). While in cells with wild-type BRCA1/2, double-strand breaks are repaired via homologous recombination, in BRCA1/2-deficient cells homologous recombination is impaired and thus, DNA strand breaks rely on PARP1 functionality for repair (78). Thus, in TNBC with BRCA mutations, the inhibition of this enzyme results in double-strand breaks, which leads to a severe and highly selective toxicity in these tumour cells, and consequent cell death (79). In addition, the use of PARP inhibitors allows also the sensitization of TNBC cells to chemotherapy and radiotherapy (80). Several PARP inhibitors are currently being tested in clinical trials, either as monotherapy or combination with chemotherapy, such as niraparib (ClinicalTrials.gov identifier: NCT01905592), rucaparib (ClinicalTrials.gov identifier: NCT02505048, NCT01074970), veliparib (ClinicalTrials.gov identifier: NCT01618357), and hold a promising future. Last year, PARP inhibitors Lynparza® (olaparib) and Talzena® (talazoparib) were approved by FDA and EMA for breast cancer treatment, in patients with germline BRCA1 or BRCA2 mutations, who have HER2 negative locally advanced or metastatic breast cancer.

EGFR is highly expressed in most of the TNBCs and has been recognized as a factor of poor prognosis for TNBC (81), which has been considered as a promising targeted treatment approach. The receptor activation promotes tumour progression and drug resistance in different cancers, such as lung, colon, head and neck, brain, pancreatic, and breast cancers (82, 83). There are two types of EGFR inhibitors – small molecular tyrosine kinase inhibitor (TKI) (e.g. erlotinib, gefitinib) and monoclonal antibody (mAb) (e.g. cetuximab, necitumumab) – and many have already been approved by FDA and EMA for the treatment of cancers, such as non-small cell lung cancer (NSCLC) and colorectal cancer. For breast cancer, however, most of the clinical trials of EGFR inhibitors have failed due to low response rates and/or acquired drug resistance (84). Currently, several phase I, II and III clinical trials are ongoing on TNBC patients as single agent (e.g. ClinicalTrials.gov identifier: NCT03692689, NCT01307891), in combination with other chemotherapeutic agents (e.g.

General introduction

ClinicalTrials.gov identifier: NCT02511847, NCT01091454, NCT01094184), or other signalling pathways inhibitors (e.g. ClinicalTrials.gov identifier: NCT01272141, NCT01307891).

Analysis of The Cancer Genome Atlas (TCGA) samples has shown activation of PAM pathway signalling in 10% – 20% of TNBCs (85), which is an important signalling pathway involved in motility regulation, metabolism, cell proliferation, migration and survival of TNBC cells (86). PAM pathway has been widely studied in several cancer types and a number of inhibitors of three main components of this pathway, namely phosphoinositide 3-kinase (PI3K), AKT and mammalian target of rapamycin (mTOR), are being investigated to be developed as therapeutic agents against cancer (87). Many different inhibitors are in phase I and II clinical trials for TNBC, as single agents or in combination with chemotherapeutic drugs, or with other signalling pathways inhibitors, as extensively reviewed by Khan *et al.* (2019) (86). The most promising inhibitors of PAM pathway are mTOR inhibitors and includes, namely, everolimus. Everolimus efficacy and OS, in combination with carboplatin, was assessed in phase II clinical trials in metastatic TNBC patients. This therapeutic combination showed efficacy with a clinical benefit rate (CBR) of 36%, and an improved progression-free survival (PFS) and OS. However, in another phase II clinical trials, when combined with the cisplatin + paclitaxel dual therapy, everolimus increased the adverse event profile of the dual therapy and did not improve the desirable clinical responses (88). This might be explained by the fact that mTOR blockade trigger a mechanism of negative feedback that leads to the activation of upstream molecules, which ultimately may increase antitumour activity in TNBC (67). Preclinical data have shown that the combination of compounds targeting the different components of the PAM pathway, such as AKT and mTOR, leads to synergistic activity, with an improved mean percentage of tumour growth inhibition compared to either one alone *in vivo* (89).

Another promising targeted therapy for the treatment of TNBC patients that have been under investigation in several clinical trials is immunotherapy. Contrarily to the other breast cancer subtypes, TNBC microenvironment present an increased tumour infiltration of CD4⁺ and CD8⁺ T-cells, which increases TNBC patients' susceptibility to immunotherapies (90). Moreover, due to the high genomic instability and elevated genetic mutation frequencies, TNBC are highly increased in immunogenicity, which also makes TNBC a cancer subtype predestined for immunomodulation (27, 91). This subject will be addressed on section 2.3.

2. The immune system

The link between the immune system and cancer is now well known, and was first highlighted by Rudolph Virchow over 150 years ago (92). The immune system is a complex network, comprising several types of soluble bioactive molecules, cytokines, proteins, and cells, involved in the control of host defences against pathogens or infected/malignant cells, that promptly reacts through an effector response (93). However, the immune system must also ignore the presence of self-antigens and innocuous microorganisms from ingested food/drink and the environment (94).

To provide protection and maintain the host's normal state of homeostasis, the immune system is divided into an innate and an adaptive branch, which mainly differ in response time and the level of specificity (**Figure 2**). Communication between those immune cells upon encountering a pathogen or infected/malignant cells is mediated by the release of signalling molecules, in particular cytokines and chemokines, which play important roles in immunity by interacting with specific receptors. Cytokines are a diverse group of proteins that have the ability to recruit and activate other cells, induce differentiation and enhance cytotoxic activity (95). Chemokines typically function as chemotactic factors, helping to guide other immune cells to the site of infection or tissue damage (96).

The innate immune system is activated almost immediately after the detection of danger signals, such as an invading pathogen, and involves the migration of phagocytic cells to the site of infection, forming the first line of defence (97). Principal components of innate immunity include epithelial barriers (skin and mucosal membranes), pattern recognition receptors (PRRs), effector cells (monocytes/macrophages, natural killer (NK) cells, dendritic cells (DCs), mast cells, neutrophils, eosinophils and basophils) and humoral components (complement proteins and collectins) (98). Innate immune cells are characterized by their lack of antigen-specificity and immunological memory. Instead, innate immune cells recognize self from non-self through genetically conserved molecular patterns that are frequently present in pathogens, but not in host cells (98, 99). These molecules are known as danger-associated or pathogen-associated molecular patterns (DAMPs or PAMPs), which are recognized by a limited number of germline-encoded PRRs present on the surface of innate immune cells (100).

Neutrophils, monocytes, and macrophages are phagocytic cells that confer immune protection by engulfing cells expressing non-self-antigens or altered self-antigens and killing them with their lysosomal enzymes (92). Eosinophils, basophils, and mast cells contribute to the cellular innate immunity by recruiting more immune cells to the inflammation/injured site (93). NK cells enable host protection inducing apoptosis of

General introduction

cell with abnormal or altered major histocompatibility complex (MHC) class I expression, by secreting perforin and granzyme (101).

Another mechanism by which the innate immunity promotes host protection is through the complement activation (93). Upon activation, these complement proteins function in opsonization, act as chemoattractant for other immune cells, and mediate cell/pathogen death after the formation of the membrane attack complex (MAC), which promotes lysis of cells and microorganisms (102).

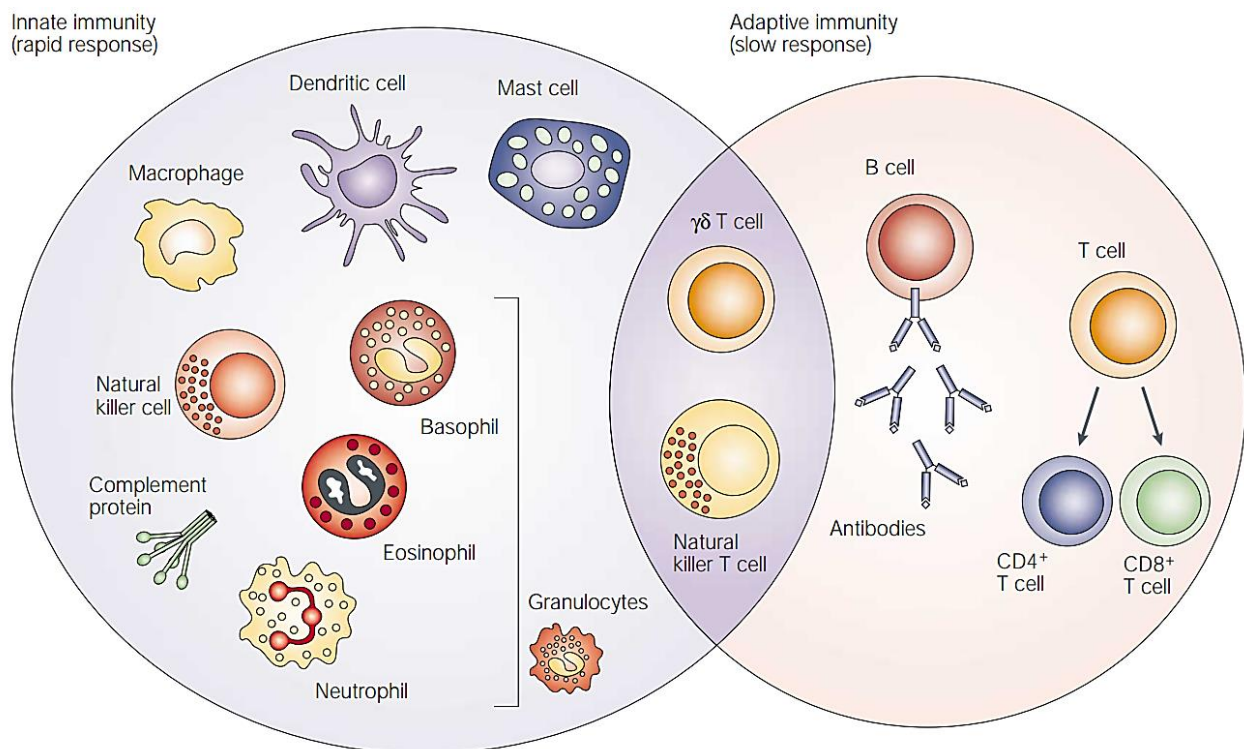


Figure 2. The innate and adaptive immune response. The innate immune response functions as the first line of defence against infection. It consists of soluble factors, such as complement proteins, and diverse cellular components including granulocytes (basophils, eosinophils and neutrophils), mast cells, monocytes/macrophages, dendritic cells and natural killer cells (NK). The adaptive immune response is slower to develop, but manifests as increased antigenic specificity and memory. It consists of antibodies, B-cells, and CD4⁺ and CD8⁺ T lymphocytes. NKT cells and $\gamma\delta$ T-cells are cytotoxic lymphocytes that straddle the interface of innate and adaptive immunity. From Dranoff G. (2004) *Nat Rev Cancer* 4(1):11.

Failure of the innate immune system to eliminate an invading pathogen leads to the activation of the adaptive immune system. The adaptive immune response is mediated primarily by T and B lymphocytes, which display specific receptors that can be tailored to recognize an extensive range of molecules, called antigens (99). The adaptive

immune responses may take 3–7 days upon first exposure to a new pathogen, as they depend on the generation of a diversity of antigen receptors on T and B lymphocytes, as well as on the specific clonal proliferation of antigen-specific B and T effector cells (110). Contrarily to the innate immune system, the adaptive immune system can form immunological memory resulting in a rapid specific response upon reinfection with the same pathogen.

Principal cells involved in adaptive immunity include T and B-cells, as well as DCs.

B-cells can differentiate into plasma cells that secrete antibodies when become activated, which in turn may bring about their effect against pathogens through a number of different mechanisms, including neutralization (direct binding to pathogen), opsonization (binding of pathogen to facilitate phagocytosis), precipitation (binding pathogens into a formation), and complement activation (93, 99).

T-cells can further differentiate into two other subsets: CD4⁺ T-cells and CD8⁺ T-cells. CD4⁺ T-cells act as helper cells and mediate the activation of B-cells, macrophage function and maturation of other T-cells. Depending on the cytokine milieu, naïve CD4⁺ T-cells can further be differentiated into different subsets, such as T helper (Th) cells (e.g. Th1 and Th2 cells), and regulatory T-cells (Tregs), which are characterised by different cytokine profiles (103). Each CD4⁺ T-cell subset has its own specific role in the immune system: Th1 cells secrete interferon (IFN)- γ and support antiviral and anti-tumour responses and autoimmunity; Th2 cells secrete interleukin (IL)-4 and IL-13 and mediate host defence against extracellular parasites and allergic diseases, and may hamper the anti-tumour response; and Tregs play a critical role in maintaining immune homeostasis (104). Tregs suppress the development of other T-cells, limit the immune response and help to maintain immunologic tolerance. Frequently, Tregs are attributed to tumour immune escape, which will be further discuss in section 2.2. CD8⁺ T-cells can generate cytotoxic T lymphocytes (CTLs) upon activation, which are able to directly eliminate virus-infected or tumour cells through the release of perforin and granzymes.

Natural killer T (NKT) cells and $\gamma\delta$ T-cells are also involved in the adaptive immunity and are considered as CTLs that function at the intersection of innate and adaptive immunity (105).

The initiation and control of adaptive immune responses depends on DCs. Along with macrophages and B lymphocytes, DCs are described as antigen-presenting cells (APCs), and more precisely, as the most powerful “professional” APCs (99, 106). First described by Steinman and Cohn in 1973, DCs are present in the majority of mammalian tissues and are organized in an intricate network throughout the human lymphatic and non-lymphatic tissues (107). DCs act as sentinels, constantly sampling their environment

General introduction

through pinocytosis, micropinocytosis, and receptor-mediated uptake. These receptors, also known as PRRs including toll-like receptors (TLRs) and scavenging receptors direct the nature of the immune response that DCs will trigger. Indeed, ligation of receptors TLR3, TLR4, TLR5, TLR 7, TLR8, TLR9 and TLR11 in human DCs leads to an anti-tumour Th1 immune response, while ligation of TLR1, TLR2 and TLR6 leads to a tolerogenic Th2 immune response (108).

An important aspect of DCs is the existence of different subsets, such as plasmacytoid DCs (pDCs), conventional/classical DCs (cDCs) and monocyte-derived DCs (moDCs), which are defined by specific transcriptional factors (109, 110). Although all subsets descend from the same precursor cells, CD34⁺ hematopoietic stem cells, present in the bone marrow (111), each one is specialized to respond to particular pathogens and to interact with specific subsets of T-cells. This increases the flexibility of the immune system to react properly to a wide range of different pathogens and danger signals (112).

Different processing pathways within DCs can occur upon the recognition of endogenous or exogenous antigens.

Extracellular antigens are generally taken up by immature DCs (iDCs) through endocytosis and cleaved into peptides of 12–25 aminoacids (aa) long within the endosomes and lysosomes. These peptides interact with MHC class II molecules and form an MHC class II-peptide complex, which is transported to the surface of APCs and further interact with the TCR of CD4⁺ T-cells (113). In this situation, cytokine priming by DCs also favours a Th2 profile, consequently inducing a predominant humoral immune response. However exogenous antigens can also be presented as a complex with MHC class I molecules, and thus activating CD8⁺ T-cell-mediated immunity, through the process known as “cross-presentation” or “cross-priming” (114). In this process, exogenous antigens are translocated from endosomal compartments into the cytosol, being further presented through MHC class I molecule to CD8⁺ T-cells (113, 267).

Opposite to exogenous antigens, endogenous antigens are transported from the cell cytoplasm into the endoplasmic reticulum, through the proteasome, where they are degraded into peptides typically 8–11 aa long. These peptide fragments exclusively bind to MHC class I molecules. A stable complex of MHC class I-peptide is expressed on the cell surface of DCs and also other nucleated cells, interacting with the T-cell receptors (TCRs) of CD8⁺ T-cells and inducing the differentiation of CTLs (115). These effector cells can directly kill infected or malignant cells, and also acquire a long-lasting memory phenotype, allowing them to fast respond in a second contact with those antigens, in the case of repeated infections or cancer recurrence (116). However, the presentation of pathogen antigens through MHC class II to CD4⁺ T-cells seems to be central for the

development of an immune response by activating antigen-specific effector cells and recruiting cells involved in the innate immune response (117). In fact, Th1 cells enhance CTL functions through the secretion of cytokines, such as IL-2, IL-12 and IFN- γ , which activate other players of the innate system, as NK cells and macrophages, thereby resulting in higher pathogen or tumour cells elimination (118). In addition, Th2 cells stimulate the secretion of antibodies by B-cells, which additionally activate other phagocytic cells (119). Thus, an immune response against intracellular pathogens or tumour cells requires the involvement of both cellular and humoral immune responses to combat the already established infections or disease.

2.1. Cancer immunoediting

For over a century, the idea that the immune system can control cancer has been a subject of debate. The immune system has three main roles in the prevention of tumours: i) it can protect the host from virus-induced tumours by eliminating or suppressing viral infections; ii) the timely elimination of pathogens and prompt resolution of inflammation can prevent the establishment of an inflammatory environment conducive to tumourigenesis; iii) the immune system can specifically identify and eliminate tumour cells in certain tissues on the basis of their expression of tumour-specific antigens (111). This third process is also known as cancer immunosurveillance, and occurs when the immune system identifies transformed cells that have escaped cell-intrinsic tumour-suppressor mechanisms and eliminates them before they can establish malignancy (112). Although the existence of this process, tumours still have the ability to escape the immune system, which is not only involved in protecting the host against tumour development, but also in promoting tumour growth by sculpting tumour immunogenicity or inhibiting host-protective anti-tumour responses (120). This conflict between the immune system and a developing tumour initiates a process named cancer immunoediting, which is divided in three phases: elimination, equilibrium and escape (**Figure 3**) (120, 121).

The first phase – elimination – represents the original concept of cancer immunosurveillance, in which both innate and adaptive immunities act combined to recognize tumour cells and to destroy them. If the developing tumour is successfully eradicated in this first phase, tumour cells are destroyed, and the immunoediting process ends without progression to the subsequent phases (121, 123).

The second phase – equilibrium – is described as a period of tumour latency. When tumour cells survive the elimination phase, the new derived tumour cells are continuously “edited” by the adaptive immunity. Tumour cell growth is thus controlled,

and immunogenicity is shaped, leading to the tumour dormancy. This phase is believed to be the longest phase of the entire process. It seems to allow cancer cells to reside in patients' body even decades before it restarts to grow and become clinically evident (122).

The third phase – escape – represents the failure of the immune system either to eliminate or to control transformed cells. In this phase some of the tumour cell variants escape the immune system and start growing, mainly due either to a lack of immunological recognition or to the induction of tolerance, which can be triggered by diverse tumour immune escape mechanisms or by the immune suppressive tumour microenvironment (TME) (112, 120, 121, 123).

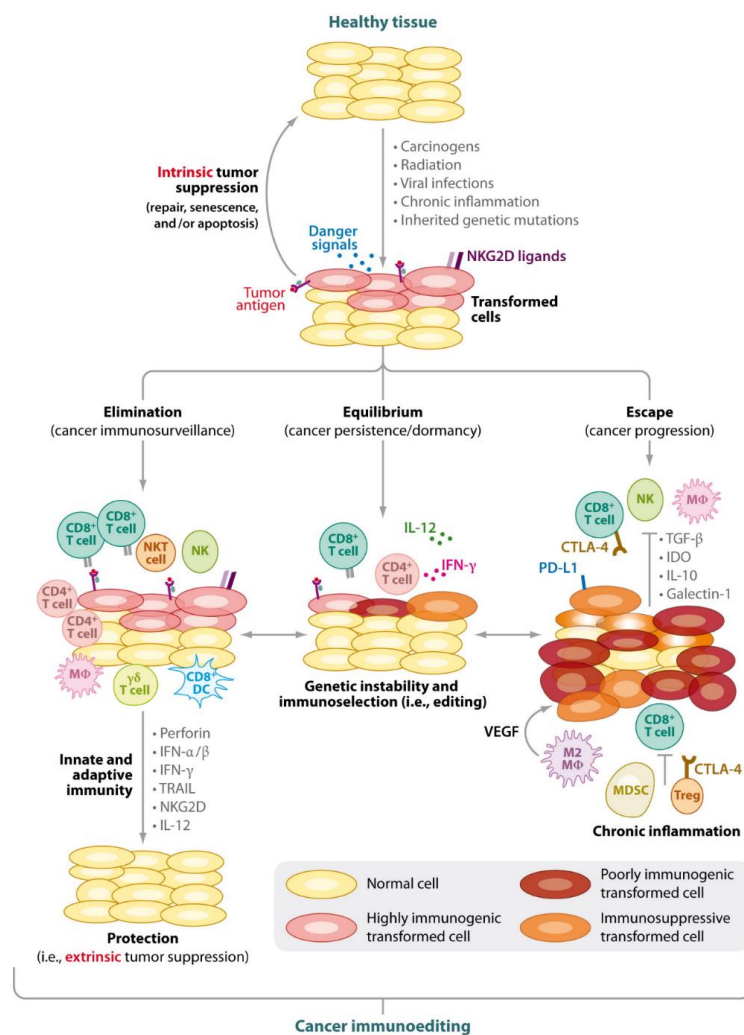


Figure 3. The three phases of cancer immunoediting process. In the elimination phase, tumour cells are recognized by innate and adaptive immune cells and are destroyed before they can become a clinical malignancy. If not destroyed, the tumour enters into the equilibrium phase and suffers genetic changes and/or becomes resistant to immune detection. In the escape phase, the tumour microenvironment becomes immunosuppressive, promoting the tumour development. From Swann JB and Smyth MJ (2007) *J Clin Invest* 117(5):1137-46.

2.2. Tumour microenvironment

The tumour mass consists not only on a heterogeneous population of cancer cells, but also on a variety of resident and infiltrating host cells, secreted factors and extracellular matrix proteins, collectively known as TME. Similarly to other solid tumours, breast TME is a complex network of bidirectional interactions established between a complete set of tumour cells, infiltrating immune cells and stromal cells with vasculature, along the extracellular matrix, which can either eradicate tumours using activated immune effectors or to promote immune evasion that ultimately leads to tumour growth and eventually metastasis, via individual or collective functions, and even shape therapeutic responses and resistance (124, 125).

The stroma plays an essential role in the tumour architecture, providing a physical support for the functions of residing cells (126, 127). Stromal cells, such as endothelial cells (EC), and cancer-associated fibroblasts (CAFs) have been identified as having an active role in breast TME (128). EC play a key role in the development and function of blood and lymph vessels. In the TME, these cells are essential to transport nutrients and oxygen for tumour survival and growth. In addition, the tips of some branched EC may penetrate the vessel lumen creating small intercellular gaps in the wall, which contribute to the metastatic spread (129). CAFs promote tumourigenesis, by aiding in tumour proliferation, vascularization, survival and metastasis. These cells are maintained and activated by growth factors, such as transforming growth factor- β (TGF- β) (130).

The immune system itself is also an important contributor to the suppressive TME. Despite the ability of the immune system to regulate the tumour biology and inhibit tumour development, as referred above, both innate and adaptive immune cells can polarize from their “tumouricidal” form to their “tumourigenic” one within the TME, further influencing the growth, proliferation, and infiltration of other immune cells into the site of injury (131).

The different subtypes of breast cancer have distinct contributions from the microenvironment to undergo malignant progression. Contrarily to the other subtypes, the TME of TNBC present a high infiltration of tumour-infiltrating lymphocytes (TILs), mainly CD8⁺ T, being thus considered as a “hot” tumour (132, 133). However, TNBCs tend also to have a higher average number of Tregs and a higher ratio of Treg/CD8⁺ cells than the other subtypes (134-136). In the TME, T-cells mediate the most important immunological response in tumour growth in the early stages of cancer but change to Tregs after chronic stimulation and interactions with tumour cells, which block anti-tumour responses and promote cancer development and progression (137). Tregs can indirectly hamper CD8⁺ T-cell activation by restraining expansion and immunogenicity of

General introduction

DCs, leading to reduce IFN- γ secretion and poor tumour control. Additionally, surface-bound TGF- β on Tregs also suppresses CTLs effector functions (138).

TME contains other cell types that make the environment suppressive to immune effectors, including M2 macrophages, N2 neutrophils, B-cells, myeloid-derived suppressor cells (MDSCs), and DCs.

Macrophages are the first line of defence against a physiological insult and present high levels of cellular plasticity and diversity, allowing them to exert dual influence of cancer depending on the activation state, with classically activated (M1) and alternatively activated (M2) cells generally exerting anti-tumoural and pro-tumoural functions, respectively (139). M2 macrophages are tumour-associated macrophages (TAMs) that aid in neovasculature formation and subsequently invasion and metastasis. While M1 macrophages typically produce a Th1-type response, M2 macrophages initiate a Th2-type response (140). The polarization toward M2 is mainly mediated by Th2 cytokines, such as IL-4, and anti-inflammatory cytokines, such as IL-10, TGF- β and macrophage colony-stimulating factor (M-CSF) (141). Although TME contains both M1 and M2 phenotypes, TNBCs secrete more granulocyte-colony stimulating factor (G-CSF) than the other breast cancer subtypes, thereby priming M1 cells to promote tumour growth by skewing them to M2 phenotype (142).

Neutrophils are involved in the first line of defence against infections, and like macrophages, these cells can also polarize from their anti-tumour and pro-inflammatory form (N1) to their “tumour-progressive and immunosuppressive” one (N2), within the TME (143). As the tumour progresses, cytokines, predominantly TGF- β and the inflammatory TME skew TANs to become N2-TANs favour tumour progression and metastasis through the release of VEGF to promote angiogenesis, and the expression of arginase 1 to suppress CTL anti-tumoural activity (144). Neutrophils are involved in various stages of tumorigenesis including tumour initiation, proliferation and metastasis (145).

B-cells can also have either tumour-promoting or tumour-suppressive properties, depending on their subtypes. Indeed, studies both in mice and humans have identified discrete subsets of regulatory B-cells (Bregs) that, similar to Tregs, enable cancer cells to escape the immune surveillance, namely by keeping the immune tolerance and suppressing both autoimmune and inflammatory responses, through the release of anti-inflammatory factors, such as TGF- β and IL-10 (146, 147). Moreover, Bregs have been shown to suppress effector T-cells and NK cells by expressing immune checkpoints, such as programmed death ligand-1 (PD-L1) (147). In addition, Bregs have been shown to promote metastasis by converting CD4⁺ T-cells into Tregs, in lung metastasis of breast cancer (148). Recently, Ishigami and collaborators demonstrated that the existence of

Bregs in TIL aggregates in breast cancer patients was closely related to that of Tregs (149).

Similar to Tregs, MDSCs are a heterogeneous population of immature myeloid cells which inhibit innate and adaptive immunity. In breast cancer, MDSCs can cause inhibition of T-cells, NK cells, and DCs, whereas they can be stimulatory to immune regulators such as Th2 cells, Tregs and M2-TAMs (150). Kumar and collaborators showed that blocking MDSCs slow TNBC metastasis (151).

As referred above, the initiation and control of adaptive immune responses against tumours is highly dependent on DCs. However, different studies have shown that DCs are not only involved in immune activation. Depending on the signals present in the TME, mDCs can be subdivided in stimulatory (sDC) and regulatory (rDC) DCs (152). Exposure to pro-inflammatory signals generates sDC, which triggers the stimulation of T-cell proliferation and impairment of Treg function, while tolerogenic signals, such as TGF- β , IL-10 and prostaglandins, generate rDC that suppress T-cell activation and proliferation, and provide signals that enable Treg differentiation and expansion (153).

Although the presence of these cells within the TME contribute to the suppression of both innate and adaptive immune responses, the absence of certain cells can also be crucial to the tumour escape. Indeed, recent findings underline the importance of CD103⁺ cDC1 into the TME (154). cDC1 form a small subset of tissue hematopoietic cells that populate most lymphoid and non-lymphoid tissues, being considered as the most important DC subsets in defeating tumour. In mice, cDC1 can be classified as lymphoid tissue resident CD8 α ⁺ cDC1 and non-lymphoid migratory CD103⁺ cDC1 (155). cDC1 excel at cross-presenting exogenous antigens to CD8⁺ T-cells and are key cells for the generation of CTL responses (156). The importance of cDC1 in anti-tumour immunity has been demonstrated by several studies with cDC1-deficient *Batf3*^{-/-} mice and other *in vivo* models of cDC1 depletion. These studies revealed that cDC1 depletion unable the animals to reject transplantable immunogenic tumours, and tolerate T-cell-based immunotherapies, such as adoptive T-cell therapy or immune checkpoint blockade (154, 157-159). In addition, further studies revealed that the loss of cDC1 cannot be compensated by other DC subsets (160), which highlights the importance of these specific DCs, and specially migratory CD103⁺ cDC1. Indeed, recently, migratory CD103⁺ cDC1 have been pointed as the responsible for the transport of the tumour-associated antigens (TAA) from the tumour to the LNs and as the only cDC population required to induce an effective CTL response against tumours (161). CD103⁺ cDC1 population constitute a small minority within the TME (162). However, gene expression data and flow cytometric analysis have shown that the overall tumour content of CD103⁺ cDC1

positively correlates with cancer patient survival in several cancers (163-165). Of note, NK cells are crucial to stimulate the recruitment of cDC1 into the TME (166).

The release of immunosuppressive cytokines by tumour cells can also contribute to the suppressive TME. The most extensively studied immunosuppressive molecules secreted by tumours are TGF- β , IL-10, and prostaglandin E2.

TGF- β , in particular, is a cytokine that plays a key role in tumour-induced immunosuppression, being considered as the most potent immunosuppressor described to date (167). TGF- β plays important roles in the regulation of various physiological processes, as maintaining tissue homeostasis by controlling the proliferation and interaction with the tissue microenvironment of diverse cell types including epithelial, endothelial, stromal fibroblastic and immune cells (168). TGF- β 1 is the only isoform known to circulate in plasma and the most rapidly induced in response to a variety of environmental stimuli. TGF- β 1 is produced by various cells within the TME including tumour cells, TAMs, DCs and Tregs (169, 170).

In cancer, TGF- β 1 plays a dual and paradoxical role (171, 172). In fact, TGF- β 1 can act as a tumour suppressor or as a promoter of invasion and metastasis depending on the context and the temporal stage of the disease. In early tumours, TGF- β 1 acts as tumour suppressor and limits the cell growth through anti-proliferative and pro-apoptotic actions (173). During tumour progression, cells lose TGF- β 1 suppressive effects resulting in tumour overproduction of TGF- β 1, which becomes an oncogenic factor and induces proliferation, angiogenesis, immunosuppression, invasion and metastasis, affecting all leukocyte populations, as summarized in **Figure 4** (172, 174).

Given the multiple immunosuppressive mechanisms that are engaged to promote tumour survival and growth, it is believed that targeting these suppressive mechanisms may be required to most effectively achieve effector T-cell activation and functionality in the TME.

2.3. Cancer immunotherapy

Due to its genomic instability, high mutational burden, and abundant infiltrating immune cells within the TME (90, 91, 175), TNBC has been considered as a good cancer subtype candidate for immunotherapeutic applications. Indeed, immunotherapy has emerged as a promising new field in TNBC treatment and represents a variety of approaches (176). During the past decades, cancer immunotherapy has evolved from a promising therapeutic option to a robust clinical reality. Diverse immunotherapeutic regimens are now approved by FDA and EMA for use in cancer patients, and many others are being investigated in clinical trials, as single agent or combined with conventional treatments or other targeted agents (177).

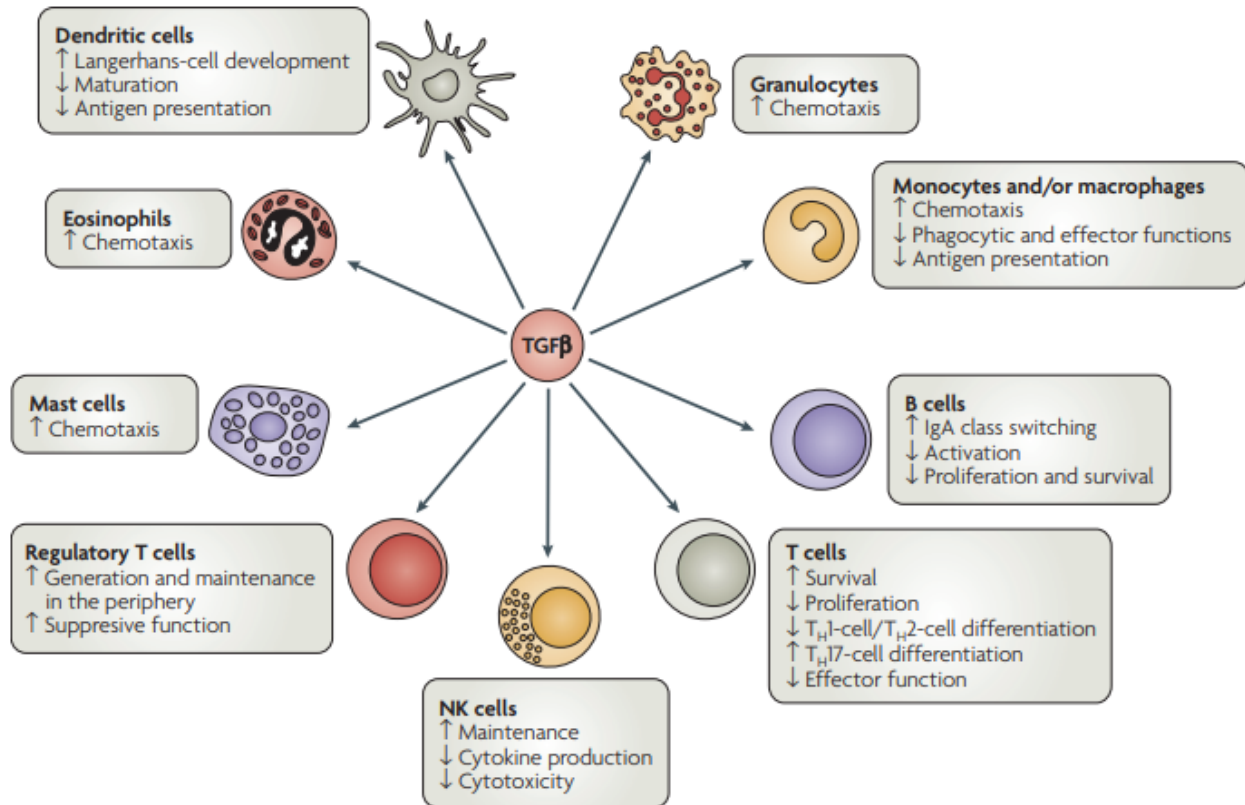


Figure 4. TGF- β signalling affects all populations of leukocytes in a stimulatory or inhibitory manner. Positive or negative effects of transforming growth factor- β (TGF- β) signalling on the indicated aspects of leukocyte biology are marked by arrows pointing up or down. Only cellular processes with a well-documented role for TGF- β are indicated in this figure. NK: natural killer; TH, T helper. From Rubtsov and Rudensky (2007) *Nat Rev Immunol* 7,443–453.

Cancer immunotherapy are related to treatments based on the modulation of the host's immune system so that they can kill their tumours, but also to alert the immune system, by generating memory response, to impede metastasis formation and further spread of the disease (178). The concept of immunotherapy relies on specific immune mechanisms and targets, which could confer greater efficacy and specificity with less toxicity than conventional treatments. Immunotherapies may be subdivided into “passive” and “active” based on their ability to engage the host immune system against cancer.

2.3.1. Immune checkpoint modulation

Immune checkpoints refer to a set of co-stimulatory molecules, such as CD28 and OX40, and co-inhibitory, including cytotoxic T-lymphocyte antigen 4 (CTLA-4), programmed death-1 (PD-1), T-cell immunoglobulin and mucin domain 3 (TIM-3), and LAG-3, involved in the activation of complex pathways that prevent the excessive activity

General introduction

of T-cells under normal conditions, protecting the host from tissue damage during an immune response against a foreign antigen (179, 180). In the presence of a tumour, the expression of immune checkpoint molecules is altered, preventing effector T-cells from mounting an effective anti-tumour immune response. mAb targeted against these molecules can reverse the inhibition of acquired immunity, and, thus contributing to higher survival rates in patients (75).

Immune checkpoint antagonists specific for CTLA-4, PD-1, and its ligand, PD-L1, have revolutionized cancer therapy, inducing durable objective responses, which in some cases translate into an OS benefit in different cancer types (181, 182). CTLA-4 is expressed exclusively on T-cells, where it regulates the amplitude of the early stages of T-cell activation, by counteracting the activity of the T-cell co-stimulatory receptor CD28 (183). Although CTLA-4 is expressed by activated CTLs, its major physiologic role seems to be through distinct effects on the two major subsets of CD4⁺ T-cells, by downmodulating Th cells activity and enhancement of Treg suppressive activity. While blockade of this immune checkpoint molecule results in a broad enhancement of immune responses dependent on Th cells, CTLA-4 engagement on Tregs enhances their suppressive function (184, 185). PD-1 is expressed on the surface of lymphocytes and APCs, while PD-L1 is expressed by tumour cells and immune cells (76). PD-L1/PD-1 pathway is a potent mechanism by which immunogenic tumours evade host immune response. Anti-PD-1 and anti-PD-L1-mAbs disrupt this ligand-receptor interaction, thereby enhancing T-cell immune response (179).

Thus far, several immune checkpoint inhibitors – ipilimumab (anti-CTLA-4), pembrolizumab (anti-PD-1), nivolumab (anti-PD-1), cemiplimab (anti-PD-1), atezolizumab (anti-PD-L1), avelumab (anti-PD-L1), and durvalumab (anti-PD-L1) – have been approved by FDA and EMA for the treatment of several cancer types, including melanoma, NSCLC, glioblastoma, mesothelioma, large-cell lung cancer, cancer, gastroesophageal cancer, primary mediastinal large B-cell lymphoma, cervical cancer, renal cancer, and head and neck cancer (186-191). Earlier this year, atezolizumab in combination with nab-paclitaxel has been approved by FDA and EMA for the treatment of metastatic TNBC whose tumours express PD-L1. This approval was based on findings from the phase III double-blinded IMpassion130 trial (ClinicalTrials.gov identifier: NCT02425891), which involved 902 patients with unresectable locally advanced or metastatic TNBC who had received no prior chemotherapy for metastatic disease. Patients receiving atezolizumab with nab-paclitaxel presented a PFS of 7.4 months (6.6–9.2 months) in the atezolizumab with nab-paclitaxel group vs 4.8 months (3.8–5.5 months) in the control group ($P < 0.0001$). The objective response rate was 53%, including pCR in 9%, vs 33%, with pCR in up to 1% (192).

Many other agents have already exhibited promising data at pre-clinical and clinical levels, for the treatment of this disease (193-196). A multitude of trials using these approved agents, alone or in combination with other conventional or targeted therapies, are currently ongoing in TNBC patients (**Table 2**) (43, 76).

Table 1. Some clinical trials using FDA and EMA approved immune checkpoint agents, alone or in combination with other agents, under investigation in TNBC.

Target	Agent	Phase	Combinatorial agent(s)	ClinicalTrials.gov identifier:
CTLA-4	Ipilimumab	II	-	NCT00083278
PD-1	Pembrolizumab	I	-	NCT01848834
			Doxorubicin hydrochloride	NCT02648477
			Enoblituzumab (anti-B7-H3 mAb)	NCT02475213
			Itacitinib (JAK inhibitor) or INCB050465 (PI3K inhibitor)	NCT02646748
			Modified vaccinia virus Ankara vaccine expressing p53	NCT02432963
			Nab-paclitaxel, doxorubicin, cyclophosphamide, carboplatin	NCT02622074
			Ruxolitinib (JAK inhibitor)	NCT03012230
			Stereotactic ablative body radiosurgery	NCT02303366
		I/II	Epacadostat (IDO inhibitor)	NCT02178722
			Eribulin mesylate	NCT02513472
			Niraparib (PARP inhibitor)	NCT02657889
			Paclitaxel or capecitabine	NCT02734290
			PEGylated doxorubicin	NCT03591276
			PLX3397 (CSF1R)	NCT02452424
		II	-	NCT02447003
			-	NCT02644369
			-	NCT02411656
			Bemcentinib (AXL inhibitor)	NCT03184558
			Carboplatin	NCT03095352
			Carboplatin + gemcitabine	NCT02755272
			Cyclophosphamide	NCT02768701
			Enobosarm (selective AR modulator)	NCT02971761
			Imprime PGG (PAMP)	NCT02981303
			Nab-paclitaxel	NCT02752685
			Nab-paclitaxel, epirubicin, cyclophosphamide	NCT03289819

General introduction

			Paclitaxel	NCT01042379
			Radiotherapy	NCT02730130
			SBRT and ADV/HSV-tk	NCT03004183
	III	-		NCT02555657
			-	NCT02954874
			Nab-paclitaxel or paclitaxel or gemcitabine or carboplatin	NCT02819518
			Carboplatin, paclitaxel, doxorubicin, epirubicin, or cyclophosphamide	NCT03036488
Nivolumab	I		Nab-paclitaxel	NCT02309177
	I/II		Ipilimumab (anti-CTLA-4 mAb)	NCT01928394
			NKTR-214 (CD122) or ipilimumab	NCT02983045
	II		Capecitabine	NCT03487666
			Carboplatin	NCT03414684
			Doxorubicin (low dose) or cyclophosphamide metronomic or radiation therapy or cisplatin	NCT02499367
PD-L1	Atezolizumab	I	-	NCT01375842
			CPI-444 (A2A receptor antagonist)	NCT02655822
			GDC-0919 (IDO inhibitor)	NCT02471846
			RO6870810 (BET inhibitor)	NCT03292172
		I/II	Entinostat (HDAC)	NCT02708680
		II	Carboplatin, paclitaxel	NCT02883062
			Carboplatin and cyclophosphamide or paclitaxel	NCT01898117
			Nab-paclitaxel	NCT02530489
			PEGylated doxorubicin	NCT03164993
			Stereotactic radiosurgery	NCT03483012
			Veliparib	NCT02849496
		III	Nab-paclitaxel	NCT02425891
			Nab-paclitaxel/ carboplatin	NCT02620280
			Nab-paclitaxel, doxorubicin, cyclophosphamide	NCT03197935
			Paclitaxel	NCT03125902
			Paclitaxel, doxorubicin, or cyclophosphamide	NCT03281954
			Paclitaxel, epirubicin, or cyclophosphamide	NCT03498716
Avelumab	II		Utomilumab (CD137)	NCT02554812

	III	-	NCT02926196
Durvalumab	I/II	Nab-paclitaxel + dose dense doxorubicin and cyclophosphamide	NCT02489448
		Olaparib (PARP inhibitor), cedinarib (VEGF inhibitor)	NCT02484404
		Olaparib	NCT02734004
		Paclitaxel	NCT02628132
		Paclitaxel, epirubicin, cyclophosphamide	NCT03356860
	II	Tremelimumab (anti-CTLA-4 mAb)	NCT02536794
		Nab-paclitaxel, epirubicin, cyclophosphamide	NCT02685059
	II/III	Vigil	NCT02725489

Abbreviations: AR: androgen receptor; CTLA-4: cytotoxic T lymphocyte-associated antigen 4; HDAC: histone deacetylase; IDO: indoleamine 2,3-dioxygenase; JAK: Janus kinase; mAb: monoclonal antibody; mTOR: mammalian target of rapamycin; PAMP: pathogen-associated molecular pattern; PARP: poly-ADP ribose polymerase; PD-1: programmed cell death protein 1; PD-L1: programmed death ligand 1; PEG: poly(ethylene glycol); PI3K: Phosphoinositide 3-kinase; VEGFR: vascular endothelial growth factor receptor.

Another immune checkpoint agent that has been targeted in TNBC patients at clinical level, but at lower extent, is OX40. Contrarily to the previous ones, OX40 is a co-stimulatory receptor, belonging to the tumour necrosis factor (TNF) family. OX40 is transiently expressed on activated T-cells, while its ligand, OX40L is expressed on activated APCs, and ECs, but also by activated T-cells (197). Upon ligation of OX40L to its receptor, OX40 induces expansion, trafficking and the survival of effector T-cells, and increases pro-inflammatory cytokine secretion (198, 199). In addition, OX40-signalling can also block the inhibitory activity of tumour-infiltrating Treg by hindering Foxp3, TGF- β and IL-10 signalling (200).

Clinical trials of OX40 agonist antibodies, such as GSK3174998, INCAGN01949, and PF-04518600, which bind specifically to OX40 to activate TIL, are in progress alone or in combination with other immune checkpoint agents such as pembrolizumab and nivolumab (anti-PD-1 mAb), avelumab (anti-PD-L1 mAb), and ipilimumab (anti-CTLA-4 mAb) for different advanced cancer types, including TNBC (ClinicalTrials.gov identifier: NCT02528357, NCT03971409, NCT03241173, NCT02554812).

Despite the promising clinical results, this immune checkpoint therapy has been associated with low percentages of effective and durable responses to single-agent therapies (201-203). For instance, response rates to PD-1 and PD-L1 blockade are very modest as single agent in advanced TNBCs. Although a durable response was obtained in many different early-phase trials, response rates were only up to 10% in unselected

TNBC patients and improved slightly to 20% to 30% when patients are selected based on IHC-based PD-L1-positive tumours (204-207).

Additionally, the use of these drugs in different cancer types has shown serious adverse events related to excessive immune activation. The clinical (systemic) use of anti-CTLA-4 mAb have been associated with severe autoimmune side effects, resulting in inflammation of multiple organs, including the gastrointestinal tract, lung, and endocrine organ (208). The most common adverse effects referred in the literature related to PD-1 and PD-L1 agents are colitis, hepatitis, adrenocorticotrophic hormone insufficiency, hypothyroidism, type 1 diabetes, acute kidney injury, and myocarditis (189). Also, excessive effects of OX40 have been associated with cytokine storm and autoimmunity (197).

In an attempt to improve the benefits of these agents, namely PD-1 or PD-L1 inhibitors, and to overcome their side effects, these drugs may be combined with other immunotherapeutic strategies, namely with cancer vaccines. In a phase I study, Ott *et al.* (2017) combined the anti-PD-1 antibody pembrolizumab with a neoantigen vaccine in melanoma patients (stage IV), showing that the vaccine worked synergistically with the immune checkpoint inhibitor (209). Also Sahin *et al.* (2017) observed this synergistic effect when combined the personalized RNA vaccine with PD-1 blockade therapy (210). More recently, Conniot and collaborators (2019) demonstrated that prophylactic and therapeutic combination regimens of DC-targeted mannosylated nanovaccines with anti-PD-1 antibody and anti-OX40 antibody triggered a synergistic effect that stimulates T-cell infiltration into tumours at early treatment stages of melanoma (211).

2.3.2. Cancer vaccines

Cancer vaccine is another promising strategy for TNBC treatment. This immunotherapeutic regimen has been developed and utilized for over 100 years with variable success, but notably with numerous reports of pCR with regression of all measurable disease in patients with advanced cancers of different types (180). Cancer vaccines have the potential to elicit tumour-specific CTLs and humoral responses, specifically against tumour-specific antigens and TAA. The main goal of vaccination is to induce tumour specific immune responses able to either eliminate the malignant cells or keep it under constant restraint, delaying tumour recurrence and prolonging survival (212).

A number of strategies have been explored for cancer treatment, including vaccination with autologous/allogeneic tumour cells, tumour-associated proteins or peptides, tumour antigen-expressing DNA or viral vectors, DC-based vaccines (124).

These therapeutic approaches offer distinct advantages over conventional therapies, including increased specificity, reduced toxicity and long-term effects via immunologic memory (213, 214). However, as cancer vaccine candidates move towards clinical investigation, it becomes clear that their biological effect depends on their optimal design to ensure their efficient transport across biological barriers and optimum presentation to innate and adaptive immune systems.

2.3.2.1. Essential elements of cancer vaccines

According to Silva *et al.* (2013), an ideal vaccination strategy needs to engage the administration of the most immunogenic TAA together with the most effective adjuvants, including delivery platforms (215). Antigens can be defined as peptides or proteins that are recognized by the immune system and are able to induce an adaptive immune response. Adjuvants are described as molecules that stimulate the innate immune system, acting as “danger signals”. Delivery systems are platforms that insure optimal delivery of single or multiple vaccine antigens and/or adjuvants to DCs in a targeted and prolonged manner (9, 215). These elements are essential for priming tumour-specific T-cells, inducing tumour-specific antibodies and killing tumour cells by host immune effector mechanisms. A large number of studies have shown that antigens and adjuvants must act in a concerted way on the same APC to obtain its full activation, which can be provided by a singular delivery system (216, 217). In many cases, the antigen itself is poorly immunogenic, thus an adjuvant is needed to intensify the immune response (218). In fact, when administered alone, the antigens tend to elicit a Th2-type immune response or even tolerance to the antigen, while when co-administered with adjuvants they tend to induce Th1-type immune response. Therefore, the efficacy of a cancer vaccine formulation can be considerably improved by the development of delivery systems able to protect and modulate the delivery of antigens and adjuvants simultaneously (216).

Antigens

The choice of the appropriate tumour antigens is one of the main issues in cancer vaccine development, since these molecular entities influence the specificity of the immune response (219). Tumour antigens can be proteins, peptides, or even lipids and carbohydrates (220-222). In a general way, the prime targets for cancer vaccines must fulfil the following criteria: i) include peptide sequences that bind to MHC class I, being also important those that bind MHC class II molecules; ii) be processed by DCs and become available for binding to MHC class I molecules; iii) be recognized by the T-cell

repertoire in an MHC class I-restricted manner, and iv) drive the expansion of CTL precursors expressing specific TCRs (215, 223).

Tumour antigens can be divided into two main categories: tumour-specific antigens and TAAs (224, 225). In the first category, antigens are completely unique to the tumour and not found in normal tissue, and include i) specific antigens for certain tumours, such as the melanocyte differentiation antigen Melan A or the prostate-specific antigen (PSA), and ii) cancer testis antigens (CTAs), that are expressed in a variety of tumours, namely the human telomerase reverse transcriptase (hTERT) and the carcinoembryonic antigen (CEA) (225). In the second category, antigens are peptides or proteins inappropriately or aberrantly expressed by tumour cells. These antigens can be mutated and thus unique (β -catenin), overexpressed (α -lactalbumin (α -Lac), mucin 1 (MUC1) and HER2), or germ line antigens that are silent in normal tissue but expressed in cancers (e.g. NY-ESO-1 in melanoma and synovial sarcoma) (124). It is widely accepted that most tumours express TAAs and that the immune system can be triggered to recognize these TAAs as non-self, thereby affecting a specific anti-tumour response (225, 226).

Although no TNBC-specific antigen has been validated, several targets have been identified and tested as a tumour vaccine to produce effective anti-tumour immunity, including α -Lac. α -Lac is a breast-specific self-protein expressed in normal breast tissues exclusively during late pregnancy and lactation, but not in aging females. However, it is also found at high levels in the vast majority, approximately 75%, of TNBCs (227, 228). The stable expression of α -Lac genes was detected in early and late stage TNBC patients. According to Tuohy (2014), in addition to the high expression of α -Lac in TNBC, there are two complementary features of the normal female aging process that together provide a basis for selecting α -Lac as antigen for vaccination against TNBC: i) 95% of breast cancer cases in the USA are diagnosed in women aged 40 and older; ii) less than 3% of children in the USA are born from women 40 years of age and older (229). In sum, most of women older than 40 no longer breastfeed, and their lactation proteins become essentially “retired” at a time in life when risk for developing breast cancer rises rapidly (229). Thus, vaccination against α -Lac would not induce any breast tissue damage since the selected protein would no longer be produced in the “retired” breast tissues. Indeed, Tuohy and collaborators steady-state studies demonstrated that healthy, cancer-free, and adult females can mount abundant pro-inflammatory T-cell responses against α -Lac, independently of the female history of breastfeeding and lactation (229). In addition, they also found that α -Lac prophylactic and therapeutic vaccination consistently inhibited the formation and growth of TNBCs in three different mouse models, commonly used in breast cancer research, such as 4T1 transplantable

tumours in BALB/c mice, with any detectable autoimmune inflammatory damage in any normal tissues examine (227, 230).

Adjuvants

In addition to the antigens, the selection of the appropriate adjuvant(s) in cancer vaccines is also important, since they define the quality and magnitude of the tumour immune response (231). Several clinical studies have already been done with different classes of compounds that present adjuvant activity, among them: mineral salts, emulsions, particulate adjuvants, nucleic acids, small molecules, bacterial products, plant derivatives, saponins and liposomes (232, 233). However, only a few of them have been approved for human use. Failures of adjuvants during the development phase may be related to the manufacturing process (lack of a reproducible formulation or negative impact on antigen stability) and/or to local or systemic adverse effects (234). Note that FDA considers adjuvants as vaccine components, and thus they are not licensed separately (235).

Alum is a mixture of aluminium salts and was the first vaccine adjuvant approved by the FDA and EMA for human use and to be widely used worldwide. Its adjuvanticity was demonstrated in the early 1920s, and since then, it has been incorporated in the majority of the vaccines currently in clinical use, such as diphtheria, tetanus and pertussis (DTaP) vaccines, the pneumococcal conjugate vaccine and the hepatitis B vaccines (232, 236). Alum adjuvants are generally well tolerated and can increase humoral-mediated immune responses against most of the antigens (237). However, alum has some disadvantages, including important side effects and safety concerns (164), also providing poor adjuvanticity for recombinant protein vaccines (238), and contributing little to or even suppressing cell-mediated immunity and subsequent CTL responses (238, 239). In fact, it was reported that vaccination using aluminium salt as an adjuvant only induces Th2 immune responses that are related to humoral immunity, but inhibits cell-mediated immune responses, which are important to eliminate the tumour cells (239).

In addition to alum, only two other adjuvants have been licensed by FDA and EMA for human use: AS03 (240), as a component of the pre-pandemic H5N1 vaccine Prepandrix®; and AS04 (241), as an adjuvant that combines alum and monophosphoryl lipid A (MPLA), used in hepatitis B virus (HBV) (Fendrix®) and human papillomavirus (HPV) (Cervarix®) vaccines (233). In addition, the oil-in-water emulsion MF59 is another adjuvant already approved for human use in Europe, as a component of the Influenza vaccine Fluad® (242). Despite its acceptable safety profile, cases of chills, fever, increased local pain at the site of administration and muscle aches have been occasionally reported (243).

TLR-agonists as adjuvants

The molecular and cellular targets of the human licensed adjuvants described above are not always understood. MPL®, a derivative of the bacterial component lipopolysaccharide (LPS), is probably the most characterized, activating TLR4. Engagement of this receptor promotes cytokine expression, antigen presentation and migration of APCs to the T-cell area of draining LNs, allowing for an efficient priming of naïve T-cells. Other TLR agonists, such as flagellin and polyinosinic-polycytidylic acid (poly(I:C)) induce a similar process and are validated vaccine adjuvants in pre-clinical models (244). Notably, cytosine phosphorothioate-guanine motifs (CpG)-containing oligodeoxy-nucleotides (CpG-ODN), which target TLR9, have also been very efficiently used in humans in a number of vaccine trials (245). These molecules mimic elements exclusively expressed on bacteria, viruses, fungi or protozoa, also known as PAMPs, and activate immune cells via TLRs, acting as TLRs agonists (246). TLRs are the largest and the most extensively studied class of PRRs, playing a crucial role in the induction of innate and adaptive immune responses. TLRs, which are mainly expressed on APCs, but also in T-cells, Treg and NKT cells, are involved in the detection of PAMPs on cell surface, but also intracellularly at endosomal membranes (247, 248). When TLRs expressed on APCs detect PAMPs or synthetic TLRs agonists, intracellular signalling pathways are activated leading to the induction of inflammatory cytokines, chemokines, interferons and upregulation of costimulatory molecules (249).

Delivery systems

Formulation of vaccines as particulate delivery systems represents a promising concept and offers some attractive features when compared with soluble agents (proteins, peptides or nucleic acids) (250), including protection of encapsulated agents that otherwise would suffer fast degradation when administered, but also facilitate co-delivery of antigens and adjuvants to the same APC which could assist in directing the type of immune response desired (94, 250).

The nature and type of the carrier used to deliver TAA and adjuvants should be carefully considered. Several particulate systems have already been used as carriers, namely whole cell vaccines, virosomes, virus-like particles or antigens formulated in particulate-based adjuvants such as liposomes, microparticles (MPs) and nanoparticles (NPs) (251-253). In particular, biodegradable polymeric NPs are being widely explored as carriers for controlled delivery of a multitude of molecules, including proteins, peptides, nucleic acids and oligonucleotides (72, 211, 254). Such NPs have the ability to stabilize vaccine antigens, but also to promote antigen sustained and controlled release to APCs, maximizing their capture, processment and presentation, and consequently

eliminating booster immunizations (253). Moreover, their subcellular size and large surfaces that may present electrostatic or receptor-interacting properties have been shown to contribute to a better interaction with APCs, comparing with soluble antigen alone (254, 255). Apart from this, these nanoscale compounds are biocompatible with tissue and cells, stable in blood, non-toxic, non-immunogenic, non-inflammatory, do not activate neutrophils, and avoid the mononuclear phagocyte system (MPS) preventing premature phagocytosis by macrophages (256).

The most commonly used biodegradable polymers for the formulation of nanoparticulate delivery systems are based on aliphatic polyesters, such as poly(lactic acid) (PLA), poly(glycolic acid) (PGA), and their copolymer poly(lactic-co-glycolic acid) (PLGA) (254). Their application in controlled release is essentially due to their high biodegradability, low toxicity, excellent biocompatibility and bioabsorbability *in vivo* (257), as it will be deeply discuss in section 3.

2.3.2.2. Applications in TNBC

Cancer vaccines may be developed as a prophylactic tool to prevent future development of cancer or as a therapeutic approach to boost the immune system to eliminate the tumour. Currently, only three prophylactic cancer vaccines have been approved by FDA: Fendrix®, Cervarix® and Gardasil®. The first one prevents the infection with HBV, while the other two prevent the infection with HPV (258). The HBV and HPV are believed to be the leading causes of liver cancer (259), and cervical cancer (260), respectively. Regarding therapeutic cancer vaccines, only one has been approved by FDA for human use. This vaccine, called Provenge® (Sipuleucel-T), is a patient-specific vaccine produced by transiently incubating the patient's own peripheral blood mononuclear cells with a fusion protein consisting of prostatic acid phosphatase (PAP; a prostate cancer-specific antigen) linked to the DC growth and differentiation factor granulocyte macrophage colony-stimulating factor (GM-CSF) (261, 262). Provenge® therapeutic intent is to generate PAP-specific T-cells capable of recognizing and killing prostate cancer cells that express this antigen (261). This tumour vaccine induced a 4-month OS benefit when compared to the control group, although the absence of objective tumour regressions or effect on time to progression (261).

Although there is no vaccine approved by FDA or EMA for the treatment of TNBC, several ongoing phase I and II clinical trials with therapeutic vaccines are being studied in combination with anticancer drugs and/or immune checkpoint inhibitors (**Table 3**) (263).

Table 2. Example of ongoing clinical studies involving cancer vaccines

Clinical trial	Agent	Combinatorial agent	Phase
NCT03362060	PVX-410	Pembrolizumab (PD-1)	I
NCT02826434	PVX-410	Durvalumab (PD-L1)	I
NCT03256344	T-VEC	Atezolizumab (PD-L1)	I
NCT03289962	RO7198457	Atezolizumab (PD-L1)	I
NCT01986426	LTX-315	Pembrolizumab (PD-1), ipilimumab (CTLA-4)	I
NCT02432963	p53MVA	Pembrolizumab (PD-1)	I
NCT02779855	T-VEC	Paclitaxel	I/II
NCT03387085	NANT	Aldoxorubicin, avelumab (PD-L1), bevacizumab (VEGF), capecitabine, cisplatin, cyclophosphamide, fluorouracil, nab-paclitaxel	I/II
NCT03328026	SV-BR-1-GM	Pembrolizumab (PD-1), ipilimumab (CTLA-4)	I/II

Abbreviations: CTLA-4, cytotoxic T lymphocyte-associated antigen 4; PD-1, programmed cell death protein 1; PD-L1, programmed death ligand 1; VEGF, vascular endothelial growth factor.

2.3.2.3. Dendritic cells as targets for cancer vaccines

DCs have been proposed as key players in cancer vaccination process, since they can function as a route of entry to the immune system and a way of controlling both innate and adaptive immune responses (264). In the early phase of the antitumour immune response promoted by cancer vaccine, DCs are strategically positioned in peripheral tissues, such as skin and mucosa, in an immature state, acting as sentinels where they sample the environment for foreign antigens (265, 266). Once detected, iDCs internalize the exogenous antigens in vesicular structures through different mechanisms of endocytosis, which can be either a receptor-dependent or receptor-independent mechanism. Receptor-dependent pathways include clathrin-mediated endocytosis, caveolae-mediated endocytosis, lipid-raft-mediated endocytosis and phagocytosis, while, receptor-independent mechanisms encompass fluid-phase endocytosis and micropinocytosis (267). After entry in the cytoplasm, the vesicles carrying extracellular antigens undergo several alterations, until they fuse with lysosomes or MHC class II compartments. There, MHC class II molecules are loaded with peptide antigens, forming an MHC class II-antigen complex, which is then transported to the cell surface, becoming available to be recognized by CD4⁺ T-cells (98, 99). However, exogenous antigens may also be exhibited by MHC class I on DC surface through cross-presentation. This process is extremely important for cancer vaccination, as TAA carried by nano-based

cancer vaccines may escape endosomes and reach the cytosol eliciting the activation of CD8⁺ T-cells, which are fundamental for the successful eradication of tumour cells.

Upon activation, iDCs start converting to mature DCs (mDCs). This transformation is accompanied by a decrease in their capacity to capture antigens, presentation of a higher number of MHC molecules at the surface, change in the expression pattern of chemokine receptors, an upregulation of co-stimulatory molecules (e.g. CD40, CD80, CD86), and secretion of cytokines and chemokines, such as IL-12 and IFN- γ . In addition, it is observed a cytoskeleton reorganization and morphological changes including the proliferation of dendrites from the membrane of these phagocytic cells (101, 102). After antigen internalization, DCs migrate to LNs in a chemokine-driven manner, where they can prime naïve T-cells (268, 269). Activated DC express CCR7, a LN-homing chemokine receptor, thereby entering lymphatic vessels towards LNs, where CCR7-ligands – CCL19 and CCL21 – are expressed (270). Once there, naïve T-cells recognize the antigens associated to MHC molecules at the surface of mDCs, through their TCRs, initiating the adaptive immunity. For T-cells to be effectively activated by DCs, three signals are required. Firstly, they need to recognize the processed antigen in the context of MHC class I (for CD8⁺ T-cells) or MHC class II (for CD4⁺ T-cells). Each T-cell carries a unique TCR and only those cells that recognize the antigens presented by DCs in the form of an MHC/antigen complex will become activated. Secondly, and referred above, DCs also upregulate other cell surface molecules during maturation, such as MHC class I and II, and costimulatory molecules, such as CD40, the receptor for CD40L expressed by naïve T-cells, and also CD80 and CD86 (B7-1 and B7-2 in humans, respectively), which are the ligands for the immunoglobulin superfamily member CD28, also expressed by naïve T-cells. Thirdly, T-cells need cytokines and chemokines, such as IL-12 and type I IFNs, which are produced by DCs and directly affect T-cells in a paracrine fashion (74, 271). After these three signals, T-cells become activated and start their proliferation and differentiation in both memory T-cells and effector T-cells (109, 272).

Several studies have already demonstrated the ability of the immune system to impact on tumour growth in several manners. It is thought that the most effective way of eradicating tumour cells *in vivo* is through the combined action of CD8⁺ T-cells and Th1 CD4⁺ T-cells (215, 273) (**Figure 5**). CD8⁺ T-cells can generate CTLs upon activation, which are able to directly eliminate tumour cells through the release of perforin and granzymes, but also acquire a long-lasting memory phenotype that allow them to promptly respond in the case of a second contact with the same antigens, like it happens in recurrent cancers (116). Th1 CD4⁺ T-cells, through the secretion of IFN- γ , improve the action of CTLs by enhancing clonal expansion at the tumour site and promoting the

General introduction

generation and maintenance of the memory phenotype (274). Moreover, IFN- γ released may also sensitize other components of the antigen-processing machinery, promoting the recruitment of cells from the innate immune system, such as NK cells, that also contribute to tumour cell lysis (94).

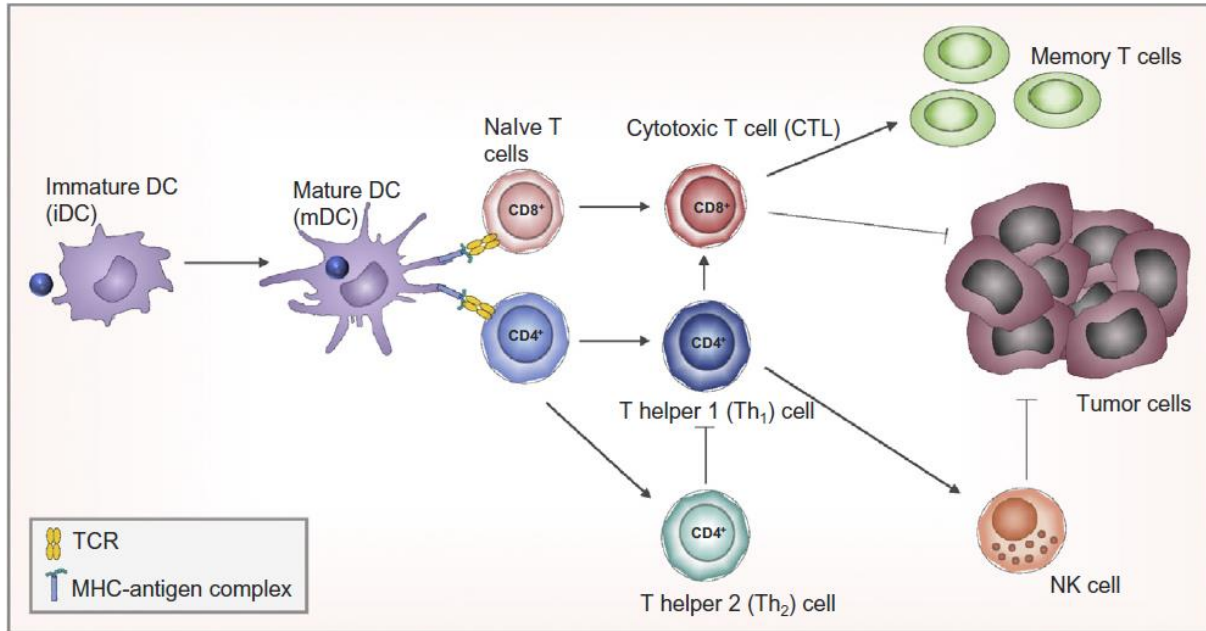


Figure 5. Desired immune response elicited by a therapeutic cancer vaccine. From Matos *et al.* (2019). *J Control Release* 307: 108-138.

3. Nanodelivery systems for DC-based vaccines

In the past decade, nanotechnology has gained significant importance for the diagnosis, prevention and treatment of a wide range of diseases. This technology makes use of materials in the nanometre scale similar to that of functional components of living cells or biological molecules (275). Nanotechnology has been explored for several applications, particularly to cancer (96, 276), gene therapy (277), regenerative medicine (278), drug delivery (279), imaging (280), and biosensors (281), which are broadly labelled “nanomedicines”. These sophisticated nanosystems have been applied for the efficient targeting of pathological sites, including the co-delivery of imaging agents and drugs, biomolecules or genes, combining diagnosis and therapy within a singular nanoplatform (282). The great impact of the successful application of nanotechnology in medicine accelerated the discovery and the design of new nanoscale systems with different compositions. Several nanosystems have been reported as potential carriers of bioactive molecules in cancer therapy, as reviewed elsewhere (215, 283-287). These nanocarriers can be formulated using different materials, such as polymers, lipids and metal or inorganic compounds. Nowadays, the most common developed nanotechnology platforms can range from micelles, liposomes, dendrimers, gold, magnetic or polymeric NPs to quantum dots (288), which are schematically represented in **Figure 6**.

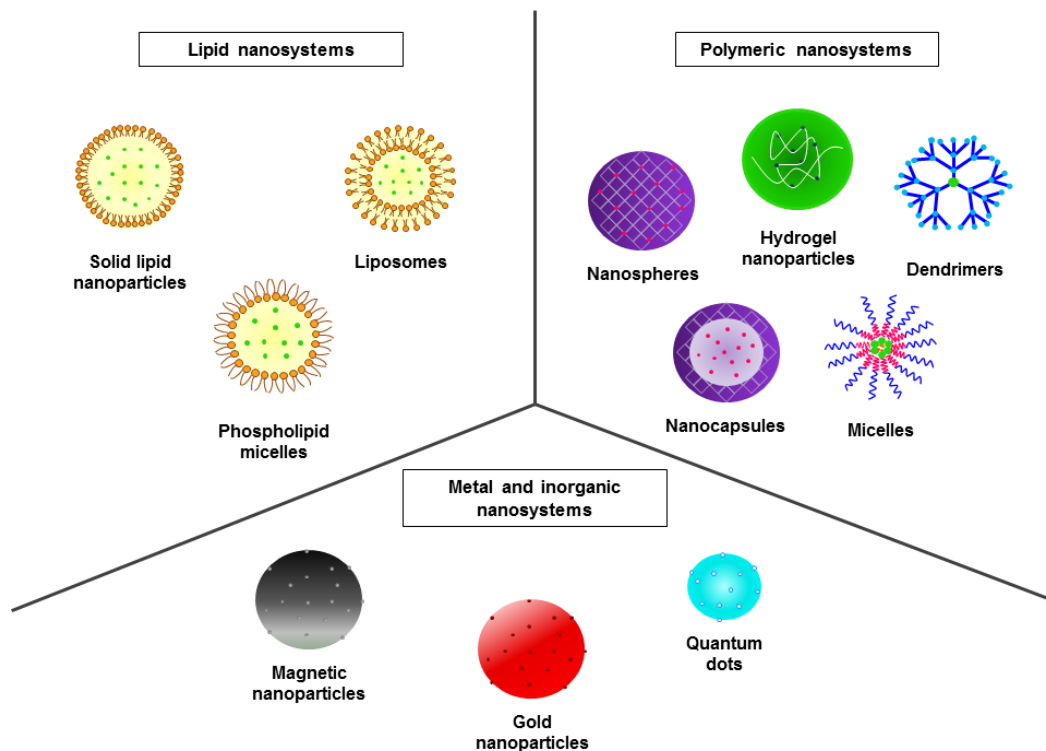


Figure 6. Schematic representation of polymeric, lipid, metal and inorganic nanocarriers. From Peres *et al.* (2017) *Acta Biomater* 15;48:41-57.

3.1. Polymeric nanoparticles

Polymeric NPs are submicron-sized colloidal systems of natural or synthetic polymers, ranging from 10 to 1000 nm, frequently used as delivery carriers of several drugs, proteins, peptides and nucleic acids, due to their high bioavailability, controlled release, biodegradable and biocompatible properties, and low toxic profile (253, 289).

Many polymers may be used to produce micro and nanodelivery systems, from aliphatic polyesters, to poly(amino acids), or even polysaccharides. PLA, PGA, PLGA, poly(methyl methacrylate) (PMMA), poly(ϵ -caprolactone) (PCL) and chitosan (Cs) are components of medicines already approved by FDA and EMA for the sustained delivery of several agents like drugs, biomolecules, and genes, via different routes of administration (287, 289). Different preparation methods have been widely explored for the preparation of polymeric NPs, being the most common the solvent evaporation, salting out, nanoprecipitation and emulsion-based formulation procedures (290). Varying the preparation method, two types of polymeric NPs can be obtained with different release properties: nanospheres and nanocapsules. Nanospheres are matrix spherical systems, which have the active agent physically and homogeneously, incorporated into the matrix system, while nanocapsules are vesicular systems containing the agent inside a cavity surrounded by a polymeric layer (291).

Polymeric NPs have had the best progress on the development of procedures for the entrapment of various bioactive molecules. Polymeric NPs are usually highly stable and have high entrapment and/or adsorption capacity, reducing the number of doses in vaccine administration (292). In fact, the antigens can be dispersed within polymeric matrix, entrapped in the core of the nanocapsule, or adsorbed onto NP surface. The nature of antigen association to polymeric carrier has been shown to have an important effect on the induction of an effective and long-lasting immune response (288).

Unlike lipid NPs, polymeric NPs can easily incorporate both hydrophilic and hydrophobic biomolecules (293). In lipid NPs, hydrophilic antigens are difficult to entrap, leading to a low entrapment efficiency and fast leakage. Also, liposomes have shown poor storage stability when compared to biodegradable polymeric NPs (294, 295). On the other hand, even though the formulation process of polymeric NPs might be considered less expensive than liposome formulation, its translation into the clinic has been challenging due to multiple reasons. Among them, the diversity of new materials, the presence of residual organic solvents, low yield, high burst and incomplete release, uncontrolled effect of NP physicochemical properties *in vivo*, difficult sterilization of the final product and variability on particle size and shape between batches (296). To date, there are about 20 PLA/PLGA-based products approved by FDA and EMA for clinical

use, but not a single nanoparticulate carrier based on these polyesters has reached the market (297). However, it is believed that by increasing the implementation of process analytical technologies (PAT), it will be possible to foster the on-line/at-line control of NP major attributes, clarifying the effect of critical points during the manufacturing process (298). In addition, the application of these “quality-by-design” concepts and the implementation of novel pharmaceutical development regulations, mostly by the USA, Europe and Japan, are expected to improve the clinical translation of these polymeric nanosystems (299).

3.1.1. Polymeric NPs as nanodelivery systems for vaccines

Polymeric nanocarriers have demonstrated the required features for developing new vaccine tools able to overcome the main hurdles related to traditional vaccines, namely safety standards and low immunogenicity, triggering the activation of the adaptive immune system (300, 301). In fact, the administration of proteins or peptides in solution has presented real pitfalls due to their limited bioavailability, short half-life *in vivo* and non-diffusion across some biological barriers. Moreover, the rapid degradation and elimination of soluble antigens dictates the need for repeated injections to attain effective levels (42, 302). To overcome these concerns, entrapped biomolecules are protected from premature enzymatic degradation (i.e., nucleases and proteases) and from the contact with unfavourable *in vivo* biological environment, being their release to intra- or extracellular compartments controlled by erosion of NP matrix (293, 303). Moreover, the maintenance of the integrity and activity of entrapped antigens favours their bioavailability and consequent ability to induce effective immune responses (304).

These nano-based systems are also able to deliver simultaneously antigens and specific adjuvants (e.g. TLRs ligands) in the same carrier. This has been shown to be essential to alert the immune system, but also enables lower doses of those immune modulating compounds, and thus limiting their toxicity (305). These nanocarriers modulate the antigen release, being a sustainable source of retained antigens by providing a continuous, prolonged and sustained delivery for a long period to APCs (depot effect), avoiding the need for several boosting administrations and the risk of tolerance (306). The continuous stimulation of effector T-cells can indeed lead to their exhaustion, and consequently to T-cell anergy. Even though, the targeted delivery of carrier contents, both immune modulators and antigens, to specific cells allow the use of low doses of cargo, minimizing the risk of a continuous stimulation of adaptive immune cells (307, 308).

3.1.1.1. Influence of NP properties in cellular uptake by dendritic cells

Several physicochemical properties, as size, morphology, surface charge, hydrophobicity and receptor interactions have been shown to influence the uptake of the nanocarrier by DCs.

Size

Size is a critical parameter that dictates the fate of nanomaterials within the body. It has a crucial impact on the recognition and capture of delivery systems by cells from MPS, thus dictating their biodistribution and payload bioavailability. However, the ideal size for particle uptake by APCs is still under discussion (304, 309). Several studies have demonstrated that larger carriers (> 500 nm) stay physically imprisoned in the skin and are efficiently internalized via phagocytosis by APC, predominantly by monocytes and skin iDC at the dermis, epidermis and to a lesser extent at the subcutis, being subsequently drained to the LN within 18-24 h (310). However, a faster pathway and independent on cell transport is attained by smaller nanovaccines (< 100 nm), which travel directly into the lymphatic drainage by interstitial flow reaching lymphoid organs to interact with LN-resident DCs, within 2–3 h after administration (310, 311). Although the rapid LN targeting by smaller NP, a compromise between NP size and retention in LN must be attained to maximize LN trafficking and retention, since larger-sized NP are retained more efficiently into LN and very small NP can bypass them (312).

DCs have demonstrated preference to take up smaller particles, as viral-sized particles (20–200 nm), whereas larger carriers (> 500 nm), as those within bacterial size range, are preferentially ingested by macrophages (313). However, iDCs can also internalize larger particles by either micropinocytosis or phagocytosis, while smaller particles are mainly taken up by receptor-mediated endocytosis (314). Generally, small-sized particles can be taken up via clathrin-dependent endocytosis (size < 200 nm) (315), or via caveolae-mediated endocytosis (size range 50–100 nm) (316).

NP size may also dictate the type of immune response. Indeed, NP with size equivalent to viruses, are usually able to initiate virus-like immune responses, with activation of CTL and Th1, while larger particles normally generate a similar immune response to those induced by bacteria, with Th2 activation and antibody production (317).

In addition, nanosized particles ranged 100–500 nm are able to cross efficiently some physiological barriers, such as blood brain barrier, tight epithelial junctions of the skin, intestinal tract and pulmonary system path, in a very efficient manner (291),

endorsing a stronger immunostimulation by promoting the antigen delivery to both peripheral and LN-resident iDC (318).

Morphology

NP morphology may influence cellular uptake and biodistribution. Non-spherical particles have been highlighted because of their increased blood circulation time, due to reduced phagocytosis by unspecific cells. However, the cellular uptake of those particles is decreased, when compared to spherical NPs. According to Gratton *et al.*, rod-shaped NPs show the highest uptake performance, followed by spheres, cylinders and finally cubical NP (319). This differential cellular uptake was also observed by Herd and collaborators who showed that spherical NPs appear to have greater degree of internalisation, when compared to worm-like NPs (320).

Surface charge and hydrophobicity

Surface characteristics of nanocarriers play an important role regarding their association with cells and their biodistribution and overall circulation time. The presence of charge influences the opsonization of nanomaterials, their capture by cells of the MPS, or their accumulation at tumour sites via the enhanced permeability and retention (EPR) effect (321). Positively charged NPs are known to have a higher internalisation rate than the negatively or neutrally charged ones, apparently, as a result of the ionic interactions established between positively charged polymers and negatively charged cell membranes (322, 323). In addition, it is well documented the more prominent aggregation of cationic particles with serum blood proteins, which is particularly important to predict the overall toxicity of those nanoparticulate systems when administered through the intravenous route due to the complement activation, and consequent hypersensitivity reaction (324). Also, particle aggregation may promote their sedimentation and diffusion, which has been shown *in vitro* to have a profound effect on the rate of particle uptake (325)

Coating particles with hydrophilic polymers, such as poly(ethylene glycol) (PEG) to neutralize the surface charge or make them more hydrophilic, may slow down the process of plasma protein adsorption, opsonization and non-specific uptake. The use of PEGylated nanocarriers has resulted in lower uptake by the MPS and increased circulation half-life, allowing for a prolonged retention and interaction with their targets, thus enhancing the intracellular delivery of targeted nanocarriers (326). However, PEGylation may hinder intracellular uptake and endosomal escape, resulting in a so-called "PEG dilemma" (327). In addition, the role of neutral charge on the internalization of nanomaterials by specific routes is still unclear (328).

3.1.1.2. Polylactic acid-based particulate systems for vaccine delivery

Aliphatic polyesters such as PLA, PGA, PLGA, PCL, and PMMA have been reported as potential biomaterials for the production of delivery systems for bioactive macromolecules, including peptides and proteins (286, 288). Among them, PLA has been one of the most well-studied for NP production. PLA is a linear aliphatic polyester composed by lactic acid building blocks (**Figure 7**), which are naturally occurring organic acids easily derived from renewable resources, such as sugarcane and corn starch (329, 330).

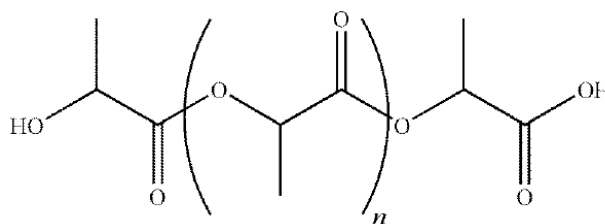


Figure 7. Schematic representation of PLA chemical structure

PLA is the most explored renewable polyester for numerous medical applications (331). PLA-based products have been approved by FDA and EMA for biodegradable packing and multiple biomedical applications, such as degradable surgical sutures, scaffolds for tissue regeneration, bone implants, bone screws and controlled delivery systems of anticancer drugs, peptides, proteins, but also vaccines (329, 330, 332, 333). PLA approval was based on its unique features of biodegradability, biocompatibility and bioabsorbability (329, 333). *In vivo*, PLA is hydrolysed into α -hydroxy acid, which is a byproduct of different metabolic pathways in the body under normal physiological conditions and is easily metabolized in the body via the Krebs cycle, being thus physiologically eliminated (334).

Different techniques have been explored for the development of PLA NP-based vaccines, including the conventional emulsion-based procedures, nanoprecipitation, supercritical fluids, dialysis, spray drying and, more recently, microfluidic techniques (297). Several studies have shown the application of PLA-based vaccines for the *in vivo* control of bacteria, including *Chlamydia trachomatis* (335-339), *Salmonella typhi* (340), and *Streptococcus equi* (341-343), among others as reviewed elsewhere (288). After internalization by DCs, PLA carriers entrapping/adsorbing bacterial antigens were able to trigger mucosal, cellular and humoral systemic immune responses *in vivo*, inducing high antibody (e.g. IgG and IgA) and cytokine (e.g. IL-2 and IFN- γ) titres. It has also been shown that the addition of adjuvants, such as alum or CpG, and/or PEG onto/into PLA MPs or NPs may improve their immunoadjuvant effect (305, 344). All of these studies

evidenced that the entrapment/adsorption of the bacterial antigens in PLA particles induced stronger immune responses than antigens and/or adjuvants in solution.

Recombinant or synthetic proteins/peptides of viral pathogens entrapped or adsorbed onto PLA particles have also been extensively used as advanced vaccines for the treatment of infections caused by HBV (345-350), HIV (351-359), and HPV (360), as reviewed (288). PLA MPs and NPs containing viral antigens and/or adjuvants induced potent cellular and humoral immune responses locally and at distant sites, *in vivo* and *ex vivo*. Indeed, PLA-based vaccines induced strong antigen-specific CD8⁺ T-cells/CTLs and Th1 responses, and high cytokine and antibody (IgG, IgA and IgM) titres. Contrarily to alum in solution, PLA particles do not induced inflammation. However, the incorporation of this adjuvant in these particulate vaccines seems to enhance the overall immune responses.

In addition to bacterial and viral antigens, PLA particles have also been studied as potential vaccine delivery systems for the prevention of malaria, eliciting strong and sustained proliferative responses and induced specific isotype/subclass antibodies (361).

Apart from their application for the prevention of infectious diseases, PLA-based vaccines are also holding great promise in tumour immunotherapy, an absolutely emerging alternative therapeutic approach against cancer that takes advantage of host immune system to specifically destroy malignant cells, thus avoiding off-target effects commonly induced by anti-tumour conventional therapies (362). However, their application in the induction of cytotoxic immune responses against cancer diseases has not been extensively reported.

Dominguez and Lustgarten prepared their cancer vaccine by covalently conjugating antibodies against RNEU, a TAA, and against CD40, a surface marker expressed by DCs, to PLA NPs. The particles trafficked to RNEU⁺ tumours and then attracted DCs into proximity of the tumour with the anti-CD40 antibodies. This PLA NP-based cancer vaccine induced an antitumour response that led to the complete tumour elimination and generation of protective memory responses. In addition, PLA NPs specifically activated an antitumour response against RNEU⁺ tumours, but not against RNEU⁻ tumours, which demonstrated the high specificity of this vaccine. Furthermore, PLA NPs allowed a reduction in the number of Tregs within the tumour and the activation of a specific cytotoxic response (363).

Egilmez and collaborators also developed a cancer vaccine based on PLA particles and tested its efficacy *in vivo*. MPs containing recombinant human PEG-IL-2, murine IL-12 or murine GM-CSF were prepared by phase inversion nanoencapsulation method, allowing high entrapment efficiency of these biologically active molecules.

General introduction

Unlike IL-2- or GM-CSF-loaded MPs, the intratumoural injection of PEG-IL-12-loaded PLA MPs have shown to induce the regression of established tumours, preventing spontaneous metastasis and promoting the development of tumour-specific immunity (364).

Despite the limited literature focused on PLA carriers for cancer vaccination, data obtained for the modulation of immune cells against infection support their promising use to increase antigen recognition and tailor its processing within target DCs. However, it is important not only to understand the effect of these polymeric carriers in the signalling pathways of these target cells, particularly those related to MHC molecules, but also to correlate particulate properties with immune-tumour cells crosstalk within TME. By correlating biological effect with particle physicochemical properties, it will be possible to rational design effective cancer vaccines towards a prolonged and specific cytotoxic immune response. In addition, a better characterization of the events involved in the interaction of NP with immune cells at molecular level can also guide the identification of the best combination treatments towards a synergistic overall anti-tumour effect.

CHAPTER II

Chapter II - Materials and Methods

This chapter is adapted from the unpublished original manuscript:

Multifunctional nanovaccine synergizes with immune checkpoint therapy against triple-negative breast cancer

Carina Peres^{a,b}, Ana I. Matos^a, Liane I. F. Moura^a, João Conniot^a, Bárbara Carreira^a, Afonso P. Basto^b, Marta Afonso^a, Ana S. Viana^c, Liana C. Silva^a, Cecília Rodrigues^a, Véronique Prémat^d, Luís Graça^b, Ronit Satchi-Fainaro^e, Helena F Florindo^a.

^a Research Institute for Medicines (iMed.U LISBOA), Faculty of Pharmacy, Universidade de Lisboa, Lisbon, Portugal;

^b Instituto de Medicina Molecular, Faculdade de Medicina da Universidade de Lisboa, Av. Prof. Egas Moniz, 1649-028 Lisboa, Portugal;

^c Center of Chemistry and Biochemistry, Faculty of Sciences, University of Lisbon, Lisbon, Portugal, Portugal;

^d Louvain Drug Research Institute, Advanced Drug Delivery & Biomaterials, Université Catholique de Louvain, 1200 Brussels, Belgium;

^e Department of Physiology and Pharmacology, Sackler Faculty of Medicine, Tel Aviv University, Tel Aviv, Israel.

(To be submitted for publication)

Chapter II - Materials and Methods

1. Materials

Poly(L-lactic acid) (PLA) with an average molecular weight (Mw) of 1,600-2,400 kDa was purchased from Polysciences Europe GmbH (Hirschberg an der Bergstrasse, Germany). Chitosan glutamate (GlutCs; Protasan UP G113) and chitosan hydrochloride (HCCs; Protasan UP C113) were purchased from NovaMatrix (Sandvika, Norway). Glycol chitosan (GCs), dichloromethane (DCM), sodium chloride (NaCl), α -lactalbumin (α -Lac) Type I from bovine milk, albumin from chicken egg white (OVA), fluorescamine, poly(vinyl alcohol) (PVA, Mw 13,000-23,000 Da), Pluronic® F-127 (PF127), hyaluronic acid (HA) sodium salt from *Streptococcus equi*, ethidium bromide solution, sodium dodecyl sulfate (SDS), N,N,N',N'-tetramethylethylenediamine (TEMED), ammonium persulfate (APS), protein marker wide range (SigmaMarker™: 6,500-200,000 Da), Fluoromount™ Aqueous Mounting Medium, Lipopolysaccharides (LPS) from *Salmonella typhosa*, bovine serum albumin (BSA) and monoclonal Anti- β -Actin antibody (A5541) were purchased from Sigma-Aldrich (Darmstadt, Germany). Cytosine phosphorothioate-guanine motifs (CpG)-oligodeoxynucleotides (ODN) 1826 (TCCATGACGTTCCCTGACGTT) was purchased from Microsynth GmbH (Balgach, Switzerland). Polyinosinic:polycytidylic acid (Poly(I:C)) (High Molecular Weight) VacchiGrade™ was purchased from Invivogen (Toulouse, France). Small interfering RNA (siRNA) anti-transforming growth factor (TGF)- β 1 (siTGF- β 1; Sense: GGGCUACCAUGCCAACUUCtt) and siRNA negative control (Silencer™ Negative Control No. 1 siRNA), phosphate buffered saline (PBS, pH 7.4), Quant-iT™ PicoGreen™ double-stranded DNA (dsDNA) Assay Kit, Quant-iT™ OliGreen™ single-stranded DNA (ssDNA) Assay Kit, RPMI 1640 Medium with no phenol red, minimum essential medium (MEM) α (nucleosides, no ascorbic acid), heat inactivated fetal bovine serum (FBS), penicillin/streptomycin (PEST; Penicillin 10,000 U/mL and - Streptomycin 10,000 mg/mL), sodium pyruvate (100 mM), Dulbecco's Modified Eagle Medium (DMEM; high glucose, pyruvate), RPMI 1640 + Glutamax™, 4-(2-hydroxyethyl)-1-piperazineethanesulfonic acid (HEPES) buffer (1 M), L-glutamine (200 mM), Minimum Essential Medium (MEM) non-essential amino acids (NEAA), β -mercaptoethanol (50 mM), trypsin-ethylenediamine tetraacetic acid (EDTA) 1x, AlamarBlue® cell viability reagent, CountBright™ Absolute Counting Beads, LIVE/DEAD™ Fixable Yellow Dead Cell Stain Kit (for 405 nm), wheat germ agglutinin (WGA)-Alexa Fluor™ 488 conjugate, Hoechst 33342, ammonium-chloride-potassium (ACK) lysing buffer, power SYBR green PCR master mix, halt protease, phosphatase inhibitor cocktail and super signal substrate

Materials and Methods

were purchased from Thermo Fisher Scientific (Bremen, Germany). Acrylamide/bisacrilamide, Mw marker for SDS-polyacrylamide gel electrophoresis (Precision Plus Protein™ standards, All Blue, 10,000-250,000 Da), Bio-Rad protein assay kit and secondary antibody conjugated with horseradish peroxidase were purchased from Bio-Rad (Hemel Hemstead, UK). Agarose, Tris-acetate-EDTA (TAE) buffer, loading buffer, sucrose, sodium phosphate, NaCl, Tris- hydrochloric acid (HCl), triton X-100, paraformaldehyde (PFA), and Ribozol™ reagent were purchased from VWR Scientific (Philadelphia, PA, USA). Recombinant Murine granulocyte macrophage colony-stimulating factor (GM-CSF) was purchased from PeproTech (Kölbe, Germany). Programmed death-1 receptor (PD-1, clone: RMP1-14) and OX40 (clone: OX-86) monoclonal antibodies (mAb) were purchased from Bio X Cell (West Lebanon, NH, USA). Ibrutinib was purchased from Selleckchem (Houston, TX, USA). Fluorochrome-labelled antibodies, Inside Stain kit, FcR blocking reagent, Anti-PE-conjugated magnetic microbeads and LS columns were purchased from Miltenyi Biotec (Miltenyi Biotec, Bergisch Gladbach, Germany). Collagenase type II, dispase and DNase were purchased from Worthington Biochemical Corp. (Freehold, NJ, USA). Rabbit polyclonal antibodies against TGF-β1 (ab92486) was purchased from Abcam (Cambridge, UK). Tumour-associated peptide MHC1-restricted gp100:209-217(IMDQVPFSV) was purchased to GeneCust (Dudelange, Luxembourg). Peptide–major histocompatibility complex (MHC) tetramer tagged with PE (H-2Kb-restricted SIINFEKL PE-labelled Class I Tetramer) was obtained from NIH Tetramer Facility (Emory, Atlanta, USA). Cyanine5 (Cy5)-carboxylic acid was purchased from Lumiprobe GmbH (Hannover, Germany). Rhodamine-6G derivative was synthesized as described elsewhere (365). Cyanine 5 carboxylic acid-grafted PLGA (PLGA-Cy5) was synthesized by esterification based on Freichels et al (366).

2. Methods

2.1. Preparation of nanovaccines

2.1.1. Preparation of chitosan-siRNA polyplexes

Water-soluble chitosan derivative – glycol chitosan (GCs), glutamate chitosan (GlutCs) or hydrochloride chitosan (HCCs) - was first dissolved in acetate buffer (0.1 M sodium acetate/0.1 M acetic acid, pH 4.5), while siRNA was resuspended in RNase-free water (60 µM). Chitosan-siRNA polyplexes were formed by adding the chitosan solution drop-wise to an equal volume of the siRNA solution (5:1 or 15:1 (m/m) Cs:siRNA ratios) and quickly mixed. This mixture was further incubated at room temperature, under stirring for 1 hour.

2.1.2. Synthesis of multifunctional biodegradable NPs

Poly(L-lactic acid) (PLA) nanoparticles (NPs) were prepared using a modified state of the art double emulsion solvent evaporation (w/o/w) technique (367). Briefly, PLA was dissolved in dichloromethane (DCM) at 50 mg/mL (oil phase). The aqueous phase containing 500 µg of the antigen (model antigen ovalbumin (OVA) or the breast tumour-associated antigen (TAA) α -lactalbumin (α -Lac)) and/or 10 µg of small interfering RNA (siRNA) (against transforming growth factor (TGF)- β 1 or negative control), dissolved or previously complexed with GlutCs, was mixed with an equal volume of 25% (m/v) PVA aqueous solution containing the TLR ligands (85 µg of cytosine phosphorothioate-guanine motifs (CpG)-oligodeoxynucleotides (ODN) 1826 and 170 µg of polyinosinic:polycytidylic acid (Poly(I:C)) (**Table 4**). This aqueous phase was added to the oil phase, while 50 µL of GlutCs in 12.5% (m/v) polyvinyl alcohol (PVA) aqueous solution were used for the synthesis of empty NP. The mixture was emulsified by sonication for 15 seconds at 70 W (Sonicator[®] Ultrasonic processor, Misonix, Inc). Then, 400 µL PVA aqueous solution (5% (m/v)) or 5% (m/v) PVA aqueous solution containing 0.05% (m/v) hyaluronic acid (HA) was added and the second emulsion was formed under the same conditions. This double emulsion was added dropwise into a 0.25% (m/v) PVA aqueous solution or 0.125% (m/v) block co-polymer Pluronic[®] F-127 (PF127) aqueous solution and stirred for 1 hour at room temperature. NP suspension was collected by centrifugation at 22,000 g for 45 minutes at 4 °C (Beckman Coulter Allegra 64R High Speed Centrifuge). NPs were washed twice with ultrapure water, collected by centrifugation and finally resuspended in phosphate-buffered saline (PBS, pH 7.4).

Cy5-grafted poly(lactic-co-glycolide) (PLGA) and rhodamine-6G-grafted PLGA were synthesized as described elsewhere (368). Cy5-labeled or rhodamine-labelled NP were prepared by adding 25 µg Cy5-grafted PLGA or 250 µg Rhodamine-6G-grafted PLGA to the polymer blend.

All solutions were prepared with ultrapure DNase/RNase-Free Distilled Water.

Table 3. Biomolecules co-entrapped in the nanovaccine formulations.

	Antigen	Gene regulator	TLR ligands
NP1	α -lac		
NP1_OVA	OVA	siTGF- β 1	CpG-ODN & Poly(I:C)
NP2	-		

Abbreviations: α -lac: α -lactalbumin; CpG: Cytosine phosphorothioate-guanine motifs; NP: nanoparticle; ODN: Oligodeoxynucleotides; OVA: ovalbumin; Poly(I:C): Polyinosinic:polycytidylic acid; TLR ligands: toll-like receptor ligands; siTGF- β 1: small interfering RNA anti-TGF- β 1.

2.1.3. Gel retardation assay

The ability of chitosan polymers to retard siRNA mobility was determined by 4% (m/v) agarose (low melting point) gel electrophoresis. Two different chitosan to siRNA weight ratios (5:1 and 15:1) were loaded (20 μ L of the sample containing 0.2 μ g of siRNA) in the agarose gel. The 1:6 dilution of loading dye was added to each well and electrophoresis was carried out at a constant voltage of 55 V for 2 hours in Tris-acetate-EDTA (TAE) buffer containing 0.5 μ g/mL ethidium bromide. The siRNA bands were then visualized under a UV transilluminator, at a wavelength of 365 nm.

2.1.4. Physicochemical characterisation of NP

2.1.4.1. Size distribution and ζ potential measurements

NP hydrodynamic mean diameter was measured by Dynamic Light Scattering (DLS) with Malvern Nano ZS (Malvern Instruments, UK). NPs were diluted at 1 mg/mL in PBS (pH 7.4) and determined at 25 °C. Z-average size was determined by cumulative analysis (13-16 measurements), in triplicate. ζ potential of NPs was measured by Laser Doppler Velocimetry (LDV) in combination with Phase Analysis Light Scattering (PALS), using the same equipment. NPs were diluted in at 1 mg/mL in ultrapure water, and electrophoretic mobility was determined at 25 °C with the Helmholtz-von Smoluchowski model, by cumulative analysis (100 measurements), in triplicate.

2.1.4.2. Particle morphology

NP surface morphology was determined using atomic force microscopy (AFM). NPs were diluted at 5 mg/mL in ultrapure water. A drop of sample was placed onto freshly cleaved mica for 15 minutes and dried with pure nitrogen. Samples were analysed in tapping mode in air at room temperature, using a Nanoscope IIIa Multimode Atomic Force Microscope (Digital Instruments, Veeco), and etched silicon tips (ca. 300 kHz), at a scan rate of ca. 1.6 Hz.

2.1.5. NP physical stability assay

Empty NPs were dispersed in PBS (pH 7.4) and maintained at 25 °C and 4 °C. After predetermined periods of time over 3 months, samples were collected and particle size, Pdl, and ζ potential were analysed.

2.1.6. Entrapment efficiency and loading capacity of antigens and immune potentiators

Supernatants collected from NP centrifugations were used for the indirect quantification of entrapped antigens (OVA and α -Lac), siRNA (anti-TGF- β 1 and negative control) and immune potentiators (CpG-ODN and Poly(I:C)). Entrapment efficiency (EE % (m/m), Eq. (1)) and loading capacity (LC μ g/mg, Eq. (2)) were calculated as follows:

$$EE(\%) = \frac{\text{Initial amount of agent} - \text{Amount of agent in the supernatant}}{\text{Initial amount of agent}} \times 100 \quad (\text{Eq. 1})$$

$$LC(\mu\text{g}/\text{mg}) = \frac{\text{Initial amount of agent} - \text{Amount of agent in the supernatant}}{\text{Total amount of polymer}} \quad (\text{Eq. 2})$$

The amount of OVA in the supernatants was evaluated using fluorescamine. The fluorescence intensity was measured at 360 nm excitation and 460 nm emission wavelengths using a microplate reader (FLUOstar Omega, BMG Labtech, Durham, NY, USA).

The amount of α -Lac was determined by high-performance liquid chromatography (HPLC). Chromatographic analyses were performed using a Beckman System Gold: UV-vis detector (Beckman 166), Beckman 126 solvent module and a Midas autosampler. Samples of 20 μ L were injected onto a Shodex PROTEIN KW-803 series (8.0 mm ID x 300 mm, 5 μ m particle size, 300 Å pore size) and eluted with 50 mM sodium phosphate buffer (pH 7.0) and 0.3 M NaCl, at a flow rate of 1 mL/minute with a run time of 20 minutes at room temperature. α -Lac elution was monitored at 220 nm by spectrophotometric analysis. The amount of α -Lac in each sample was calculated using a standard curve generated with known concentrations of the surfactant, which demonstrated to be linear over the range of 0 to 40 μ g/mL of α -Lac, with a correlation coefficient higher than $r^2=0.99$.

Loading of siRNA (siTGF- β 1 and negative control) and Poly(I:C) in NPs was quantified using the Quant-iT™ PicoGreen™ dsDNA Reagent, following manufacturers' instructions. Fluorescence generated by the binding of PicoGreen™ to siRNA or Poly(I:C) was measured using a microplate reader (FLUOstar Omega, BMG Labtech, Durham, NY, USA) at 480 nm excitation and 520 nm emission wavelengths.

The amount of CpG-ODN in the supernatant was determined by the Quant-iT™ OliGreen™ ssDNA Reagent, following manufacturers' instructions. Fluorescence generated was measured using the microplate reader (FLUOstar Omega, BMG Labtech, Durham, NY, USA) at 485 nm excitation and 530 nm emission wavelengths.

2.1.7. Integrity of α -Lac entrapped in NP

After 3 hours at 37 °C under continuous stirring, NP suspensions (20 mg/mL) or α -Lac solution (250 μ g/mL), used as control, were mixed with SDS-containing loading buffer and digested at 95 °C for 20 minutes. Samples at room temperature were loaded onto a 12.5% polyacrylamide gel prepared with an acrylamide:bisacrylamide solution 29:1 at 30% (m/v) (Bio-Rad, UK). Electrophoresis was then performed at a constant voltage of 150 V for 90 minutes using a Bio-Rad 300 power pack (Bio-Rad, Hercules, CA, USA). Mw marker (6,500-200,000 Da) was used as a control. Gels were further stained with Coomassie Blue G 250 0.025% (m/v) to reveal protein bands.

2.1.8. NP antigen release

Alexa Fluor™ 647 OVA conjugate-loaded NPs were prepared as described above and dispersed in RPMI medium 1640, with no phenol red. The final NP suspension (5 mg/mL) was divided by Eppendorf® tubes of 2 mL, two for each time point (0 hours, 6 hours, 24 hours, 72 hours, 1 week, 3 weeks, 4 weeks and 8 weeks) and incubated at 37 °C, under gentle stirring (150 rpm). At each time point, NP suspensions were centrifuged at 22,000g for 20 minutes, at 4 °C. The supernatants were recovered and displayed in a 96 well-plate. A calibration curve was prepared using Alexa Fluor™ 647 OVA solution, with concentrations ranging from 0 to 8 μ g/mL. Fluorescence values were read in a microplate reader (FLUOstar Omega, BMG Labtech, Durham, NY, USA) at 480 nm excitation and 560 nm emission wavelengths.

2.2. Cell line culture conditions

Murine bone marrow dendritic cells (DCs) JAWSII cell line (ATCC® CRL-11904™) were cultured in MEM- α , nucleosides, with no ascorbic acid, supplemented with 10% (v/v) FBS, 1% (v/v) PEST (Penicillin 10,000 U/mL and - Streptomycin 10,000 mg/mL), 1% (v/v) sodium pyruvate (100 mM), and 5 ng/mL GM-CSF Recombinant Mouse Protein, in an incubator at 37 °C equilibrated with 5% CO₂. Murine mammary carcinoma 4T1 cells (ATCC® CRL-2539™) were cultured in DMEM, high glucose with pyruvate, supplemented with 10% (v/v) FBS, and 1% (v/v) PEST (Penicillin 10,000 U/mL and - Streptomycin 10,000 mg/mL), in an incubator at 37 °C equilibrated with 5% CO₂. Highly metastatic B16 melanoma cell line transfected with OVA gene (B16.MO5) was cultured in RPMI 1640 with 10% (v/v) heat-inactivated FBS, 1% (v/v) PEST (Penicillin 10,000 U/mL and - Streptomycin 10,000 mg/mL), 2 mmol/L glutamine, 1% (v/v) sodium pyruvate (100 mM), 25 mM HEPES, and 1% (v/v) non-essential amino acids, in an incubator at 37 °C equilibrated with 5% CO₂.

2.3. Animal studies

Female BALB/c mice (8-12-weeks-old) and female C57BL/6J mice (10-weeks old) were purchased from Charles River (France), and housed in the animal facility of the Faculty of Pharmacy at University of Lisbon. All animal procedures were completed in compliance with Faculty of Pharmacy, University of Lisbon guidelines and protocols were reviewed and approved by the Direção-Geral de Alimentação e Veterinária (DGAV, Portugal). Animals were housed under a 12 hours light, 12 hours dark cycle, with food and water available *ad libitum* and handled in compliance with the National Institutes of Health (NIH) guidelines and the European Union (EU) rules for the care and handling of laboratory animals (Directive 2010\63\EU). Mice body weight change was monitored 3 times a week. Mice were euthanized according to ethical protocol when showing signs of distress or with rapid weight loss (above 10% within a few days or 20% from the initial weight). For tumour-bearing mice, tumour volume was monitored 3-times a week. Animals were also euthanized in case the tumour size exceeded 1000 mm³ or if the tumour was necrotic/ulcerative. Tumour volume (mm³) was determined using a caliper by $d^2 \times D \times 0.5$ where d and D are the shortest and longest diameter in mm, respectively.

2.4. Isolation of murine hematopoietic stem cells from bone marrow and differentiation into BMDC

Immature bone marrow-derived DCs (BMDCs) were generated as described by Inaba *et al.* (1992) (369), with some modifications. Fresh bone marrows flushed from femurs and tibias from female BALB/c mice (8-12-weeks-old, purchased from Charles River, France) were depleted of erythrocytes by ACK lysing buffer for 5 minutes at 37 °C, and cultured for 7 days in RPMI 1640 + GlutamaxTM with 10% (v/v) FBS, 1% (v/v) PEST (Penicillin 10,000 U/mL and - Streptomycin 10,000 mg/mL), 1% (v/v) sodium pyruvate (100 mM), 1% (v/v) HEPES buffer (1 M), 0.1% (v/v) β-mercaptoethanol (50 mM), and 20 ng/mL murine GM-CSF Recombinant Mouse Protein, in an incubator at 37 °C equilibrated with 5% CO₂. On days 3 and 6, plates were gently swirled, and medium replaced. On day 7, loosely and non-adherent cells were harvested for further assays. BMDC purity was assessed by flow cytometric analysis of CD11c-APC monoclonal antibody-surface stained cells (Miltenyi Biotec, Cat.# 130-102-800, mouse, clone: N418, 1:10).

2.5. *In vitro* and *ex vivo* cell viability in the presence of NP

Cell viability of JAWSII DCs and BMDCs was assessed by AlamarBlue[®] assay. Briefly, 1x10⁴ cells were seeded in 96-well plates and incubated overnight, at 37 °C and

5% CO₂. Cells were then treated with different NP concentrations (up to 1 mg/mL) for 48 hours, at 37 °C and 5% CO₂. AlamarBlue® reagent was added at 10% (v/v) and incubated for 4 hours, at 37 °C and 5% CO₂. Fluorescence measurements were performed at excitation wavelength of 570 nm and emission of 600 nm with a FLUOstar Omega microplate reader (BMG Labtech, Ortenberg, Germany). The 0.5% (v/v) triton X-100 solution and PBS were used as negative and positive controls, respectively.

2.6. *In vitro* and *ex vivo* NP internalisation by targeted cells by flow cytometric analysis

Dendritic cells (JAWSII DCs and BMDCs, 3x10⁴ cells/well) or 4T1 breast carcinoma cells (1x10⁴ cells/well) were seeded in 96-well plates and incubated overnight, at 37 °C and 5% CO₂. Cells were then incubated with rhodamine-grafted NP (0.5 mg/mL, 465 nm excitation and 559 nm emission wavelengths) for 3, 12 and 24 hours, at 37 °C and 5% CO₂. Cells were then washed with PBS 1x (pH 7.4) and resuspended in flow cytometry buffer. Non-treated cells and non-labelled NPs were used as negative controls. The individual fluorescence of 10,000 cells was collected for each sample using LSR Fortessa cytometer (BD Biosciences) and analysed with FlowJo software version 7.6.5 (TreeStar, San Carlos, CA).

2.7. *In vitro* NP internalisation by DCs by confocal microscopy

JAWSII DCs (1x10⁵ cells/well) were seeded in 8-well Ibidi® μ -Slide microscopy chambers, previously coated with fibronectin, and incubated with empty Cy5-grafted PLGA/PLA NPs (647 nm excitation and 664 nm emission wavelengths) at 0.5 mg/mL for 3 hours, 12 hours and 24 hours, at 37 °C and 5% CO₂. Cells were then washed with PBS (pH 7.4) and incubated with a solution containing paraformaldehyde (PFA, 4% (m/v)), WGA-Alexa Fluor® 488 Conjugate (5 μ g/mL) for plasma membrane and Golgi apparatus staining (495 nm excitation and 519 nm emission wavelengths), and Hoechst 33342 (2 μ g/mL) for nucleus staining (350 nm excitation and 461 emission wavelengths), for 20 minutes at room temperature and protected from light. JAWSII DCs were then washed three times with PBS (pH 7.4) and after covered with Fluoromount™ Aqueous Mounting Medium. Images were obtained by confocal microscopy (Leica TCS SP8, Solms, Germany) and processed using LAS X software.

2.8. *Ex vivo* analysis of NP effect on DC activation and maturation

Immature BMDCs (1x10⁵ cells/well) were seeded in 96-well plates and incubated overnight, at 37 °C and 5% CO₂. Cells were then incubated with 0.5 mg/mL NP (empty

or entrapping antigen/adjuvants) for 48 hours, at 37 °C and 5% CO₂. After this period, BMDCs were washed with PBS and stained with fluorochrome-labelled antibodies (CD11b-APC-Vio770 (Miltenyi Biotec, Cat.# 130-109-288, mouse, clone: REA592, 1:10), CD11c-APC (Miltenyi Biotec, Cat.# 130-102-493, mouse, clone: N418, 1:10), MHC Class II-VioBlue (Miltenyi Biotec, Cat.# 130-102-145, mouse, clone: M5/114.15.2, 1:10), CD40-VioBright FITC (Miltenyi Biotec, Cat.# 130-105-109, mouse, clone: FGK45.5, 1:10), CD80-PE-Vio770 (Miltenyi Biotec, Cat.# 130-116-462, mouse, clone: REA983, 1:50), CD86-PE (Miltenyi Biotec, Cat.# 130-102-604, mouse, clone: PO3.3, 1:10)), following manufacturers' instructions. Samples were then analysed using a LSR Fortessa (BD Biosciences) and FlowJo software version 7.6.5 (TreeStar, San Carlos, CA). LPS (100 ng/mL), free antigens (25 µg/mL) and free adjuvants (5 µg/mL) were used as controls.

2.9. NP *in vivo* biodistribution

Female BALB/c mice ($N = 3$) were injected subcutaneously with empty Cy5-grafted PLGA/PLA NPs (20 mg/mL) at inguinal site on the left flank, and with PBS (pH 7.4) on the right flank, as negative control. After 24 hours, the animals were sacrificed and analysed by fluorescence using an IVIS Lumina imaging system (Xenogen, CA, USA). Major organs (spleen, kidneys, lymph nodes (LNs), lungs, liver, and heart) were recovered and analysed by fluorescence.

2.10. Intervention combination therapies in triple-negative breast carcinoma

On day 0, female BALB/c mice were orthotopically inoculated in the fourth inguinal mammary fat pad with 50 µL of cell suspension, containing 7×10^5 4T1 breast carcinoma cells (mycoplasma-free) in PBS, as reported by Gregório *et al.* (2016) (370). On day 5 after tumour inoculation, animals were randomized into different groups ($N = 9$ -10) according to **Table 5**. Three different intervention combinational studies with distinct treatment schedules (**Figure 14a, 16a and 18a**) were performed by combining nanovaccines (NP1 + NP2; **Table 4**) with i) αOX40, ii) αOX40 + ibrutinib, and iii) αOX40 + αPD-1.

Treatments such as PBS and cancer vaccine (antigens and immune regulators in solution or entrapped in NPs (NP1)) were injected by hock immunization, via subcutaneous (SC) injection proximal to popliteal and axillary LNs (100 µL). Half dose was injected into the right side and the other half into the left side. Cancer vaccine (antigens and immune regulators in solution or NP1 (23.5 mg/mL)) contained 100 µg of the TAA α-Lac, 2 µg of siTGF-β1 (or siRNA negative control), 20 µg CpG-ODN and 40

Materials and Methods

µg poly(I:C). NP2 were injected directly into the tumour site (IT) (50 µL at 47 mg/mL) and did not contain the TAA. αOX40 and αPD-1 were administered intraperitoneally (IP) at 10 mg/kg. Ibrutinib was also administered IP at 6 mg/kg. On day 19, three mice from each group were sacrificed and the tumour and spleen were isolated aseptically for characterising the tumour-infiltrating immune population (see section 2.10.1) and assessing the antigen-specific nature of the T-cell response (see section 2.10.3), respectively. The remaining animals were maintained for the survival assay. Mice were sacrificed when the tumour size exceeded 1000 mm³.

Table 4. Treatment groups and the respective route(s) of administration in the three combination assays.

	Group	Treatments	Route(s) of administration
1 st Combi. Assay	G1	PBS	SC
	G2	α-Lac + siTGF-β1 + CpG-ODN/Poly(I:C)	SC
	G3	αOX40	IP
	G4	NP1	SC
	G5	NP2	IT
	G6	NP1 + NP2	SC + IT
	G7	NP1 + NP2 (with siRNA negative control)	SC + IT
	G8	NP1 + NP2 + αOX40	SC + IT + IP
2 nd Combi. Assay	G9	Ib	IP
	G10	NP1 + NP2 + αOX40 + Ib	SC + IT + IP + IP
3 rd Combi. Assay	G11	αOX40 + αPD-1	IP
	G12	NP1 + NP2 + αOX40 + αPD-1	SC + IT + IP + IP

Abbreviations: α-Lac: α-lactalbumin; αOX40: monoclonal antibody against OX40 receptor; αPD-1: monoclonal antibody against programmed death-1 receptor; Combi: combination; CpG: Cytosine phosphorothioate-guanine motifs; Ib: Ibrutinib; IP: intraperitoneal; IT: intratumoural; ODN: Oligodeoxynucleotides; PBS: Phosphate-buffered saline; Poly(I:C): Polyinosinic:polycytidylic acid; siTGF-β1: Small interfering RNA anti-TGF-β1; SC: subcutaneous. NP1: NP entrapping α-Lac + siTGF-β1 + CpG-ODN/Poly(I:C); NP2: NP entrapping siTGF-β1 + CpG-ODN/Poly(I:C).

2.10.1. Characterization of tumour-infiltrating immune populations by flow cytometry

Tumours were isolated from three animals per group, directly after euthanasia, and placed in cold sterile PBS (pH 7.4). Tumour single-cell suspensions were obtained by mechanical disruption of the tissues and enzymatic digestion for 1 hour at 37° C. Enzymatic digestion solution was prepared in RPMI medium with 0.5% (m/v) BSA, 0.1% (m/v) collagenase type II, 0.1% (m/v) dispase and DNase. After digestion, the cell

suspension was filtered through a 70 µm filter (BD Biosciences) with cold PBS to remove the debris. The cell suspension was centrifuged at 300 g for 5 minutes at 4° C and washed with cold PBS. The centrifugation was repeated, and the cell pellet was resuspended in cold PBS and seeded in medium in sterile 96-well tissue culture plates (1x10⁶ cells per well). The obtained single-cell suspension was then stained with fluorochrome-labelled antibodies for surface markers, fixed with PFA 3.7%, and stained with fluorochrome-labelled antibodies for intracellular markers (Inside stain kit, Miltenyi Biotec, Germany), following manufacturer's protocols. Cells were analysed using a LSR Fortessa (BD Biosciences) and FlowJo software version 7.6.5 (TreeStar, San Carlos, CA).

Lymphocyte panel: CD3-PerCP-Vio700 (Miltenyi Biotec, Cat.# 130-109-240, mouse, clone: REA606, 1:10), CD8a-PE (Miltenyi Biotec, Cat.# 130-109-247, mouse, clone: REA601, 1:10), CD107b-APC-Vio770 (Miltenyi Biotec, Cat.# 130-106-292, mouse, clone: M3/84, 1:10), CD279 (PD-1)-VioBlue (Miltenyi Biotec, Cat.# 130-102-741, mouse, clone: HA2-7B1, 1:10).

Treg panel: CD3-PerCP-Vio700 (Miltenyi Biotec, Cat.# 130-109-841, mouse, clone: REA641, 1:10), CD4-VioBlue (Miltenyi Biotec, Cat.# 130-110-310, mouse, clone: REA604, 1:10), CD8a-APC-Vio770 (Miltenyi Biotec, Cat.# 130-109-328, mouse, clone: REA601, 1:10), CD25-PE (Miltenyi Biotec, Cat.# 130-109-051, mouse, clone: REA568, 1:10), FoxP3-Vio515 (Miltenyi Biotec, Cat.# 130-109-051, mouse, clone: REA568, 1:10).

Cytokine panel: CD3-PerCP-Vio700 (Miltenyi Biotec, Cat.# 130-109-841, mouse, clone: REA641, 1:10), CD8a-APC-Vio770 (Miltenyi Biotec, Cat.# 130-109-328, mouse, clone: REA601, 1:10), IL-2-PE (Miltenyi Biotec, Cat.# 130-110-154, mouse, clone: REA638,1:10), TNF-α-APC (Miltenyi Biotec, Cat.# 130-109-767, mouse, clone: REA636,1:10), IFN-γ-FITC (Miltenyi Biotec, Cat.# 130-109-768, mouse, clone: REA665,1:10).

DC Panel: CD11c-FITC (Miltenyi Biotec, Cat.# 130-102-800, mouse, clone: N418, 1:10), CD11b-APC-Vio770 (Miltenyi Biotec, Cat.# 130-109-288, mouse, clone: REA592, 1:10), MHC Class II-VioBlue (Miltenyi Biotec, Cat.# 130-102-145, mouse, clone: M5/114.15.2, 1:10), CD8a-APC-Vio770 (Miltenyi Biotec, Cat.# 130-109-328, mouse, clone: REA601, 1:10), CD103-APC (Miltenyi Biotec, Cat.# 130-111-686, mouse, clone: REA789, 1:50), CD24-PerCP-Vio700 (Miltenyi Biotec, Cat.# 130-110-830, mouse, clone: REA743, 1:50).

MDSC Panel: CD11b-APC-Vio770 (Miltenyi Biotec, Cat.# 130-109-288, mouse, clone: REA592, 1:10), Gr-1-APC (Miltenyi Biotec, Cat.# 130-112-307, mouse, clone: REA810, 1:50).

2.10.2. Assessment of TGF- β 1 expression in tumours

Tumours were isolated from three animals of groups 1 and 6 (treated with PBS and NP1+NP2, respectively), directly after euthanasia, to quantify TGF- β 1 expression, at both mRNA and protein levels.

2.10.2.1. Quantitative RT-PCR

Total RNA was extracted from animal tumour samples using the Ribozol™ reagent according to the manufacturer's instructions. Quantitative real-time RT-PCR (qPCR) was performed in the QuantStudio™ 7 Flex Real-Time PCR System (Life Technologies Corp., Carlsbad, CA, USA). The following primer sequences were used: for TGF- β 1 gene 5' CTG CTG ACC CCC ACT GAT AC 3' (forward) and 5' GTG AGC GCT GAA TCG AAA GC 3' (reverse); for the glyceraldehyde-3-phosphate dehydrogenase (GAPDH) gene 5' ATT CAA CGG CAC AGT CAA GG 3' (forward) and 5' TGG ATG CAG GGA TGA TGT TC 3' (reverse). Three independent reactions for each primer set were assessed in a total volume of 5 μ L containing 2x Power SYBR green PCR master mix and 0.6 μ M (each) primer. The relative amount of TGF- β 1 was calculated based on the standard curve and was normalized to the level of GAPDH, being expressed as fold change from PBS controls.

2.10.2.2. Protein extraction and immunoblotting

For isolation of total protein extracts, tumour pieces were homogenised using a motor-driven grinder on ice-cold lysis buffer (10 mM Tris-HCl, pH 7.6, 5 mM MgCl₂, 1.5 mM potassium acetate, 1% Nonidet P-40, 2 mM dithiothreitol) and 1x Halt Protease and Phosphatase Inhibitor Cocktail. The lysate was sonicated at 80% power for 10 seconds and centrifuged at 10,200 g for 10 minutes at 4 °C. The supernatants were recovered and stored at -80 °C. Protein concentrations were determined using the Bio-Rad protein assay kit, according to the manufacturer's specifications. Forty μ g of total protein extracts were separated on an 14% SDS-PAGE. Following electrophoretic transfer onto nitrocellulose membranes and blocking with 5% (m/v) milk solution, blots were incubated overnight at 4 °C with primary rabbit polyclonal antibodies against TGF- β 1 (1:1000), and with a secondary antibody conjugated with horseradish peroxidase diluted 1:5000 in blocking solution, for 2 hours at room temperature. Membranes were processed for protein detection using Super Signal substrate. β -actin (1:40000) was used as housekeeping gene. The relative intensities of protein bands were analysed using the Image Lab densitometric analysis program (version 5.1; Bio-Rad Laboratories, Hercules, CA, USA).

2.10.3. Functional assessment of T-cells

Spleens from animals treated with NP1+NP2 (group 8) were aseptically removed from three animals, 23 days after tumour inoculation, and placed in cold sterile PBS (pH 7.4). Splenocyte suspensions were obtained by mechanical disruption of the tissues and filtered through a 70 µm filter (BD Biosciences) in cold PBS to remove the debris. Suspensions were depleted of erythrocytes by ACK lysing buffer for 5 minutes at 37 °C, and cultured for 5 days in RPMI 1640 + Glutamax™ with 10% (v/v) FBS, 1% (v/v) PEST (Penicillin 10,000 U/mL and - Streptomycin 10,000 mg/mL), 1% (v/v) sodium pyruvate (100 mM), 1% (v/v) HEPES buffer (1 M), 0.1% (v/v) β-mercaptoethanol (50 mM) containing PBS, 100 µg/mL of α-Lac aqueous solution or 100 µg/mL of gp100, in an incubator at 37 °C equilibrated with 5% CO₂. After 5 days, splenocytes were recovered and stained with fluorochrome-labelled antibodies for surface markers, fixed with 3.7% PFA solution, and stained with fluorochrome-labelled antibodies for intracellular markers (Inside stain kit, Miltenyi Biotec, Germany), following manufacturer's protocols. Splenocytes were then analysed using a LSR Fortessa (BD Biosciences) and FlowJo software version 7.6.5 (TreeStar, San Carlos, CA). **Panel:** CD45-VioBlue (Miltenyi Biotec, Cat.# 130-110-663, mouse, clone: REA737, 1:50), CD3-PerCP-Vio700 (Miltenyi Biotec, Cat.# 130-109-841, mouse, clone: REA641, 1:10), CD8a-APC-Vio770 (Miltenyi Biotec, Cat.# 130-109-328, mouse, clone: REA601, 1:10), IL-2-PE (Miltenyi Biotec, Cat.# 130-110-154, mouse, clone: REA638, 1:10), TNF-α-APC (Miltenyi Biotec, Cat.# 130-109-767, mouse, clone: REA636, 1:10), IFN-γ-FITC (Miltenyi Biotec, Cat.# 130-109-768, mouse, clone: REA665, 1:10).

2.11. Intervention combination therapies in B16.MO5 murine model

The efficacy and specificity of the NP vaccine – NP1, using OVA as antigen (NP1_OVA), and NP2, combined with αOX40 was confirmed in a B16.MO5 melanoma murine model.

On day 0, all female C57BL/6J mice were anaesthetized with isoflurane and the right dorsal area was treated with depilatory cream before the subdermal injection of 50 µL of cell suspension, containing 2x10⁵ B16.MO5 melanoma cells (mycoplasma-free) in PBS. On day 10 after tumour inoculation, mice were randomized into one of the following groups (*N* = 5) (**Table 6**) and started to be treated (**Figure 10a**).

Treatments such as PBS and cancer vaccine (either free in solution or entrapped in NP1) were injected by hock immunization, via subcutaneous (SC) injection into inguinal areas, twice (once a week) with 100 µL (**Figure 10a**). Half dose was injected into the right side and the other half into the left side. Cancer vaccine (either free in

Materials and Methods

solution or entrapped in NP1_OVA (23.5 mg/mL) contained 100 µg of OVA, 2 µg of siTGF-β1, 20 µg CpG-ODN and 40 µg poly(I:C). Contrarily to NP1, NP2 were injected directly into the tumour site (IT) (50 µL at 47 mg/mL) and did not contain the antigen. The αOX40 was administered intraperitoneally (IP) at 10 mg/kg, twice (once a week).

Table 5. Treatment groups and the respective route(s) of administration for the functional assessment of T-cell.

Group	Treatments	Route(s) of administration
G1	PBS	SC
G2	OVA + siTGF-β1 + CpG-ODN/Poly(I:C)	SC
G3	αOX40	IP
G4	NP1_OVA + NP2	SC + IT
G5	NP1_OVA + NP2 + αOX40	SC + IT + IP

Abbreviations: αOX40: monoclonal antibody against OX40 receptor; CpG: Cytosine phosphorothioate-guanine motifs; IP: intraperitoneal; IT: intratumoural; ODN: Oligodeoxynucleotides; OVA: ovalbumin; PBS: Phosphate-buffered saline; Poly(I:C): Polyinosinic:polycytidylic acid; siTGF-β1: Small interfering RNA anti-TGF-β1; SC: subcutaneous. NP1: NP entrapping OVA + siTGF-β1 + CpG-ODN/Poly(I:C); NP2: NP entrapping siTGF-β1 + CpG-ODN/Poly(I:C).

2.12. Functional assessment of T-cells

For the assessment of T-cell specificity using tetramer staining, spleens were harvested 7 days after the second injection, homogenized in a single-cell suspension and plated in a 96-well plate for staining. First, the peptide–major histocompatibility complex tetramer tagged with PE (H-2Kb-restricted SIINFEKL PE-labelled Class I Tetramer (NIH Tetramer Facility at Emory, Atlanta, USA) was added to the single-cell suspension, including FcR blocking, following the supplier instructions. After 30 minutes of incubation at 4 °C, the cells were washed to remove unbound tetramers and centrifuged at 1,300 rpm for 10 minutes at 4 °C. Cell population was enriched using anti-PE-conjugated magnetic microbeads and passed over a magnetized column. Cell samples were eluted and centrifuged at 1,300 rpm for 10 min at 4 °C. The cells were resuspended in ice-cold sorter buffer and plated in 96-well plates. After adding a mix of the antibodies (LIVE/DEAD™ -BV605, CD19-APC (Miltenyi Biotec, Cat.# 130-112-036, mouse, clone: REA749, 1:50), CD3-APC-Vio770 (Miltenyi Biotec, Cat.# 130-119-793, mouse, clone: REA641, 1:50) and CD8α-Vio770 (Miltenyi Biotec, Cat.# 130-119-123, mouse, clone: REA601, 1:50), the cells were incubated for 10 minutes at 4 °C, protected from light. Cells were then washed, centrifuged and resuspended in 200 µL of ice-cold sorter buffer to determine the specificity of CD3⁺CD8α⁺ T-cells, by flow cytometry. The

absolute number of OVA-specific T-cells within each sample was determined as described by Moon *et al.* (2009) (371).

2.13. Statistical Methods

Data are presented as mean \pm standard deviation (SD) for *in vitro* and *ex vivo* studies, and as mean \pm standard error of the mean (SEM) for *in vivo* studies. *T*-test, one-way ANOVA followed by Tukey's post-hoc test, or Log-Rank test were performed to demonstrate statistical differences ($P < 0.05$), using the software GraphPad Prism version 6 (GraphPad Software, Inc, CA, USA). * $P < 0.05$; ** $P < 0.01$; *** $P < 0.001$.

CHAPTER III

Chapter III - Results

This chapter is adapted from the unpublished original manuscript:

Multifunctional nanovaccine synergizes with immune checkpoint therapy against triple-negative breast cancer

Carina Peres^{a,b}, Ana I. Matos^a, Liane I. F. Moura^a, João Conniot^a, Bárbara Carreira^a, Afonso P. Basto^b, Marta Afonso^a, Ana S. Viana^c, Liana C. Silva^a, Cecília Rodrigues^a, Véronique Prémat^d, Luís Graça^b, Ronit Satchi-Fainaro^e, Helena F Florindo^a.

^a Research Institute for Medicines (iMed.U LISBOA), Faculty of Pharmacy, Universidade de Lisboa, Lisbon, Portugal;

^b Instituto de Medicina Molecular, Faculdade de Medicina da Universidade de Lisboa, Av. Prof. Egas Moniz, 1649-028 Lisboa, Portugal;

^c Center of Chemistry and Biochemistry, Faculty of Sciences, University of Lisbon, Lisbon, Portugal, Portugal;

^d Louvain Drug Research Institute, Advanced Drug Delivery & Biomaterials, Université Catholique de Louvain, 1200 Brussels, Belgium;

^e Department of Physiology and Pharmacology, Sackler Faculty of Medicine, Tel Aviv University, Tel Aviv, Israel.

(To be submitted for publication)

Chapter III – Results

1. Multifunctional nanoparticles as antigen delivery systems and regulators of TGF- β levels

Three different water-soluble chitosan derivatives - glycol chitosan (GCs), glutamate chitosan (GlutCs) and hydrochloride chitosan (HCCs) - were used at two different chitosan/small interfering RNA (siRNA) ratios to prepare the polymer-siRNA complexes by electrostatic-based interactions. An electrophoretic mobility shift assay (EMSA) was used to determine the optimal chitosan/siRNA ratio, using free siRNA as control. Chitosan/siRNA polyplexes were analysed by electrophoresis on an EMSA to assess the ability of the different water-soluble chitosan derivatives to retard the siRNA mobility on the agarose gel. GlutCs and HCCs were able to form a complex with siRNA with an optimal Cs:siRNA ratio of 15:1, contrarily to GCs (**Figure 8**).

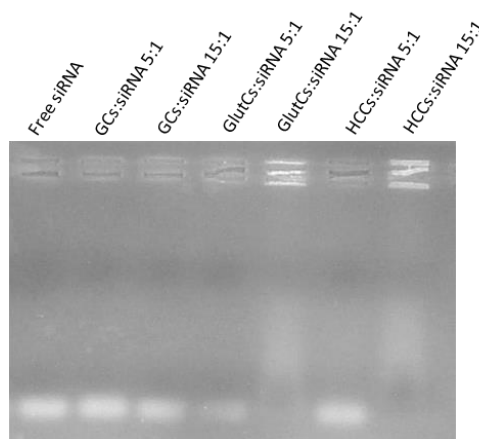


Figure 8. Electrophoretic mobility of chitosan–siRNA polyplexes formed with different chitosan derivatives (glycol chitosan (GCs), glutamate chitosan (GlutCs) and hydro-chloride chitosan (HCCs)) with siTGF- β 1 at two different Cs-siRNA ratios (5:1 and 15:1). Free siRNA was used as control.

Poly(lactic) acid-based nanovaccines were prepared by a modified state of the art double emulsion solvent evaporation technique. Different surface active agents - poly(vinyl alcohol) (PVA) and block co-polymer Pluronic[®] F-127 (PF127), and hydrophilic stabilizers/viscosity enhancers with adjuvant properties (water-soluble chitosan derivatives (GCs, GlutCs and HCCs), and hyaluronic acid (HA)) were used to optimize nanovaccine formulations, in order to achieve a stability suitable for the co-entrapment of bioactive molecules with distinct physico-chemical properties (**Figure 9a**). The size, shape and surface morphology of empty NP were assessed by atomic force microscopy (AFM) (**Figure 9b**). The section analyses of empty NP revealed homogenous spherical

Results

particles with a slightly rough surface, and a diameter close to 180 nm, which correlates with the data measured by dynamic light scattering (DLS) analyser (**Table 6**).

The stability of empty NP in terms of size (mean diameter and Pdl) and surface charge (ZP) was assessed by DLS and doppler velocimetry (LDV), respectively. Empty NPs were resuspended in phosphate-buffered saline (PBS, pH 7.4) and followed for 88 days, at 4 °C and 25 °C. During this period, no significant changes were observed for all three parameters, at both storage conditions (**Figure 9c-e**).

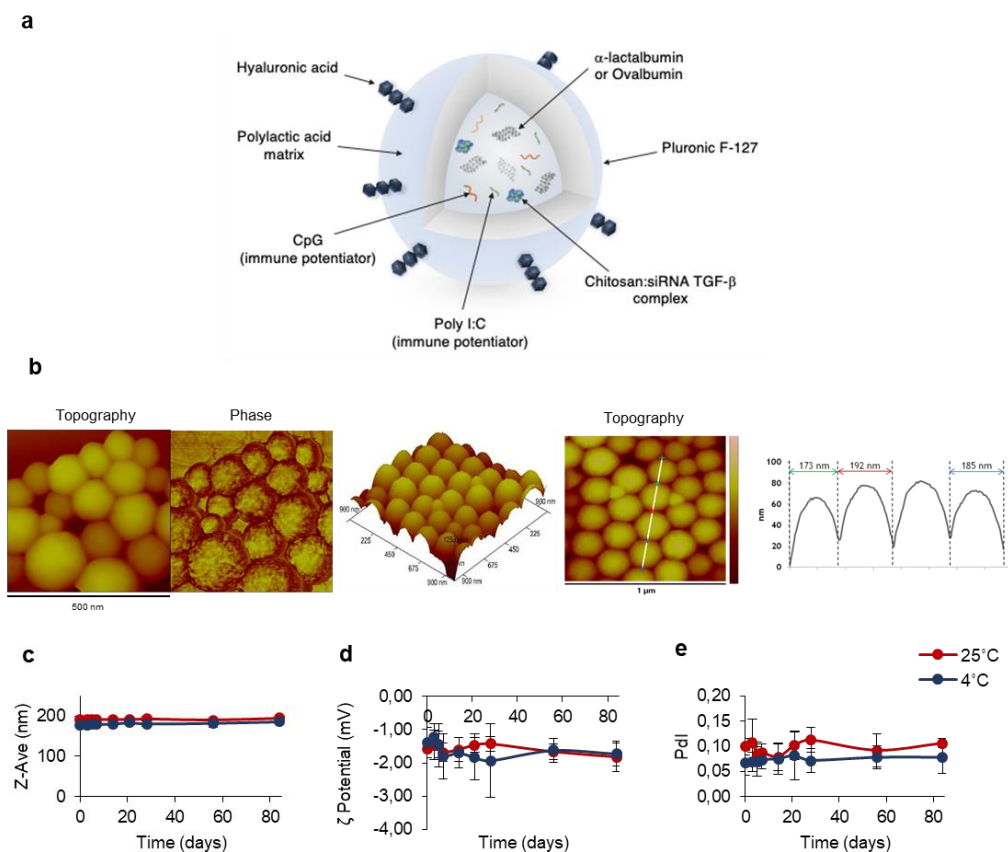


Figure 9. Physical properties of nanoparticles (NPs) and stability. **a**, Schematic representation of nanoparticles (NP). **b**, AFM images of empty NPs showing spherical shape, slight roughness on the surface and a narrow size polydispersity ($N = 3$). **c-e**, Empty NP physicochemical stability in PBS (pH 7.4) at 25 °C ($n = 3$).

Two different NP were synthesised (**Table 4**) according to targeted cells: nanovaccine NP1 to deliver the combination of antigens (α -lactalbumin (α -Lac) or ovalbumin (OVA)), Toll-like receptors (TLR) ligands (CpG-ODN and poly(I:C)) and gene regulator siRNA molecules (siTGF- β 1 or negative control) to DCs; nanovaccine NP2 to deliver the combination of immune potentiators and siRNA to tumour cells, aiming at the modulation of tumour-infiltrating immune cell sub-populations.

Each biomolecule entrapped in the NPs was selected based on their synergistic role: α -Lac as tumour-associated antigen, siTGF- β 1 to silence the expression of this

potent immune suppressor by DCs (NP1) and tumour cells (NP2), and CpG-ODN and Poly(I:C) as agonists of the TLR9 and TLR3, respectively, within DCs and tumour niche.

Empty NP, NP1 and NP2 presented similar average hydrodynamic diameters, ranging from 167 ± 7 nm to 202 ± 8 nm, with a narrow particle size distribution (Pdl, range between 0.09 ± 0.01 and 0.17 ± 0.09) and a near-neutral surface charge (Z-Ave, ranging -4.53 ± 1.43 and -1.08 ± 0.43), depending on the entrapped molecules (**Table 7**). All three parameters (Z-Ave, Pdl and ZP) did not depend on both the surface-active agents (PVA or PF127) and the coating with HA (**Table 7**).

High EE and LC values were obtained for α -Lac into the different NPs, ranging from 88.2 ± 2.1 and 92.1 ± 1.8 for the EE and 44.1 ± 1.1 and 46.1 ± 0.9 for the LC, suggesting that the entrapment of α -Lac into the different NPs was not affected by both the surface-active agents (PVA or PF127) or the HA coating (**Table 7**). The incorporation of the TAA into NP did not change the nanovaccine ability to entrap the other bioactive immune regulatory molecules, including the TLR ligands and the siRNA molecules, since high EE and LC values were obtained for these biomolecules co-entrapped into the nanovaccines (**Table 7**).

The structure of the α -Lac protein (14 kDa) entrapped within NP1 was not affected by the formulation procedure, as a single band can be seen at a molecular weight similar to the one obtained for the α -Lac standard solutions (**Figure 10a**). Alexa Fluor 647®-ovalbumin conjugate was used to assess the release profile of the biomolecules entrapped into the nanovaccine. OVA-Alexa 647® was slowly released from the NPs, being 22% (w/w), 33% (w/w) and 72% (w/w) released after 1, 3 and 4 weeks of incubation, respectively (**Figure 10b**).

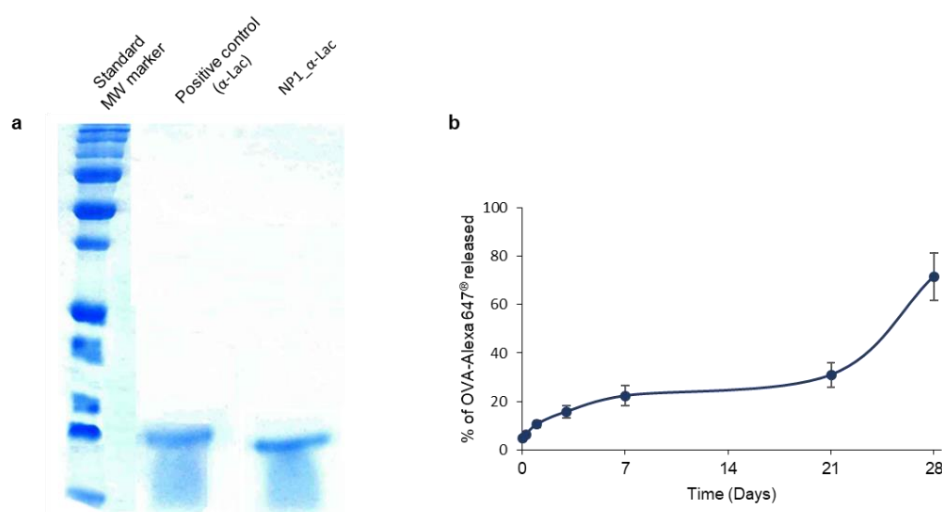


Figure 10. a, SDS-PAGE of α -Lac protein (14 kDa) in solution (positive control) or entrapped into NPs ($n = 3$). **b**, Release profile of OVA-Alexa 647® entrapped in the nanovaccine over 28 days ($N = 3$; $n = 3$).

Results

Table 6. Size, polydispersity index (Pdl), ζ potential, and entrapment efficiency (EE) and loading capacity (LC) of the different biomolecules within nanovaccines.

Nanovaccine				Antigen		siRNA		CpG-ODN		Poly(I:C)	
	Size (nm \pm SD)	Pdl \pm SD	ζ Potential (mV \pm SD)	EE (% \pm SD)	LC (μ g/mg)	EE (% \pm SD)	LC (μ g/mg)	EE (% \pm SD)	LC (μ g/mg)	EE (% \pm SD)	LC (μ g/mg)
NP PVA	166 \pm 1	0.05 \pm 0.02	-5.60 \pm 1.13	-	-	-	-	-	-	-	-
NP PVA + HA	167 \pm 7	0.09 \pm 0.01	-4.21 \pm 1.70	-	-	-	-	-	-	-	-
NP PF127	167 \pm 4	0.08 \pm 0.01	-6.90 \pm 0.96	-	-	-	-	-	-	-	-
NP PF127 + HA	164 \pm 6	0.10 \pm 0.04	-7.16 \pm 0.97	-	-	-	-	-	-	-	-
NP PVA + α -Lac	173 \pm 9	0.10 \pm 0.01	-3.78 \pm 0.57	90.2 \pm 1.3	45.1 \pm 0.7	-	-	-	-	-	-
NP PVA + HA + α -Lac	177 \pm 8	0.08 \pm 0.05	-4.37 \pm 1.77	92.0 \pm 1.5	46.0 \pm 0.8	-	-	-	-	-	-
NP PF127 + α -Lac	195 \pm 9	0.13 \pm 0.05	-4.53 \pm 1.43	92.1 \pm 1.8	46.1 \pm 0.9	-	-	-	-	-	-
NP PF127 + HA + α -Lac	180 \pm 1	0.13 \pm 0.01	-3.05 \pm 0.56	88.2 \pm 2.1	44.1 \pm 1.1	-	-	-	-	-	-
NP1: NP α -Lac + siTGF- β 1	193 \pm 6	0.14 \pm 0.05	-1.08 \pm 0.43	86.2 \pm 10.9	43.1 \pm 5.5	95.1 \pm 1.2	1.0 \pm 0.0	93.0 \pm 0.9	7.9 \pm 0.1	96.4 \pm 1.7	16.4 \pm 0.3
NP1_OVA: NP OVA + siTGF- β 1	199 \pm 4	0.17 \pm 0.09	-2.89 \pm 0.62	81.7 \pm 5.7	40.9 \pm 2.9	92.2 \pm 3.1	0.9 \pm 0.0	93.2 \pm 1.1	7.9 \pm 0.1	96.2 \pm 2.3	16.4 \pm 0.4
NP2: NP siTGF- β 1	202 \pm 8	0.14 \pm 0.01	-1.53 \pm 0.10	-	-	93.9 \pm 2.3	0.9 \pm 0.0	95.1 \pm 0.5	8.1 \pm 0.0	97.1 \pm 2.9	16.5 \pm 0.5

Abbreviations: α -Lac: α -lactalbumin; CpG: Cytosine phosphorothioate-guanine motifs; EE: entrapment efficiency; HA: hyaluronic acid; LC: loading capacity; NP: nanoparticle; ODN: Oligodeoxynucleotides; OVA: ovalbumin; Pdl, polydispersity index; PF127: Pluronic F-127; PVA: polyvinyl alcohol; Poly(I:C): polyinosinic:polycytidylic acid; SD: standard deviation; siTGF- β 1: small interfering RNA anti-TGF- β 1. NP PVA: empty NP prepared with PVA as surfactant; NP PVA + HA: empty NP prepared using PVA as surfactant and HA as stabilizer and immunomodulator; NP PF127: empty NP prepared with PF127 as surfactant and immunoregulator; NP PF127 + HA: empty NP prepared using PF127 as surfactant and immunoregulator, and HA as stabilizer and immunoregulator; NP PVA + α -Lac: NP prepared with PVA entrapping α -Lac. NP PVA + HA + α -Lac: NP prepared with PVA and HA entrapping α -Lac. NP PF127 + α -Lac: NP prepared with PF127 entrapping α -Lac. NP PF127 + HA + α -Lac: NP prepared with PF127 and HA entrapping α -Lac. NP1: NP entrapping α -Lac, the TLR ligands (CpG, Poly (I:C)), and siTGF- β 1; NP1_OVA: NP entrapping OVA, the TLR ligands (CpG, Poly (I:C)), and siTGF- β 1; NP2: NP entrapping the TLR ligands (CpG, Poly (I:C)), and siTGF- β 1. For each formulation, 4 independent batches ($N = 4$) were prepared and measured in triplicate ($n = 3$).

2. Multifunctional nanovaccines activate and improve the maturation of dendritic cells

An AlamarBlue® assay was performed to determine the effect of empty NP on the viability of dendritic cells (DC, murine immature JAWSII cell line and primary murine bone marrow DC (BMDC)) and 4T1 breast tumour cells. Cells were incubated with increasing concentrations (250 to 1000 µg/mL) of the different NPs, for 48 hours. Empty NPs did not affect DC viability (JAWSII (> 94%), BMDC viability (> 80%)) nor 4T1 breast tumour cells (> 91%), in the concentration range tested, independently of their composition, supporting NP safety and physiological biocompatibility (**Figure 11a**).

The internalization pattern of empty NP by immature DCs (JAWSII and BMDC) and 4T1 breast tumour cells was assessed by flow cytometric analysis. DC and tumour cells were incubated with Rho-labelled NP for 3, 12 and 24 hours. The NPs synthesized using PF127 as surfactant and coated with HA were taken up by DCs and breast tumour cells at higher extent ($P = 0.0001$) than the NP containing only HA or PF127 (**Figure 11b**). Therefore, and having in consideration the results above, the NPs synthesised using GlutCs + PF127 + HA were selected for further studies.

Cy5-labelled NP were prepared to assess the internalisation pattern of NP by immature JAWSII DC by confocal microscopy. Z-stacks and maximum projections showed that the optimised empty nanoplatform were effectively internalised by DCs and that the internalisation levels increased with incubation time until 24 hours of incubation, being the highest internalisation extent obtained after 12 hours of incubation (**Figure 11c**). These results corroborated the ones obtained with NP PF127+HA (**Figure 11b**), by flow cytometric analysis.

To assess the ability of NP (empty or entrapping antigen and/or immune regulators) to induce the maturation of primary BMDC, a flow cytometric analysis of the expression of co-stimulatory molecules (CD40, CD80 and CD86) in the CD11b⁺CD11c⁺MHCII⁺ population was performed after 48 hours of incubation. PBS and LPS-treated cells were used as negative and positive controls, respectively. α-Lac, and α-Lac + TLR ligands (CpG-ODN/Poly(I:C)) were also tested. The highest levels for each surface co-stimulatory molecule were obtained for BMDCs treated with NPs entrapping α-Lac and both adjuvants (**Figure 12**).

3. Combination of therapeutic multifunctional nanovaccines with αOX40 immune checkpoint therapy restricts tumour growth and prolongs survival

The Cy5-labeled NP1 remained at the site of injection after the subcutaneous administration of these multifunctional nanocarriers in the left hind ($N = 3$) (**Figure 13a**).

Results

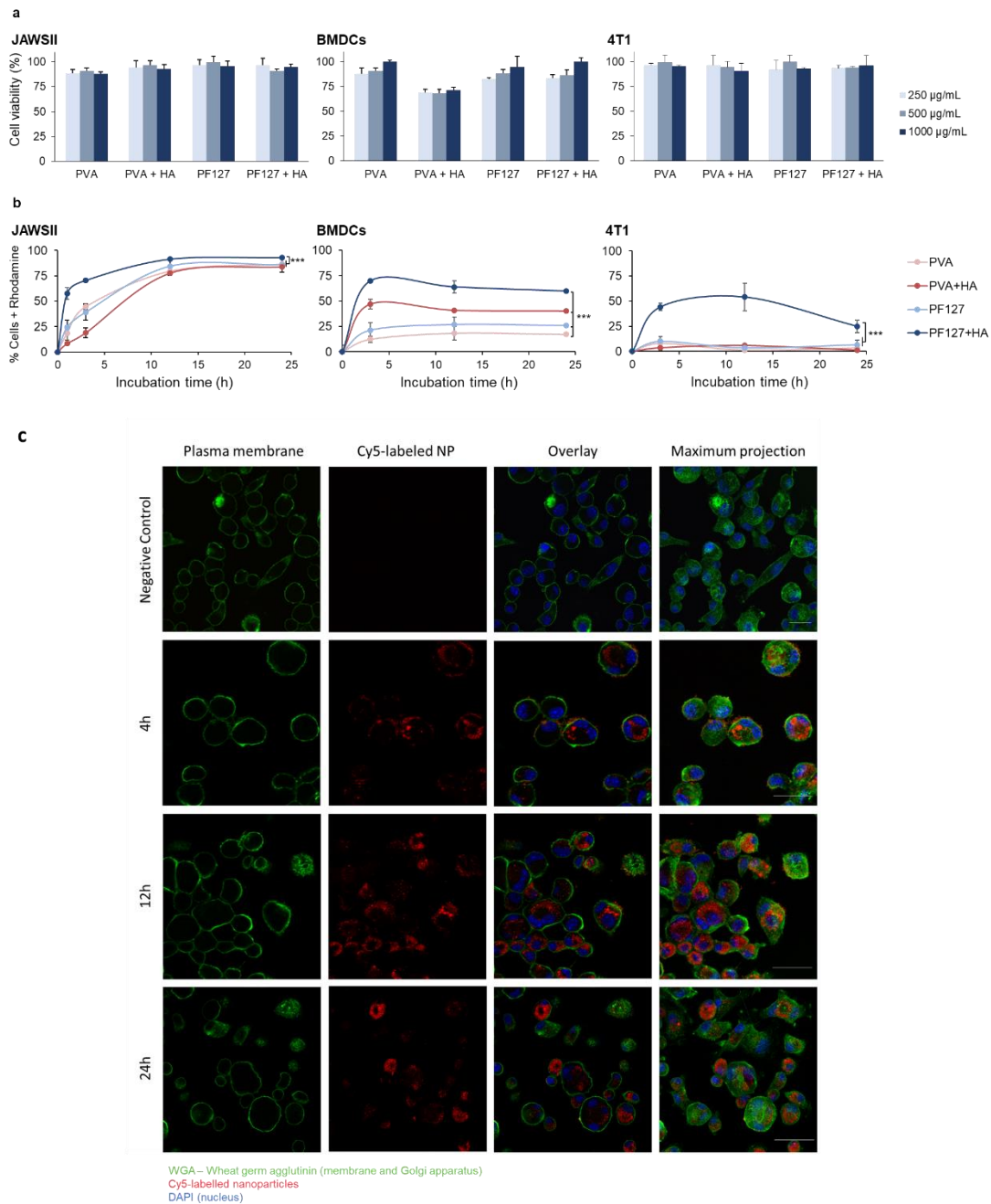


Figure 11. a, Cell viability of DC (JAWSII ATCC[®] CRL-11904[™] and BMDC) and breast tumour cells (4T1 ATCC[®] CRL-2539[™]) after incubation of NPs for 48 hours. Mean \pm SD ($N = 3$ independent experiments, $n = 6$ replicate measurements). **b**, Rho-labelled NP internalisation by murine immature DCs (JAWSII and BMDCs), and by murine 4T1 breast tumour cells, determined by FACS. Non-treated cells and non-labelled NPs were used as negative controls. Data are presented as mean \pm SD, $N = 4$ independent samples, with 3 technical replicates ($n = 3$). One-way ANOVA followed by Tukey Post-Hoc test. *** $P = 0.0001$. **c**, Confocal images (Z-stack and maximum projection) of murine immature DC (JAWSII) after 4, 12 and 24 hours of incubation with Cy5-labelled NPs ($N = 3$; $n = 3$). Scales bar: 25 μ m.

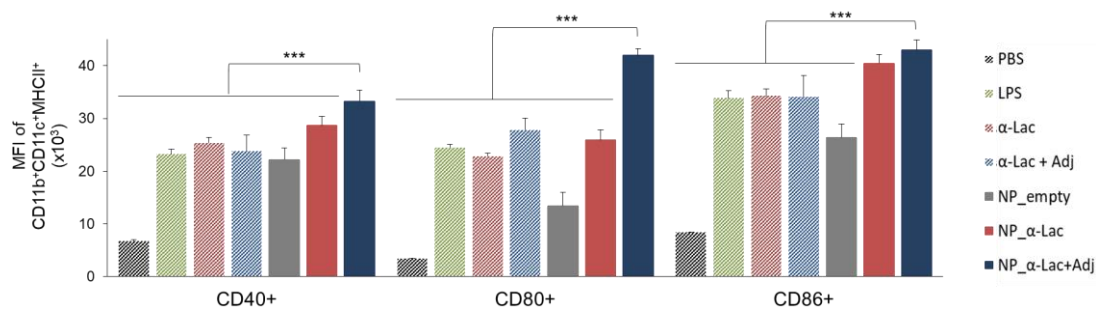


Figure 12. Median fluorescence intensity (MFI) of activated DCs that internalised NP1, present in the lymph nodes, 17 hours after immunisation. Mean \pm SD; $N = 3$, $n = 3$, where N denotes the number of independent experiments and n denotes the number of measurements per experiment. One-way ANOVA followed by Tukey Post-Hoc test. *** $P < 0.001$.

In addition, *ex vivo* images of dissected organs (liver, spleen, kidneys, heart, lungs and lymph nodes (LNs) (inguinal)) showed a fluorescent signal in inguinal LNs recovered from the left side of mice, contrary to the one recovered from the right side. Moreover, no fluorescent signal was detected in any other organ (**Figure 13b**).

To determine the anti-tumour effect of our nanovaccine against triple-negative breast carcinoma (TNBC), we administered three doses of our nanovaccine, seven days apart, to 4T1 mouse model and tested if the induced immune response would synergize with the agonist antibody anti-OX40 (α OX40).

To test this hypothesis, 4T1-bearing BALB/c mice were treated according to the dosing schedule described in **Figure 14a**. On day 22 after tumour inoculation, the average tumour volume of mice groups treated with α -Lac and immune stimulators (CpG-ODN and Poly(I:C)) free in solution or the nanovaccines with siRNA negative control were identical to the PBS-treated group. There was no evidence of body weight change in all groups, attesting the vaccine tolerability and safety (**Figure 14b**). Although mice treated with NP1 and NP2 presented similar average tumour volumes, they are slightly lower than the obtained by the previous groups. Also, α OX40 treatment slightly decreased the average tumour volume when compared with the PBS-treated group ($P > 0.05$) (**Figure 14d**). It is important to highlight that this group presented variable tumour volumes (**Figure 14e**). The tumour volume of the animals treated with the nanovaccines alone or combined with α OX40 was significantly lower compared with the PBS-treated group ($P = 0.0037$ and $P = 0.0001$, respectively). The tumour volume of the nanovaccine + OX40 group was more than 5-fold smaller than the one presented by the PBS-treated animals.

Results

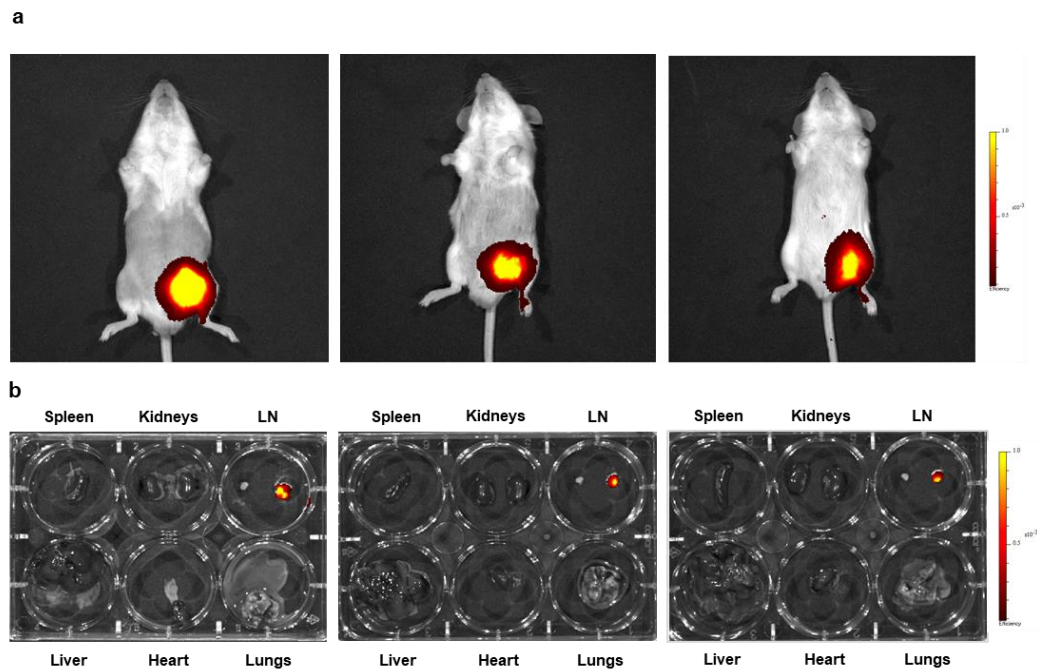


Figure 13. Non-invasive intravital fluorescence imaging 24 hours following hock immunisation with NP (left) and PBS (right) of **a**, BALB/c mouse. **b**, Organ biodistribution. $N = 3$ animals. LN: lymph nodes.

Moreover, the tumour volume of this treatment group was significantly lower than the one obtained in all other treatment groups ($P = 0.0001$ relative to the α -Lac + siTGF- β 1 + Adjs group, $P = 0.0011$ relative to the NP1 group, $P = 0.0022$ relative to the NP2 group, $P = 0.0194$ relative to the nanovaccine group and $P = 0.0003$ relative to the NP1 + NP2 (siRNA negative control) group (**Figure 14d**). Additionally, these immunized animals presented a long-term survival: 50% (4 out of 8) of the animals treated with NP1 + NP2 + α OX40 remained alive at day 35 after tumour inoculation, in comparison to the remaining treated groups ($P = 0.0006$) (**Figure 14c**).

At the endpoint (day 19 after tumour inoculation), 3 animals from each treatment group were sacrificed and the main organs were recovered. Tumour mass from each animal was weighted. The tumour mass of animals treated with the multifunctional nanovaccines or treated with nanovaccine + α OX40 was significantly smaller than those presented by the PBS-treated group ($P = 0.0369$ and $P = 0.0011$, respectively) (**Figure 14f**).

Murine mammary carcinoma 4T1 is known to induce splenomegaly (372). For this reason, the spleen was also recovered from each animal and weighted, revealing a significant decrease in the group treated with NP1 + NP2 + α OX40, when compared with PBS-treated group ($P = 0.0224$) (**Figure 14e**).

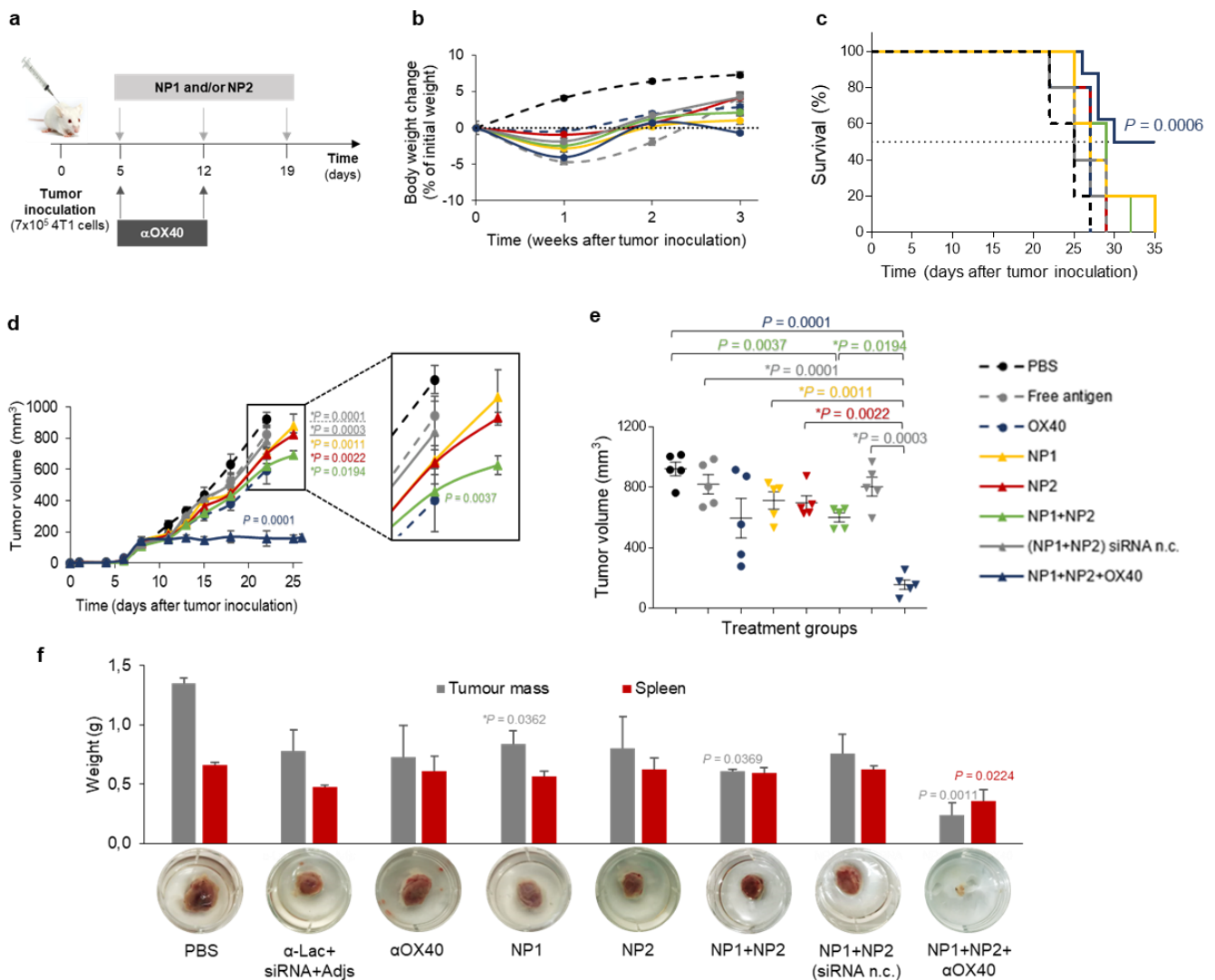


Figure 14. Nanovaccines synergize with αOX40 immune checkpoint against TNBC. **a**, Timeline (days) of tumour inoculation in BALB/c mice, immunisation scheme, and immune checkpoint therapy. **b**, Body weight change, expressed as percent change from the day of treatment initiation. Data are presented as mean ± SEM (N = 5 animals per group). **c**, Kaplan-Meier overall survival over time graph for mice inoculated with 7 x 10⁵ 4T1 cells (two independent assays were performed with N = 8 animals for NP1+NP2+αOX40 group and N = 5 animals for the remaining groups). Log-Rank test, for the combination NP1+NP2+αOX40 compared to all other treatment groups. **d**, Tumour growth curve. Data are presented as mean ± SEM (N = 5 animals). P values correspond to tumour volume at day 22 after tumour inoculation relative to PBS-treated group and *P values are relative to the nanovaccine + αOX40 group. One-way ANOVA followed by Tukey Post-Hoc test. **e**, Individual tumour volume at day 22 (N = 5 animals) with mean ± SEM. P values correspond to tumour volume at day 22 after tumour inoculation relative to PBS-treated group and *P values are relative to the nanovaccine + αOX40 group. One-way ANOVA followed by Tukey Post-Hoc test. **f**, Tumour mass and spleen weight recovered after mice sacrifice. N = 3, Mean ± SD. One-way ANOVA followed by Tukey Post-Hoc test. P values relative to the PBS-treated group and *P values relative to the nanovaccine + αOX40 group.

Results

When analysed by flow cytometry, the multifunctional nanovaccine combined with α OX40 stimulated T-cell infiltration (**Figure 15a**) into tumours at an early stage of the treatment (day 19), resulting in an increase of CD4⁺ T-cells (CD3⁺CD4⁺ cells) (**Figure 15b**) and CD8⁺ T-cells (CD3⁺CD8⁺ cells) (**Figure 15b**), specially of activated CD8⁺ T-cells (CD3⁺CD8⁺CD107b⁺ cells) (**Figure 15c**), expressing tumour necrosis factor (TNF)- α , interleukin (IL)-12 and interferon (IFN)- γ (in CD3⁺CD8⁺ population) (**Figure 15g-i**). Additionally, an increase of CD8⁺ T-cells expressing programmed death-1 receptor (PD-1) was observed into tumours treated with the nanovaccines combined with α OX40 (**Figure 15d**), but also in the ones treated only with α OX40.

Besides the infiltration of T-cells, tumours recovered from mice treated with the combination therapy (nanovaccines + α OX40) also revealed a high infiltration of myeloid cells, such as DCs (CD11c⁺MHCII⁺CD11b⁺ cells) (**Figure 15j**), monocyte-derived DCs (CD11c⁺MHCII⁺CD11b⁺) (**Figure 15k**) and macrophages (CD11c⁺MHCII⁺CD11b⁺) (**Figure 15l**). More importantly, a high infiltration of CD103⁺ DC (CD11c⁺MHCII⁺CD11b^{dim}CD8⁺CD103⁺) (**Figure 15n**) was only found in the tumours of these animals. These CD103⁺ DC are essential to promote an effective anti-tumour immune response. However, these animals also presented levels of tumour-infiltrating MDSCs (CD11b⁺Gr-1⁺) (**Figure 15m**) higher than those observed in tumours of animals treated with α OX40 alone, NP1, NP2 and NP1 + NP2.

4. Ibrutinib does not improve the antitumour effect of the therapeutic multifunctional nanovaccines with α OX40

Motivated by the results obtained above, two additional combination treatments were performed to possibly improve the anti-tumour effect obtained in animals treated with the combination of the nanovaccines with α OX40. In one hand, the nanovaccines were combined with α OX40 + ibrutinib (Ib), according to the dosing schedule described in **Figure 16a**, as an attempt to decrease the infiltration of MDSCs observed in these animals (**Figure 15m**). On the other hand, the nanovaccines were combined with α OX40 + α PD-1, according to the dosing schedule described in **Figure 18a**, to decrease the immune suppressor-mediated effect of the PD-1 expression in CD8⁺ T-cells, previously found in the tumours of nanovaccine + α OX40 treatment group (**Figure 15d**).

Concerning the combination of the nanovaccines with α OX40 + Ib, the groups α OX40, Ib and PBS-treated group showed similar average tumour volume at day 22 after tumour inoculation. However, the group treated with Ib showed variable individual tumour volumes (**Figure 16e**).

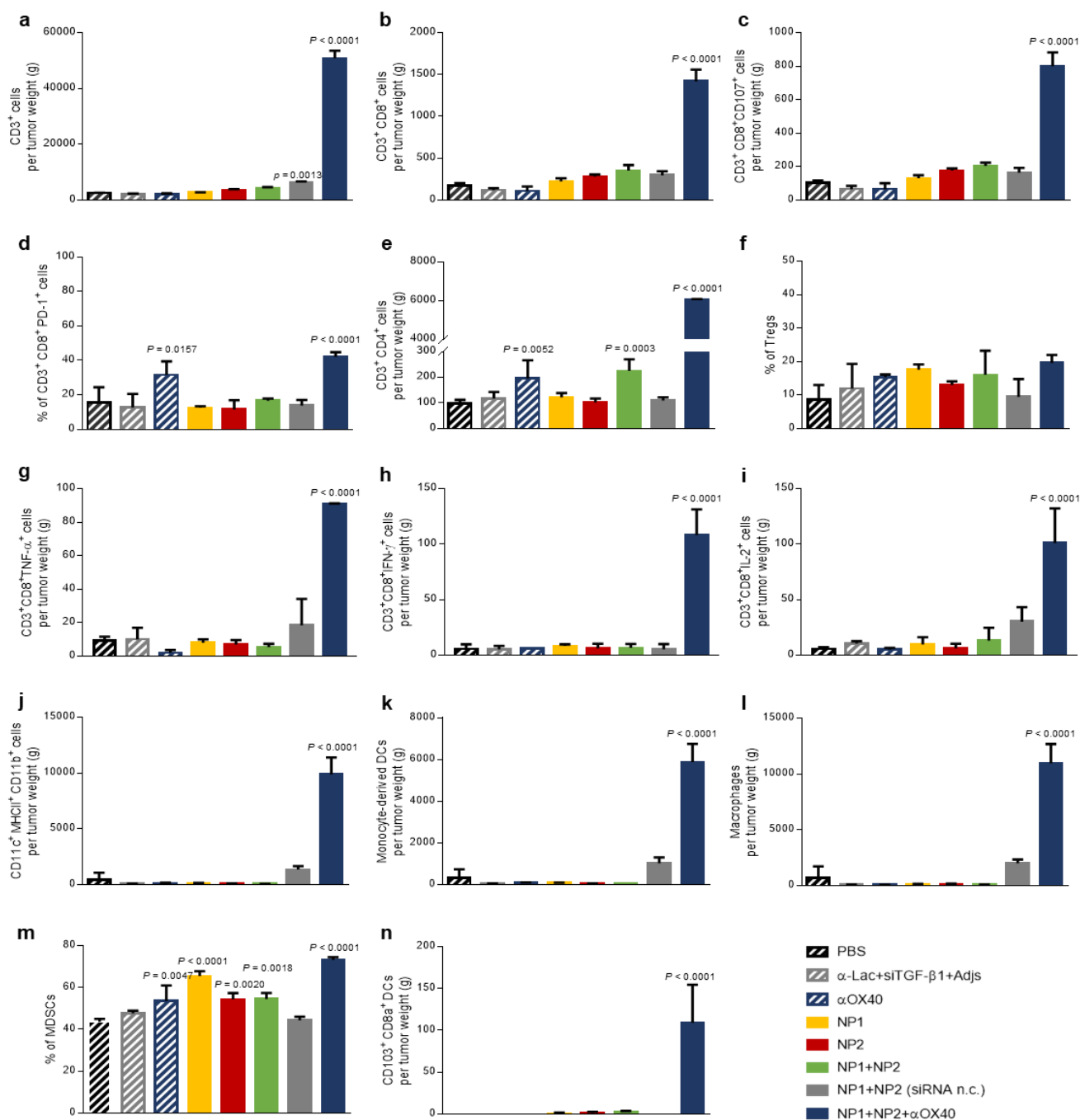


Figure 15. Tumour-infiltrating immune cell populations after the combination of nanovaccines with α OX40. a-n, Tumour-infiltrating immune cell populations for CD3⁺ (a), CD3⁺CD8⁺ (b), CD3⁺CD8⁺CD107b⁺ (c), CD3⁺CD8⁺PD-1⁺ (d), CD3⁺CD4⁺ (e), CD3⁺CD4⁺CD25⁺FoxP3⁺ (f), CD3⁺CD8⁺TNF- α ⁺ (g), CD3⁺CD8⁺IFN- γ ⁺ (h), CD3⁺CD8⁺IL-2⁺ (i), CD11c⁺MHCII⁺CD11b⁺ (j), CD11c⁺MHCII⁺CD11b^{hi} (k), CD11c⁺MHCII⁺CD11b⁺ (l), CD11b⁺Gr-1⁺ (m), CD11c⁺MHCII⁺CD11b^{dim}CD8⁺CD103⁺ (n). Tumours were isolated on day 19 after tumour cell inoculation. Quantification was performed by flow cytometric analysis. Data are presented as mean \pm SD, $N = 3$ animals, $n = 3$ measurements per experiment. One-way ANOVA followed by Tukey Post-Hoc test. P values relative to PBS-treated group.

Results

Although mice treated with the nanovaccine + α OX40 + Ib showed a significantly smaller average tumour volume when compared with PBS-treated group (1.8-fold) ($P = 0.0089$), with negligible systemic toxicity observed (**Figure 16b**), the average tumour volume observed in nanovaccines + α OX40 group was significantly lower when compared with the previous group ($P = 0.0288$) (**Figure 16d**).

In addition, the triple combination treatment did not improve the overall animal survival, since none of those animals survived after 35 days (**Figure 16c**), neither showed a decrease on tumour mass or spleen weight (**Figure 16f**).

The analysis of tumour-infiltrating immune cells by flow cytometry showed that the nanovaccines combined with α OX40 + Ib also improved the infiltration of CD4⁺ (**Figure 17e**) and activated CD8⁺ T-cells (**Figure 17b, c**) into tumours at an early stage of the treatment (day 19), but at a lower extent than nanovaccines + α OX40 group. Also the expression of TNF- α and IL-2 was significantly higher than PBS-treated group, but lower than the one induced by the nanovaccines combined with α OX40 (**Figure 17g, i**). Moreover, and contrarily to the latter group, the nanovaccines combined with α OX40 + Ib did not stimulate the infiltration of monocytes (**Figure 17j-l,n**). However, and as expected, the nanovaccines combined with α OX40 + Ib reduced significantly the MDSCs infiltration into the tumours, when compared with the nanovaccines + α OX40 group ($P < 0.0001$).

5. PD-1 blockade does not improve the antitumour effect of the therapeutic multifunctional nanovaccines with α OX40

Regarding the combination of the nanovaccines with α OX40 + α PD-1, this treatment decreased significantly the average tumour volume of the animals at day 22 after tumour inoculation, when compared with PBS-treated group (2.4-fold) ($P = 0.0015$) (**Figure 18c**), with negligible systemic toxicity observed (**Figure 18b**). However, the average tumour volume was similar to the one obtained while combining the nanovaccines with α OX40. The control groups (PBS-treated group, α OX40 and α OX40 + α PD-1) also presented similar tumour volumes (**Figure 18c**). However, the group treated with α OX40 + α PD-1 showed variable individual tumour volumes (**Figure 18d**). Moreover, α OX40 + α PD-1 and the triple combination (nanovaccines + α OX40 + α PD-1) also decreased the tumour mass weight when compared with PBS-treated group ($P = 0.0039$ and $P = 0.0118$, respectively), but not the spleen weight (**Figure 18e**).

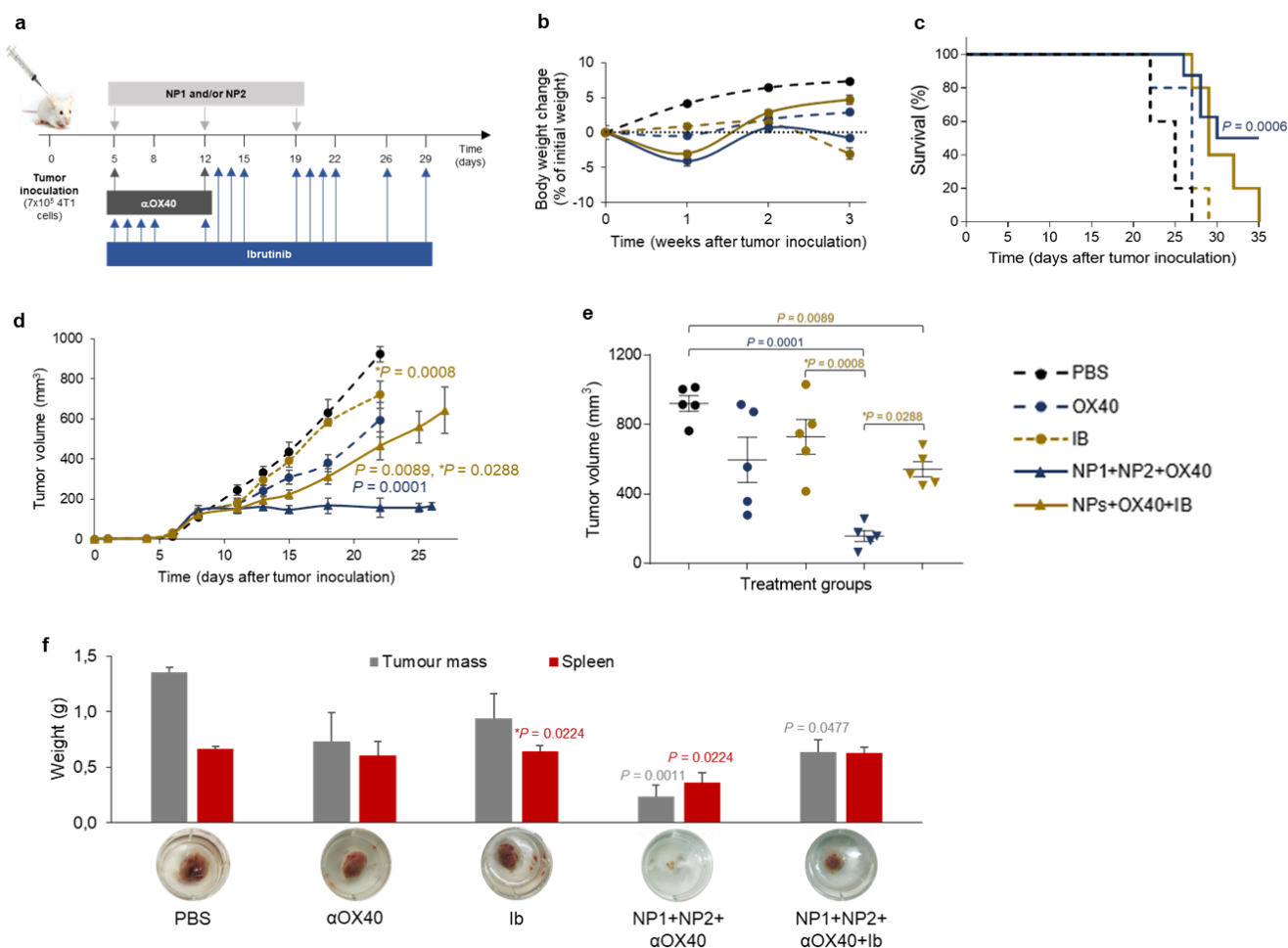


Figure 16. Ibrutinib did not improve the antitumour effect of the dual therapy. **a**, Timeline (days) of tumour inoculation in BALB/c mice, immunisation scheme, and treatments. **b**, Body weight change, expressed as percent change from the day of treatment initiation. Data are presented as mean \pm SEM ($N = 5$ animals per group). **c**, Tumour growth curve. Data are presented as mean \pm SEM ($N = 5$ animals). P values correspond to tumour volume at day 22 after tumour inoculation relative to PBS-treated group. $*P$ value correspond to tumour volume at day 22 after tumour inoculation relative to the nanovaccine + α OX40 group. One-way ANOVA followed by Tukey Post-Hoc test. **d**, Kaplan-Meier overall survival over time graph for mice inoculated with 7×10^5 4T1 cells (two independent assays were performed for groups nanovaccine + α OX40 and nanovaccines + α OX40 + Ib with $N = 8$ animals for nanovaccine + α OX40 group and $N = 5$ animals for the remaining groups). Log-Rank test, $P = 0.0006$ for the combination nanovaccine + α OX40 compared to all other treatment groups. **e**, Individual tumour volume at day 22 ($N = 5$ animals) with mean \pm SEM. P values correspond to tumour volume at day 22 after tumour inoculation relative to PBS-treated group and $*P$ values are relative to the nanovaccine + α OX40 group. One-way ANOVA followed by Tukey Post-Hoc test. **f**, Tumour mass and spleen weight recovered after mice sacrifice. $N = 3$, Mean \pm SD. One-way ANOVA followed by Tukey Post-Hoc test. P values relative to PBS-treated group and $*P$ values relative to the nanovaccine + α OX40.

Results

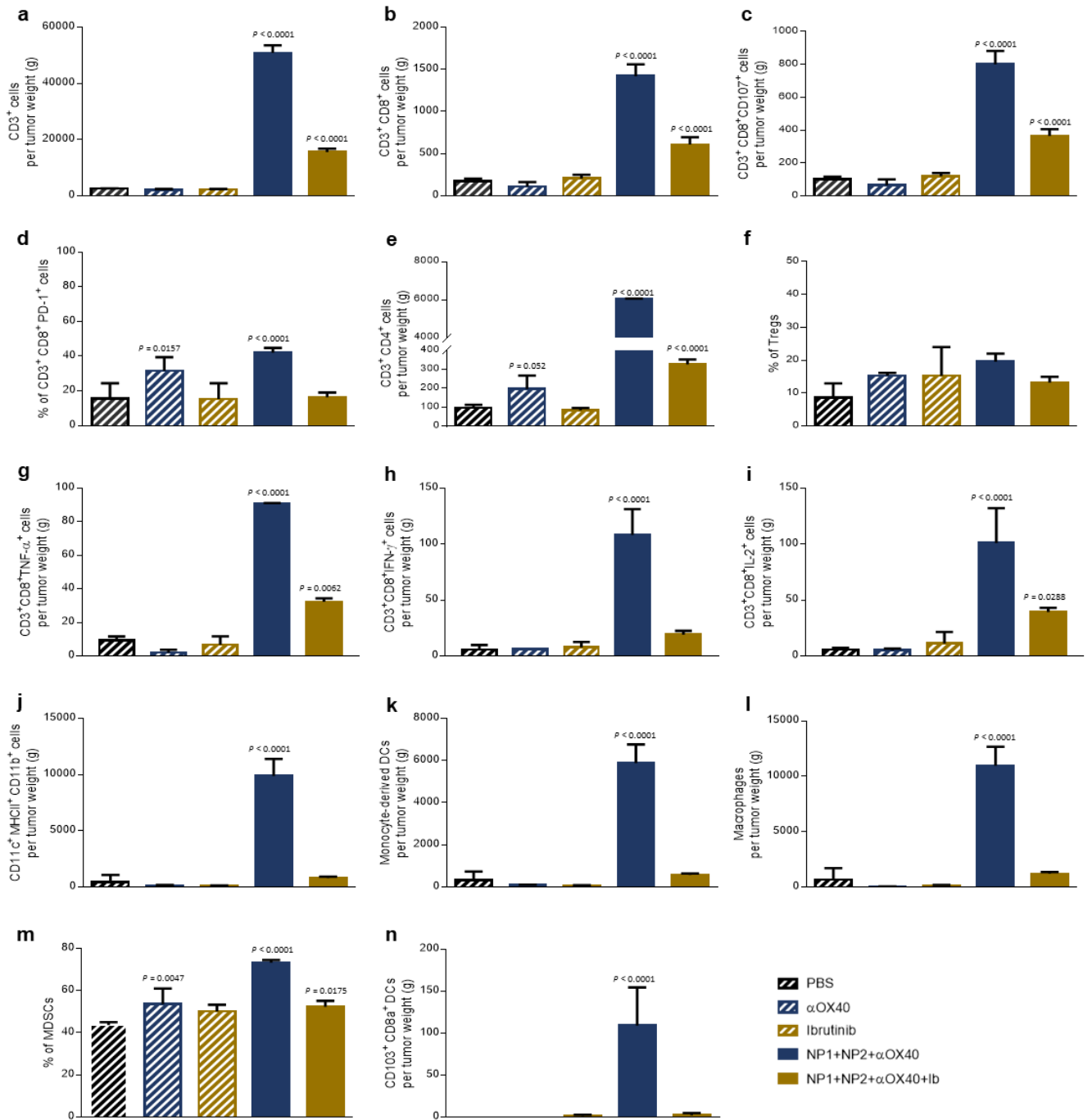


Figure 17. Tumour-infiltrating immune cell populations after the combination of nanovaccines + α OX40 with Ibrutinib showed a decrease on the MDSCs, besides not improving the antitumour effect of the dual therapy. a-n, Tumour-infiltrating immune cell populations for CD3⁺ (a), CD3⁺CD8⁺ (b), CD3⁺CD8⁺CD107b⁺ (c), CD3⁺CD8⁺PD-1⁺ (d), CD3⁺CD4⁺ (e), CD3⁺CD4⁺CD25⁺FoxP3⁺ (f), CD3⁺CD8⁺TNF- α ⁺ (g), CD3⁺CD8⁺IFN- γ ⁺ (h), CD3⁺CD8⁺IL-2⁺ (i), CD11c⁺MHCII⁺CD11b⁺ (j), CD11c⁺MHCII⁺CD11b^{hi} (k), CD11c⁺MHCII⁺CD11b⁺ (l), CD11b⁺Gr-1⁺ (m), CD11c⁺MHCII⁺CD11b^{dim}CD8⁺CD103⁺ (n). Tumours were isolated on day 19 after tumour cell inoculation. Quantification was performed by flow cytometric analysis. Data are presented as mean \pm SD, $N = 3$ animals, $n = 3$ measurements per experiment. One-way ANOVA followed by Tukey Post-Hoc test. P values relative to PBS-treated group.

Flow cytometric analyses of the tumour cell suspension from mice treated with the triple combination nanovaccines + α OX40 + α PD-1 revealed a higher infiltration of CD4⁺ (**Figure 19e**) and activated CD8⁺ T-cell (**Figure 19b, c**), compared to PBS-treated group, at an early stage of the treatment (day 19). However, the infiltration observed was at a lower extent than the nanovaccines + α OX40 group. CD8⁺ T-cells were shown to overexpress TNF- α , but not IFN- γ nor IL-2, contrarily to what was observed in mice treated with the nanovaccines + α OX40 (**Figure 19g-i**). However, and as expected, the expression of PD-1 by CD8⁺ T-cells decreased in group treated with the nanovaccines + α OX40 + α PD-1 (**Figure 19d**). Although this treatment induced monocyte-derived DCs (**Figure 19k**) and macrophages (**Figure 19l**) infiltration into the tumour, the DCs and CD103⁺ DCs infiltration was not significant (**Figure 19j, n**).

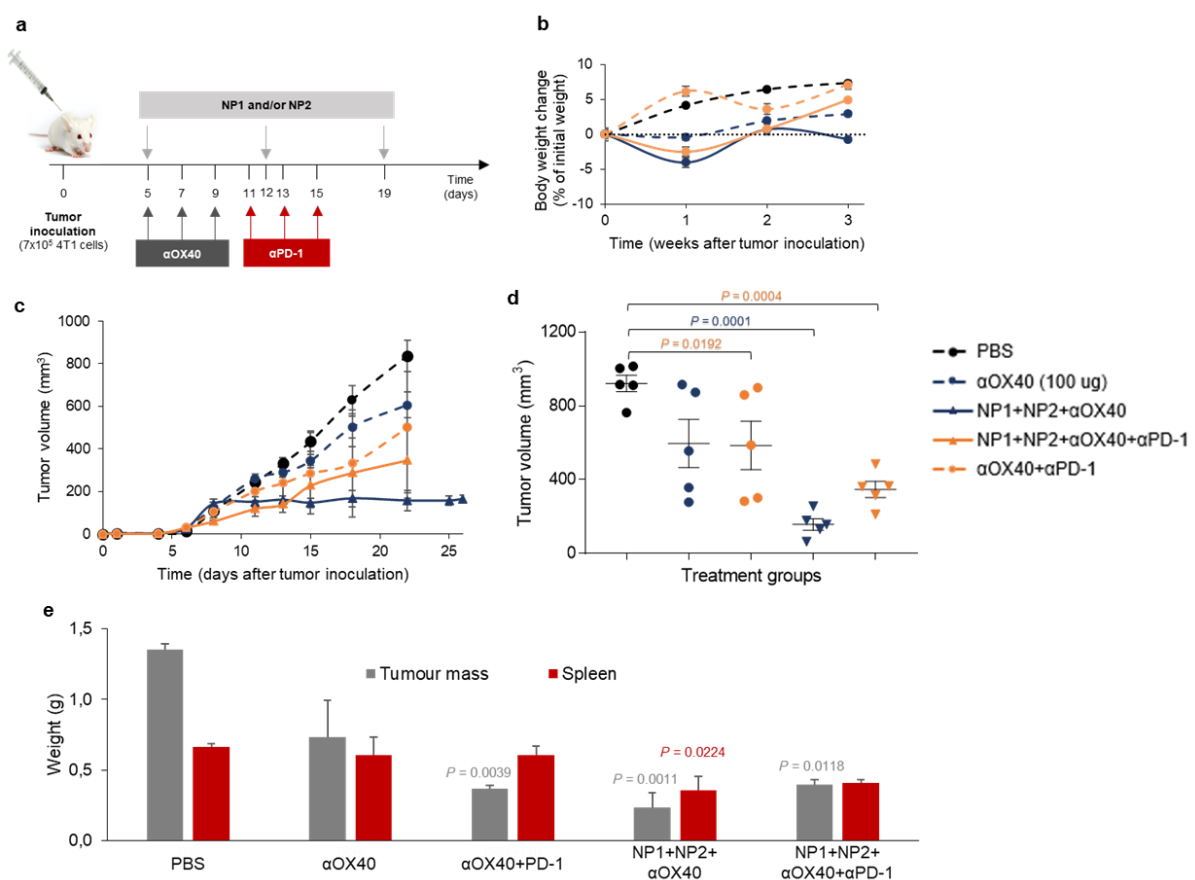


Figure 18. PD-1 blockade did not improve the antitumour effect of the dual therapy. a, Timeline (days) of tumour inoculation in BALB/c mice, immunisation scheme, and immune checkpoint therapy. **b,** Body weight change, expressed as percent change from the day of treatment initiation. Data are presented as mean \pm SEM (N = 5 animals per group). **c,** Tumour growth curve. Data are presented as mean \pm SEM (N = 5 animals). One-way ANOVA followed by Tukey Post-Hoc test. P values correspond to tumour volume at day 22 after tumour inoculation relative to PBS-treated group. **d,** Tumour mass and spleen weight recovered after mice sacrifice. N = 3, Mean \pm SD. One-way ANOVA followed by Tukey Post-Hoc test. P values relative to PBS-treated group.

Results

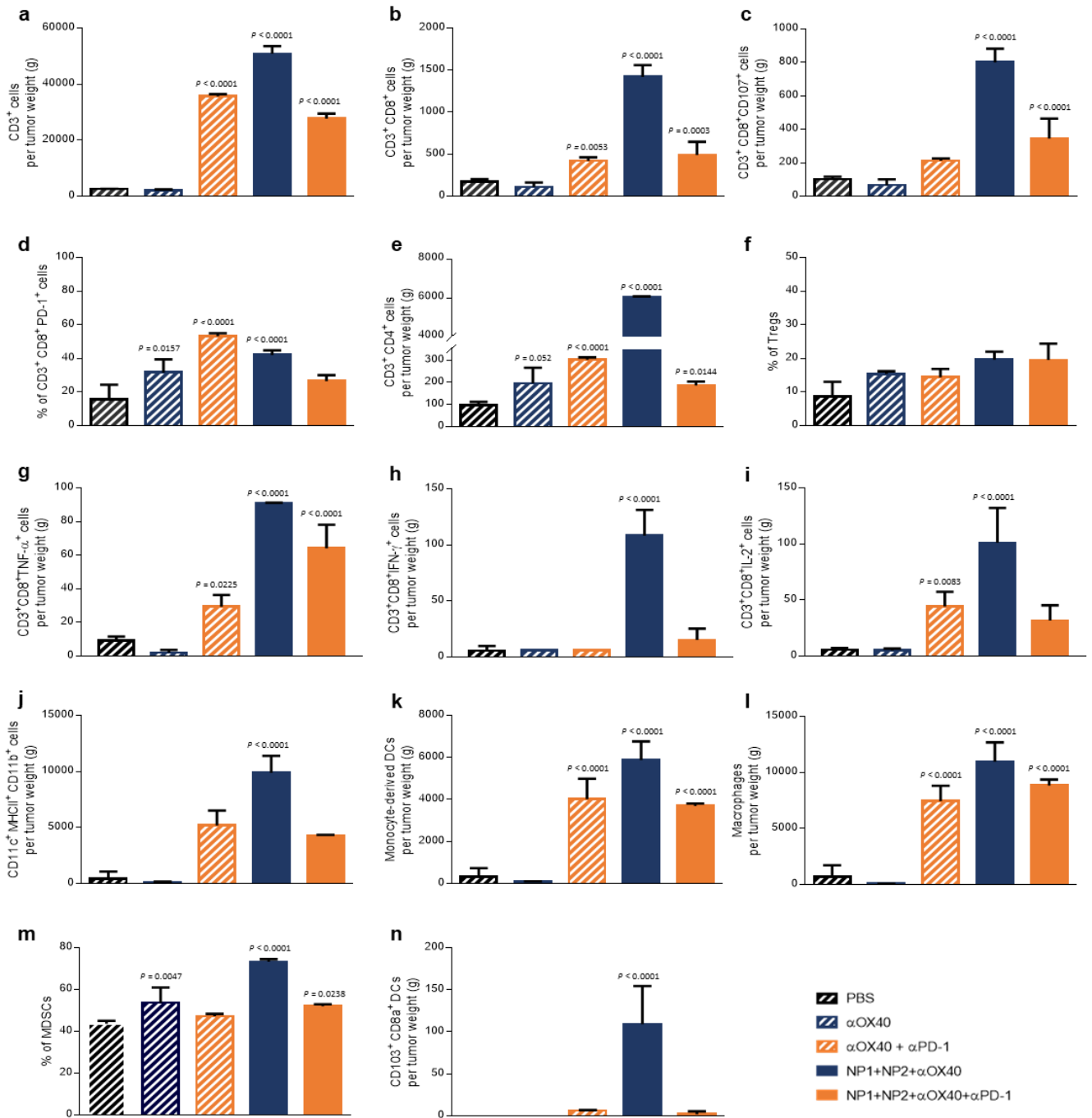


Figure 19. Tumour-infiltrating immune cell populations after the combination of nanovaccines + αOX40 with αPD-1 monoclonal antibody decreased the PD-1 expression on CD8⁺ T-cells, besides not improving the antitumour effect of the dual therapy. a-n, Tumour-infiltrating immune cell populations for CD3⁺ (a), CD3⁺CD8⁺ (b), CD3⁺CD8⁺CD107b⁺ (c), CD3⁺CD8⁺PD-1⁺ (d), CD3⁺CD4⁺ (e), CD3⁺CD4⁺CD25⁺FoxP3⁺ (f), CD3⁺CD8⁺TNF-α⁺ (g), CD3⁺CD8⁺IFN-γ⁺ (h), CD3⁺CD8⁺IL-2⁺ (i), CD11c⁺MHCII⁺CD11b⁺ (j), CD11c⁺MHCII⁺CD11b^{hi} (k), CD11c⁺MHCII⁺CD11b⁺ (l), CD11b⁺Gr-1⁺ (m), CD11c⁺MHCII⁺CD11b^{dim}CD8⁺CD103⁺ (n). Tumours were isolated on day 19 after tumour cell inoculation. Quantification was performed by flow cytometry. Data are presented as mean ± SD, N = 3 animals, n = 3 measurements per experiment. One-way ANOVA followed by Tukey Post-Hoc test. P values relative to PBS-treated group.

6. Nanovaccines knockdown TGF- β expression and induce systemic CD8⁺ T-cell-mediated immune response

The ability of the nanovaccines (NP1+NP2) to decrease the expression of TGF- β 1 was confirmed *in vivo*. Both qRT-PCR and immunoblotting analysis revealed a significant decrease in the TGF- β 1 expression in mice treated with the nanovaccines compared to the PBS-treated group (2.6-fold and 2-fold, respectively) ($P = 0.0287$ and $P = 0.0008$, respectively) (**Figure 20a, b**).

The antigen-specific nature of the CD8⁺ T-cell-mediated immune response was evaluated. Flow cytometric analysis showed that the CD8⁺ T-cells within the spleens of animals treated with the nanovaccines presented the highest expression of IFN- γ , IL-2 and TNF- α , following their incubation with the specific antigen α -Lac (**Figure 20c-e**), when compared with the same sample incubated with PBS or with a non-specific antigen (gp100).

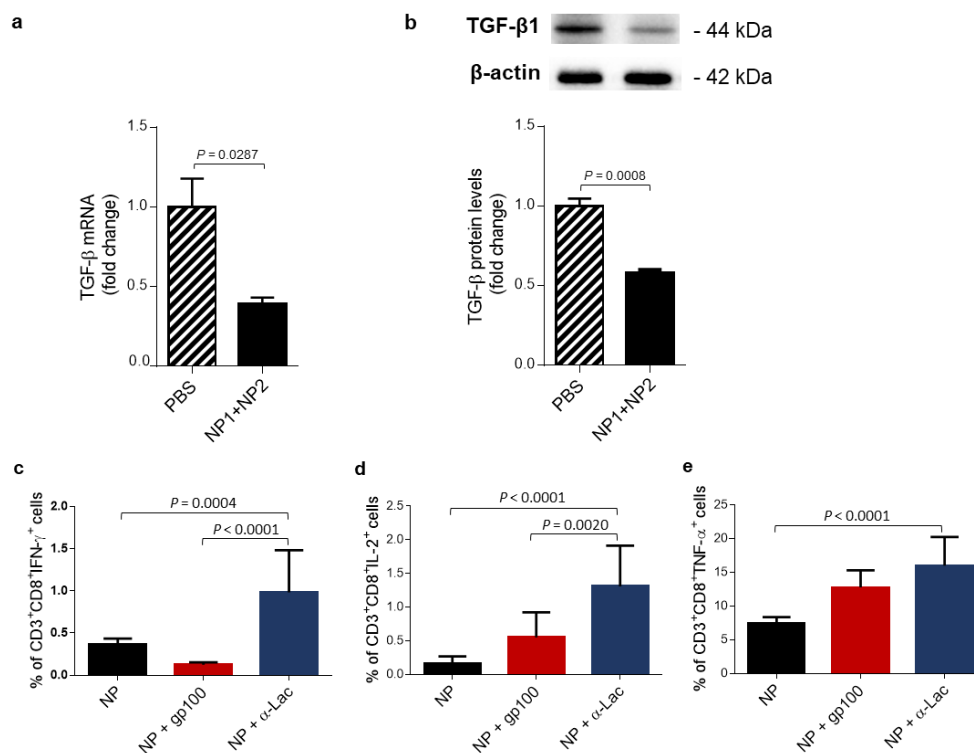


Figure 20. **a**, qRT-PCR analysis of TGF- β 1 in tumours. Data are shown as mean \pm SD fold change of 3 individual animals ($N = 3$). Unpaired two-tailed t test. **b**, Immunoblotting and densitometry of TGF- β 1. Blots were normalised to the endogenous β -actin. Representative immunoblots are shown. Results are expressed as mean \pm SD fold change of 3 individual animals ($N = 3$). Unpaired two-tailed t test. **c-e**, Flow cytometric analysis of T-cell specificity. Spleens from animals treated with NP1+NP2 were recovered on day 23 (after tumour inoculation) and co-cultured in medium, medium with gp100 or medium with α -Lac. Data are presented as mean \pm SD of 3 individual animals ($N = 3$).

7. Nanovaccines induce CD8⁺ T-cell-mediated immune response within the tumour microenvironment

Additionally, the antigen-specific nature of the immune response induced by our nanovaccine was also confirmed following the immunization of B16.MO5 melanoma-bearing mice with OVA-loaded nanovaccine (NP1_OVA), according to the dosing schedule described in **Figure 21a**. Contrarily to the remaining treatment groups, the combination of the nanovaccines (NP1_OVA + NP2) with α OX40 reduced significantly the average tumour volume, at day 22 after tumour inoculation, when compared with the PBS-treated group (**Figure 21c**), with negligible systemic toxicity observed (**Figure 21b**).

Flow cytometric analysis revealed that mice treated with the nanovaccines (NP1_OVA + NP2) combined with α OX40 induced the highest expression of SIINFEKL (OVA)-specific CD8⁺ T-cells (**Figure 21d**).

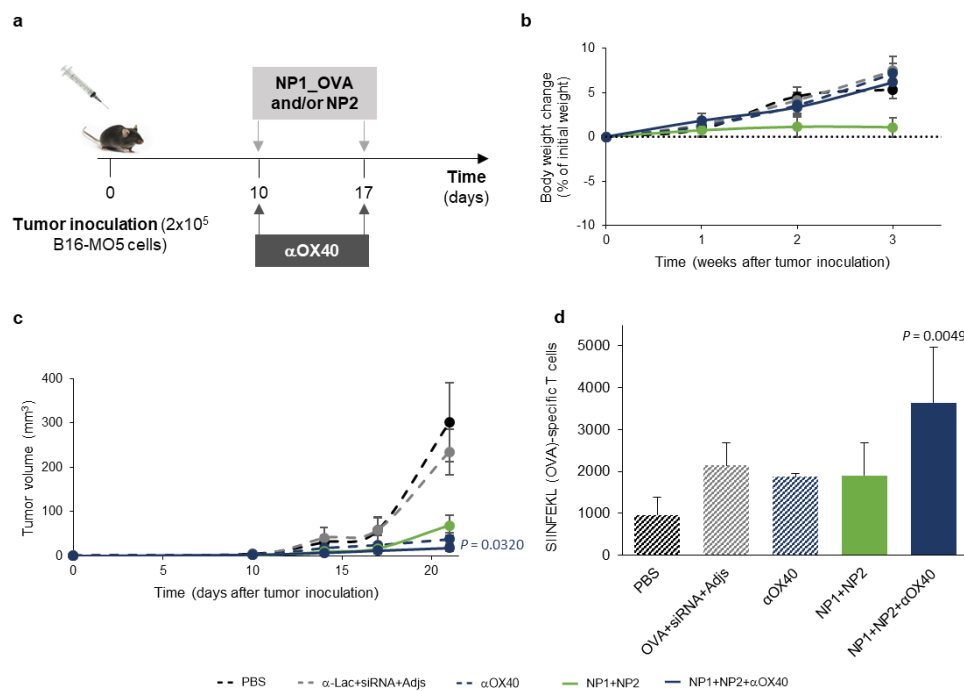


Figure 21. T cell induced response by nanovaccine on B16.MO5 model is specific for OVA antigen. **a**, Timeline (days) of B16.MO5 inoculation in C57BL/6J mice, immunisation scheme, and immune checkpoint therapy. **b**, Body weight change, expressed as percent change from the day of treatment initiation. Data are presented as mean \pm SEM ($N = 5$ animals per group). **c**, Tumour growth curve. Data are presented as mean \pm SEM ($N = 5$ animals). P values correspond to tumour volume at day 22 after tumour inoculation. One-way ANOVA followed by Tukey Post-Hoc test. **d**, Frequency of SIINFEKL (OVA)-specific CD8⁺ T-cells (in live CD3⁺CD19⁻ cell population) in spleen. Data are presented as mean \pm SD ($N = 5$ animals per group, $n = 3$ measurements per experiment). One-way ANOVA followed by Tukey Post-Hoc test. P values relative to PBS.

CHAPTER IV

Chapter IV - Discussion

This chapter is adapted from the unpublished original manuscript:

Multifunctional nanovaccine synergizes with immune checkpoint therapy against triple-negative breast cancer

Carina Peres^{a,b}, Ana I. Matos^a, Liane I. F. Moura^a, João Conniot^a, Bárbara Carreira^a, Afonso P. Basto^b, Marta Afonso^a, Ana S. Viana^c, Liana C. Silva^a, Cecília Rodrigues^a, Véronique Prémat^d, Luís Graça^b, Ronit Satchi-Fainaro^e, Helena F Florindo^a.

^a Research Institute for Medicines (iMed.U LISBOA), Faculty of Pharmacy, Universidade de Lisboa, Lisbon, Portugal;

^b Instituto de Medicina Molecular, Faculdade de Medicina da Universidade de Lisboa, Av. Prof. Egas Moniz, 1649-028 Lisboa, Portugal;

^c Center of Chemistry and Biochemistry, Faculty of Sciences, University of Lisbon, Lisbon, Portugal, Portugal;

^d Louvain Drug Research Institute, Advanced Drug Delivery & Biomaterials, Université Catholique de Louvain, 1200 Brussels, Belgium;

^e Department of Physiology and Pharmacology, Sackler Faculty of Medicine, Tel Aviv University, Tel Aviv, Israel.

(To be submitted for publication)

Chapter IV – Discussion

Immunotherapy, notably cancer vaccines and immune checkpoint therapy, has recently emerged as a promising strategy for the treatment of triple-negative breast cancer (TNBC) patients. Although cancer vaccines have been greatly improved, most of them still fail in providing clinical benefits as monotherapy in patients with advanced cancers. This can be explained by several immune escape mechanisms developed by tumours, which includes the recruitment of immunosuppressive cells and overexpression of potent inhibitory molecules, leading to an ineffective antitumour immune response (373). Additionally, despite the promising long-term responses of different immune checkpoint modulators, the use of these drugs as monotherapy has shown serious adverse events related to excessive immune activation, as well as primary resistance in the majority of patients (374). Thus, in an attempt to overcome the main disadvantages presented by these two therapeutic options, when used individually, and considering the heterogeneity of TNBC, combination therapies should be considered to treat this specific breast cancer subtype. Combination therapy has been a hot topic in the immunotherapy field. By combining two or more therapeutic agents that have different mechanisms of action, more cancer cells should be killed, thereby improving the overall patient's response.

Here we report the synergism of a multifunctional nanovaccine, composed of two nanosystems, with an immune checkpoint OX40 agonist. Additionally, we also report the lack of improvement in the overall immune response by adding to this dual therapy a programmed death-1 receptor (PD-1) inhibitor and a modulator of the function and generation of myeloid-derived suppressor cells (MDSCs).

1. Multifunctional nanoparticles as antigen delivery systems and regulators of TGF- β levels

The first step of the nanovaccine development consisted of polyplexes preparation. Interaction between the positively charged chitosan backbone and the negatively charged small interfering RNA (siRNA) leads to the spontaneous formation of nano-size complexes (polyplexes) in the aqueous milieu (375). Three different chitosan salts were tested to evaluate their ability to complex with the siRNA molecules, at different ratios. Contrarily to the two other chitosan derivatives, glycol chitosan (GCs) was not able to complex efficiently the oligonucleotide at low ratios (1:5 and 1:15 (w/w)). Although both glutamate chitosan (GlutCs) and hydrochloride chitosan (HCCs) were found to complex efficiently the oligonucleotides at a siRNA-Cs ratio of 1:15 (w/w),

Discussion

GlutCs was chosen as chitosan derivative for the polyplexes preparation, based on Mao *et al.* studies, who stated that GlutCs allowed a higher gene silencing than HCCs (375).

In an attempt to obtain the best physicochemical characteristics, two different external aqueous phase surfactants, polyvinyl alcohol (PVA) and Pluronic® F-127 (PF127), were used for polylactic acid (PLA) nanoparticle (NP) preparation, and their surface was modified by hyaluronic acid (HA). Overall, all nanosystems presented similar morphology and physicochemical characteristics in terms of size, polydispersity index (PDI), surface charge, entrapment efficiency (EE) and loading capacity (LC) of the antigen, without affecting dendritic cells (DCs) nor breast cancer cell line viability. Comparing all nanosystems, NP synthesised with PF127 as surfactant showed a higher and faster internalisation by DCs and tumour cells, than the ones synthesized with PVA. NP internalisation by tumour cells herein observed is in accordance with Menon *et al.* study, where they attest that cancer cells internalised more poly(lactic-co-glycolic) acid (PLGA) NPs coated with PF127 than the ones coated with PVA (162). Additionally, despite PVA is the most well-known and the most commonly used surfactant in the formulation of polymeric NPs (376), diverse side effects have been related to this surfactant, namely hypertension, organ lesions, anaemia, and depression of the central nervous system, upon subcutaneous and intravenous administration *in vivo* (377, 378).

As it was expected, the modification of the NP surface with HA also improved their ability to be taken up by tumour cells when compared with the other nanosystems ($P < 0.0001$). This can be explained by the fact that HA is a targeting moiety that specifically recognizes the receptor CD44, which is overexpressed on several tumour cell surfaces, including TNBC cell lines, such as 4T1 (379). Upon encountering tumour cells, these NP are internalised via HA-CD44 interaction. On the other way, immature DC also internalised at higher extent the NP modified with HA than the other nanosystems ($P < 0.0001$). Although there is no evidence in the literature that HA may target DCs, Do *et al.* revealed that HA induced the activation of DCs, enhancing their ability to stimulate allogeneic and antigen-specific T-cells markedly (380).

NPs synthesised with PF127 as surfactant and coated their surface with HA were shown to be the safest nanosystem, with the ability to target both DCs and the tumour microenvironment (TME).

We observed that this optimized nanosystem was able to co-entrap whole proteins (α -lactalbumin (α -Lac) and ovalbumin (OVA)), the toll-like receptor (TLR) ligands cytosine phosphorothioate-guanine motifs (CpG) and polyinosinic:polycytidylic acid (Poly(I:C)), and siRNA molecules with high EE and LC values. Importantly, the entrapment of α -Lac into the NP did not affect its structure, which is fundamental to induce the specific and desired immune response. This nanosystem also promoted

antigen prolonged/sustained release overtime, which is highly desired in vaccination since this release profile has been shown to elicit more efficiently antigen-specific immune responses, and activate cytotoxic T lymphocyte cells (CTLs) and immune memory cells *in vivo*, reducing or even eliminating the need for booster immunisations (303). The co-entrapment of these biomolecules into these nanosystem originated NP with an average diameter slightly lower than 200 nm, which is suitable for their trafficking through the lymphatic drainage directly to the lymphoid organs (381), narrow PDI values, and a surface charge close to neutrality, owing to lower toxicity and prevention of their premature phagocytosis by macrophages in circulation.

2. Multifunctional nanovaccines activate and improve the maturation of dendritic cells

The co-entrapment of the antigen and both CpG and Poly(I:C) TLR agonists in a single polymeric matrix showed to be relevant for the efficient activation and maturation of DCs, since an increase in the stimulatory molecules' expression (CD40, CD80 and CD86) was observed, in contrast with their levels upon incubation with the biomolecules free in solution ($P < 0.0001$). This highlights the important role of the nanovaccine in this process, since a residual immune response was obtained when the antigen and the TLR ligands were added to BMDCs free in solution. The efficient activation of those antigen-presenting cells (APCs) is crucial for the priming of naïve T-cells, and the consequent induction of tumour-specific T-cell responses (382). When entrapping the antigen only, NPs did not increase co-stimulatory molecules expression at the same extent, specially CD40 and CD80, which showed the importance of having both the tumour antigen and the TLR ligands entrapped within the nanovaccine. CpG-ODN and Poly(I:C) were specifically chosen because they have been described as potent Th1-inducing immunoadjuvants (383). Recently, Poly(I:C) has been shown to stimulate specialized DC subsets that are involved in the cross-presentation of antigens to CTL precursors in humans, known as BATF3-dependent, CD141⁺ DCs (known as CD103⁺ in mice) (384). Their receptors, TLR3 and TLR9 respectively, are both localized in the endosomal membrane where NPs can easily get access, upon internalisation by DCs (385). When both TLR ligands are successfully delivered to the same DC, these biomolecules may potentiate the efficient maturation of those APCs towards balanced Th1- and Th2-type immune responses, which has a crucial role in controlling homeostasis within tumour site (386).

When injected s.c. by hock immunization, the optimized nanosystem remained near the local of injection, which may anticipate an extended contact with DCs at the

periphery, as well as proximity to the axillary lymph nodes (LNs). This may explain the obtained preferential accumulation of the nanovaccines in these tissues, which is extremely important for the induction of antigen-specific adaptive immune responses and vaccine efficacy (387).

3. Nanovaccines knockdown the expression of TGF- β , induce systemic CD8+ T-cell-mediated immune response, and, when combined with α OX40 immune checkpoint therapy, restrict tumour growth and prolongs survival

Here we also report the ability of the dual therapy (multifunctional nanovaccine combined with α OX40) to induce an antitumour immune response, which resulted in a noteworthy tumour remission, with a higher overall survival and a tumour volume 4-fold lower than those obtained in α OX40-treated mice. The multifunctional nanovaccine was composed by two nanosystems, one targeting DCs (NP1) and the other targeting the TME (NP2). Both polymeric NP entrap the TLR ligands CpG-ODN and Poly(I:C) and the siRNA against transforming growth factor (TGF)- β 1, with the addition of the tumour-associated antigen (TAA) α -Lac in the NP1. Although α -Lac is expressed in healthy breast tissue during late pregnancy and lactation, this protein is also expressed at high levels in the vast majority of TNBC cases (227). Contrarily to what could be expected, Tuohy *et al.* showed that prophylactic vaccination of adult women against α -Lac provided a substantial proinflammatory T-cell response to human α -Lac, and that a history of lactation and breastfeeding has no impact on α -Lac-induced immunity and on the protection that such immunity will provide against the development of breast cancer (227). As far as we know, this is the first time α -Lac is entrapped in any kind of nanosystem to develop a nanovaccine for the treatment of breast cancer.

Contrarily to NP1 which was injected s.c. by hock immunization, NP2 was administered by i.t. injection aiming at delivering the combination of immune potentiators and siRNA to the TME, and thus modulate the tumour-infiltrating immune cell sub-populations. Although the use of this administration route has been controversial in immunotherapy, i.t. has numerous advantages. In our case, we can highlight the proximity of the siRNA molecules to their target to deplete Tregs population within the TME. Important components of the NP2 are the TLR ligands. Indeed, some studies have referred that the i.t. delivery of CpG alters the TME by improving the antitumour activity of both innate and adaptive immune cells. Lou *et al.* showed that the direct activation of the immune potentiators within the tumour promote an extensive infiltration of tumour antigen-specific T-cells and natural killer (NK) cells, and subsequent tumour suppression *in vivo* (388). More recently, Humbert *et al.* also referred the inhibition of the tumour

growth upon i.t. injection of this TLR9 agonist. They also showed the ability of CpG to activate conventional DCs, subsequent increasing antitumour T-cell priming at draining LNs, and enhancing the effector T-cell infiltration within TME (389). Poly(I:C) has also been shown to modulate the TME upon i.t. injection. Salmon *et al.* demonstrated that i.t. administration of this TLR3 agonist avoids systemic toxicity, but also activates directly tumour-resident classical DC (cDC)1 in mice (158). Interestingly, among many innate immune receptors, TLR3 has been shown to be expressed almost exclusively by mouse CD8 α ⁺ cDCs and CD103⁺ cDCs (390) and human CD141⁺ cDCs (384, 391), which excel in the priming and cross-presentation of cell-associated antigens to CD8⁺ T-cells (155). These facts support our interest in delivering these TLR agonists into the TME.

It is important to highlight that despite the ability of CpG and Poly(I:C) to activate these immune cells, these agents alone do not induce a therapeutically effective systemic antitumour immune response.

Our nanovaccine significantly reduced the average tumour volume of mice when compared with the group treated with the antigen, TLR ligands and siTGF- β free in solution. This highlights the role of our nanosystem on delivering these biomolecules, protecting them from early degradation and promoting their continuous release *in vivo*, which was already demonstrated by many different studies of our research group and others (211, 392-398). Mice treated with the nanovaccine entrapping the siRNA negative control, instead of siTGF- β , showed an average tumour volume markedly higher, suggesting the effective function of siTGF- β by decreasing the expression of this immune suppressive cytokine upon delivered by our nanosystem. This was further confirmed by qRT-PCR and immunoblotting analysis, where mice treated with the nanovaccine showed a significant decrease in TGF- β expression in comparison with the PBS-treated group. Additionally, our nanovaccine controlled tumour growth at a similar level than the α OX40. However, a synergistic effect was shown when combining these two treatments, inducing a noteworthy tumour remission, but also increasing the overall survival of the treated group, with minimal reversible systemic toxicity, reflected by slight body weight changes relative to the initial body weight. In addition, we further confirmed the antigen-specific nature of the CD8⁺ T-cell-mediated immune response, systemically and the tumour site.

Anti-OX40 agonistic monoclonal antibodies (mAbs) are currently being tested in four different clinical trials for the treatment of TNBC, in combination with other immune checkpoint modulators (ClinicalTrials.gov identifier: NCT02528357, NCT03971409, NCT02554812, NCT03241173). Although tumour regression was obtained in several preclinical models, conflicting results and controversies between *in vitro* and *in vivo* data have been also observed (399). Additionally, clinicians have reported some

inconsistency in terms of patient's response when treated with α OX40, as well as, several side effects (400).

When combined with our nanovaccine, the immune response was not only improved, by presenting lower variability in terms of tumour volumes of treated mice, but also the α OX40-related toxicity was reduced. This may be explained by a significant increase of TILs within the TME, specially CTLs. Here we also reported the impressive infiltration of CD103⁺ cDCs, which are as the most important DC subsets in defeating tumour. These cells excel at cross-presenting exogenous antigens (e.g., tumour antigens) to CD8⁺ T cells and are key cells for the generation of CTL responses (156).

Despite the impressive results, animals treated with our dual combination treatment also showed an increased infiltration of MDSCs and PD-1 expression in CD8⁺ T-cells.

4. Ibrutinib does not improve the antitumour effect of the therapeutic multifunctional nanovaccines with α OX40

MDSCs have emerged as an important contributor to tumour progression, promoting tumour angiogenesis, chemoresistance, and tumour metastasis (401) and have been implicated in limiting the efficacy of cancer immunotherapy (402-404) in different cancer types. Therefore, in an attempt to revert their immune suppressive effect within the TME, we combined our dual therapy (nanovaccine + α OX40) with ibrutinib, an irreversible inhibitor of Bruton's tyrosine kinase (BTK) and IL-2-inducible T-cell kinase, to modulate the MDSC generation and function (405, 406). By inhibiting MDSCs, this drug has been shown to improve DC maturation and migration, inducing T-cell activation and proliferation *in vivo* (407, 408), but also to enhance the efficacy of immune checkpoint modulators (409).

As we expected by combining ibrutinib with our dual treatment, MDSC infiltration was significantly reduced. However, the overall immune response (average tumour volume, survival and infiltration of immune cell populations) was not improved. This results suggest that this immature myeloid cell population was not totally involved in the major immune suppressive mechanism that was preventing the combined action of our dual treatment, contrarily to what we observed in a similar study in melanoma (211).

Another important aspect to take into account is the non-specificity of ibrutinib to MDSCs, being able to affect other immune cells, as B-cells, T-cells, NK cells, macrophages and neutrophils (410-415), which certainly affect the overall anti-tumour immune response. To avoid this, more specific inhibitors to MDSCs should be used in combination with our nanovaccine. MDSC inhibitors can modulate these cells by i)

inhibiting their immunosuppressive activity (e.g. PDE5 and STAT3 inhibitors and class I histone deacetylase); ii) blocking their recruitment to the tumour site (e.g. vitamins, tyrosine kinase inhibitors and chemotherapeutic agents); iii) regulating the myelopoiesis and/or their depletion in the tumour-bearing hosts (e.g. CCL2 inhibitors and CCR5 antagonists) (416). Recently, CXCR2/CCR4 inhibitors have shown to reduce MDSC recruitment, angiogenesis, and metastasis in TNBC patients (151).

Despite the non-specificity for MDSCs, systemic administration of ibrutinib has shown to enhance the antitumour immune response induced by the intratumoural injection of CpG-ODN in mouse lymphoma (417), which reinforce our interest in combining this agent with our nanovaccine.

In an attempt to improve the overall immune response achieved by our dual therapy, it would be important to genetically characterize the tumour-infiltrating cell populations to better understand the immune suppressive mechanisms involved in the TME of TNBC and thus, select the appropriate inhibitors to decrease their suppressive functions.

5. PD-1 blockade does not improve the antitumour effect of the therapeutic multifunctional nanovaccines with α OX40

PD-1 is an inhibitory receptor expressed at the surface of diverse immune cells, namely T-cells, NK cells, B-cells, macrophages and several subsets of DCs. Its ligand, programmed death ligand-1 (PD-L1), is frequently overexpressed on tumour cells, but also DCs. Upon its binding to PD-1 or CD80 (B71) located on T-cells, an inhibitory signal is delivered to T-cells, leading to T-cell exhaustion and thus ineffective T-cells. With the inhibition of PD-L1 or PD-1, T-cell exhaustion is reversed, and the antitumour response is improved (418).

Several mAbs targeting PD-L1 (Atezolizumab, Durvalumab and Avelumab) and PD-1 (Nivolumab and Pembrolizumab) are currently in clinical trials, as monotherapy or in combination with other agents. However, α PD-1 monotherapy has shown a limited therapeutic benefit in TNBC. Indeed, although TNBC patients have a high number of TILs, and express higher level of PD-L1 compared to other breast cancer subtypes, most of them do not, or only incompletely, respond to PD-1 blockade therapy. Recently, phase III KEYNOTE-119 clinical trial using Pembrolizumab as a monotherapy in TNBC failed to extend overall survival in patients (ClinicalTrials.gov identifier: NCT02555657). Earlier this year, Atezolizumab in combination with nab-paclitaxel chemotherapy has been approved by FDA and EMA for the treatment of locally advanced or metastatic TNBC, based on findings from the phase III double-blinded IMpassion130 trial (ClinicalTrials.gov

Discussion

identifier: NCT02425891). Although its acceptance, the results were not impressive. Indeed, this dual therapy presented a progression-free survival (PFS) of 7.4 months, against 5.5 months presented by the control group (nab-paclitaxel chemotherapy). Despite statistically significant ($P < 0.0001$), the improvement of PFS was only of 1.9 months. Contrarily, the improvements in the overall survival (OS) were impressive (23.7 months for the dual therapy against 17.6 months for the control group), however they were not statistically significant ($P = 0.08$).

In an attempt to revert the immune suppressive effect, induced by the overexpression of PD-1 and consequent exhaustion of tumour-specific effector T-cells, our dual therapy (nanovaccine + α OX40) was combined with an anti-PD-mAb. The combination of α OX40 and PD-1 blockade has already been studied in different cancer types, including, melanoma (211), ovarian cancer (419), lung cancer (420), and TNBC (421). However, the immune effect of this combination and the interaction of the two molecules on the downstream immune outcome remain unclear. In ovarian cancer and melanoma, the combined of these two immune checkpoint modulators induced a significant increase of CD8⁺ T-cells relative to Treg at the tumour site (211, 419). Interestingly, Messenheimer *et al.* demonstrated that the combination of α PD-1 and α OX40 is additive in metastatic breast cancer, but for such effect, they require to be given in the right sequence (421). In fact, simultaneous addition of α PD-1 to α OX40 negated the antitumour effects of α OX40, leading to a lower infiltration of antigen-specific CD8⁺ T-cell into the tumour, weak antitumour response, and lower overall survival (420, 421). However, the sequential administration of Abs targeting OX40 first and then PD-1, but not vice versa, was effective and additive (421). This study corroborates the results obtained by Shrimali *et al.* who showed that the simultaneous addition of anti-PD-1 to anti-OX40 negated the antitumour effects of OX40 antibody, by inducing T-cell apoptosis (420). As it can be seen in ClinicalTrials.gov, few clinical trials have started, and others are being planned to test this combination. However, response results have not yet been reported.

As expected, by combining α PD-1 with our dual treatment, the PD-1 expression was significantly reduced in CD8⁺ T-cells within the TME. However, here also the overall immune response (average tumour volume, survival and infiltration of immune cell populations) was not improved.

Additionally, we also highlight the inconsistency in the average tumour size of the mice treated with α OX40 + α PD-1.

Different studies have emphasised the dual role of PD-1 in defining efficient or ineffective immune T-cell responses. Indeed, although an inhibition signal is triggered upon ligation to PD-L1, PD-1 expression is firstly a marker of T-cell activation, allowing

the identification of the tumour-reactive CD8⁺ T-cell and of high avidity CD8⁺ T-cells specific for their specific antigens (422, 423). The level of PD-1 expression has been related to the strength of TCR signalling, and thus to the functional avidity of specific T-cells (424). Thus, PD-1 expression can also be considered as a marker of activated tumour-reactive T-cells.

CHAPTER V

Chapter V – Conclusions and Future Perspectives

Triple-negative breast cancer (TNBC) is the most aggressive subtype of breast cancer and due to the lack of expression of important receptors, TNBC patients do not benefit from endocrine and human epidermal growth factor receptor 2 (HER2)-targeted therapies. Considering the limitations of traditional treatment methods, immunotherapy might improve the survival rate and prognosis of TNBC patients based on its high specificity and immune memory, and thus hopefully, providing a new turning point for the treatment of TNBC.

In this research project, we proposed an immunotherapeutic strategy to treat the aggressive TNBC, combining a polymeric nanoparticle (NP)-based cancer vaccine with the immune checkpoint agonist, OX40. Here, we demonstrated the potential of NPs as cancer vaccines and their synergistic effect with the monoclonal antibody anti-OX40 (α OX40), obtaining a noteworthy tumour remission and improved overall survival, in TNBC-bearing mice. These results may be explained by the ability of i) these polymeric NPs to prime antigen-specific T cell responses, by targeting DCs, and ii) to decrease the expression of the immune suppressive cytokine transforming growth factor (TGF)- β overexpressed by DCs and the tumour cells; and iii) α OX40 to increase T-cell expansion, trafficking and the survival (197, 198), and block the inhibitory activity of tumour-infiltrating regulatory T-cells (199).

Although these findings provide important insights for the establishment of novel combination regimens against this aggressive tumour, there is still limited knowledge underlying the mechanisms of action of these immunotherapeutic strategies, and thus additional studies are needed. A better characterization of their mechanisms of action would help in identifying possible other immune cell populations involved in the overall anti-tumour immune response observed, and thus, adding important knowledge into better combinatorial therapies and schedules. In addition, deeper understanding of these mechanisms would also allow the identifications of additional biomarkers, which would facilitate the selection of the appropriate tumour patients to receive immunotherapeutic treatments.

Currently, there have been few studies on immunotherapy for TNBC patients. However, most of them are still at the basic research stage, and many problems remain to be solved, which may be improved by chosen the best tumour antigen and the best administration route for both cancer vaccines and immune checkpoint modulators.

Considering the tumour heterogeneity and phenotypic diversity, targeting of a single antigen may not be sufficient to achieve a complete tumour remission. By using

Conclusions and Future Perspectives

multiple tumour antigens or tumour lysates, the immune system can generate strong and long-lasting anti-tumour responses against each antigen and, thus, to target a higher number of cancer cells. However, the weak immunogenicity of tumour cells has led to the search for antigens with stronger immunogenicity, such as neoantigens. Neoantigens are a class of tumour-specific antigens that are generated from somatic mutations in tumours, but not in healthy tissue. These molecules have emerged as a promising path to personalized cancer immunotherapy that may overcome some challenges presented by tumour-associated antigens (TAA) (425). Advancements in sequencing technology, mass spectrometry, bioinformatics, and peptide manufacturing have simplified the identification of cancer neoantigens and the production of synthetic neoantigen peptides within a reasonable time course, making it possible to use them as cancer vaccines (426). The presence of these peptides is one of the essential differences between tumour cells and normal cells, and therefore, the idea of using them as vaccines to actively stimulate patients' immune system and, thus, generate anti-tumour response has gained recognition. Theoretically, compared to other types of antigens used in cancer vaccines, neoantigen vaccines, can induce stronger specific immune response and elicit stable therapeutic effects.

Another important aspect that may influence the overall anti-tumour response is the route of administration of the immunotherapeutic agents. Regarding cancer vaccines, few studies have shown that the route of administration influences the distribution of the vaccine upon injection and, consequently, lead to different anti-tumour immune responses (427, 428). Recently, intravenous administration of cancer vaccine has shown to elicit higher CTL response, when compared with the subcutaneous injections, resulting in more successful anti-tumour effects in mice (428). These differences depending on the administration routes were also observed upon the injection of a monoclonal antibody against the immune checkpoint agonist OX40 (α OX40), in mice. Indeed, it has been shown that the systemic delivery of α OX40 may favour the activation of peripheral lymphocytes rather than the intratumoural lymphocytes. Therefore, the intratumoural administration of α OX40 could enforce local priming of tumour-specific immune responses, while avoiding systemic toxicity (399).

Although some of the cancer immunotherapeutic agents presented impressive pre-clinical results, most of them failed in clinical trials. This may be explained by the unsuccessful translation from the pre-clinical models to humans. Animal models have been the major preclinical tool for the evaluation of novel diagnostic and therapeutic anticancer therapies before clinical testing. Mouse models, and more specifically syngeneic models, are the most commonly used preclinical model for the evaluation of immunotherapies, due to their ease of use and experimental reproducibility. However,

these models are frequently poor predictive of clinical challenges being the average rate of successful translation less than 8% (429). These models lack the genomic and microenvironmental (intra and inter) heterogeneity that defines cancer, and the implanted tumours develop as *de novo* poorly differentiated malignancies and do not undergo the natural steps of tumour evolution (pre-malignant transformation, tumour development, and progression) (430). The rapid kinetics for tumour growth in these models often provides an inadequate time window to evaluate immunotherapy efficacy, which impairs the evaluation of immunotherapeutics in earlier stages of disease (430). As an alternative, humanized patient-derived xenograft (PDX) mouse models have been developed for cancer immunotherapy research. Contrarily to syngeneic models, humanized mouse models present the complexity involved in natural tumour development, including genomic heterogeneity, tumour architecture, and microenvironment factors (430), that are critical to evaluate immunotherapeutic agents, as cancer vaccines and immune checkpoint modulators. Nevertheless, humanized mouse models are also associated with diverse drawbacks, namely: i) cost and time required for their development; ii) the success rate of engraftment of human tumour tissue into the mouse is variable; iii) humanized models present a short lifespan, which precludes, for instance, long survival assays; iv) they do not represent a complete immune system, lacking important immune cell populations (B cells, T cells, myeloid cells or NK cells) depending on the humanized model. Given these issues and the scientific limitations, it is important to assess whether these humanized models represent the best pre-clinical models to assess the efficacy of cancer immunotherapeutics.

Contrarily to the immune checkpoint modulators, few cancer vaccines have been approved so far by the American (FDA) and European (EMA) medicine agencies. Despite their tremendous potential for the treatment of a diversity of cancers, including TNBC, either as monotherapy or in combination with other therapeutic modalities, such as chemotherapy, radiotherapy, surgery, and immune checkpoint modulators, so far most of cancer vaccine trials have failed to show improvement in clinical outcome. In addition, the inconsistent data obtained from clinical studies and the lack of understanding of the mechanisms of action of cancer vaccines has unfortunately biased the view of many people against this therapeutic approach. For this reason, the pharmaceutical industry has tended to favour other anti-tumour options for production and marketing with the security of more financial return, such as cytotoxic chemotherapies and more recently, monoclonal antibodies (180). However, taking in consideration the multiple T cell-suppressive activities in TME, cancer vaccines cannot be expected to show optimal anticancer efficacy by themselves. As so, cancer vaccines

Conclusions and Future Perspectives

need to be used in combination treatments that are designed to inactivate the most important immunosuppressive mechanisms in this environment.

References

1. Bosetti C, Bertuccio P, Malvezzi M, Levi F, Chatenoud L, Negri E, et al. Cancer mortality in Europe, 2005–2009, and an overview of trends since 1980. *Ann Oncol*. 2013;24(10):2657-71.
2. DeSantis C, Ma J, Bryan L, Jemal A. Breast cancer statistics, 2013. *CA Cancer J Clin*. 2014;64(1):52-62.
3. Cancer: Breast cancer: World Health Organization; [cited 15/10/2018].
4. Redig A, McAllister S. Breast cancer as a systemic disease: a view of metastasis. *J Intern Med*. 2013;274(2):113-26.
5. Organization WH. Women and health: today's evidence tomorrow's agenda. 2009.
6. Howlader N, Noone A, Krapcho M, Garshell J, Miller D, Altekruse S, et al. SEER Cancer Statistics Review, 1975–2012. National Cancer Institute (Bethesda, MD), 2015.
7. Polyak K. Heterogeneity in breast cancer. *J Clin Invest*. 2011;121(10):3786-8.
8. Turashvili G, Brogi E. Tumor heterogeneity in breast cancer. *Front Med (Lausanne)*. 2017;4:227.
9. Yersal O, Barutca S. Biological subtypes of breast cancer: Prognostic and therapeutic implications. *World J Clin Oncol*. 2014;5(3):412.
10. Perou CM, Sørlie T, Eisen MB, Van De Rijn M, Jeffrey SS, Rees CA, et al. Molecular portraits of human breast tumours. *Nature*. 2000;406(6797):747.
11. Sørlie T, Perou CM, Tibshirani R, Aas T, Geisler S, Johnsen H, et al. Gene expression patterns of breast carcinomas distinguish tumor subclasses with clinical implications. *Proceedings of the National Academy of Sciences of the United States of America*. 2001;98(19):10869-74.
12. Sørlie T, Tibshirani R, Parker J, Hastie T, Marron JS, Nobel A, et al. Repeated observation of breast tumor subtypes in independent gene expression data sets. *Proceedings of the National Academy of Sciences of the United States of America*. 2003;100(14):8418-23.
13. Fragomeni SM, Sciallis A, Jeruss JS. Molecular subtypes and local-regional control of breast cancer. *Surg Oncol Clin N Am*. 2018;27(1):95-120.
14. Dai X, Li T, Bai Z, Yang Y, Liu X, Zhan J, et al. Breast cancer intrinsic subtype classification, clinical use and future trends. *Am J Cancer Res*. 2015;5(10):2929.
15. Subik K, Lee J, Baxter L, Strzepek T, Costello D, Crowley P, et al. Patterns of ER, PR, HER2, CK5/6, EGFR, Ki-67 and AR by immunohistochemical analysis in breast cancer cell lines. *Breast cancer: Basic and clinical research*. 2010; . 2018.
16. Voduc KD, Cheang MC, Tyldesley S, Gelmon K, Nielsen TO, Kennecke H. Breast cancer subtypes and the risk of local and regional relapse. *J Clin Oncol*. 2010;28(10):1684-91.
17. Sanpaolo P, Barbieri V, Genovesi D. Prognostic value of breast cancer subtypes on breast cancer specific survival, distant metastases and local relapse rates in conservatively managed early stage breast cancer: A retrospective clinical study. *Eur J Surg Oncol*. 2011;37(10):876-82.
18. Sihto H, Lundin J, Lundin M, Lehtimäki T, Ristimäki A, Holli K, et al. Breast cancer biological subtypes and protein expression predict for the preferential distant metastasis sites: a nationwide cohort study. *Breast Cancer Res*. 2011;13(5):R87.

19. Jatoi I, Anderson WF, Jeong J-H, Redmond CK. Breast cancer adjuvant therapy: time to consider its time-dependent effects. *J Clin Oncol*. 2011;29(17):2301.
20. Cheang MC, Chia SK, Voduc D, Gao D, Leung S, Snider J, et al. Ki67 Index, HER2 Status, and Prognosis of Patients With Luminal B Breast Cancer. *Journal of the National Cancer Institute*. 2009;101(10):736-50.
21. Inic Z, Zegarac M, Inic M, Markovic I, Kozomara Z, Djuricic I, et al. *Clin Med Insights Oncol*. *Clinical Medicine Insights: Oncology*. 2014;8:CMO.S18006.
22. Buonomo OC, Caredda E, Portarena I, Vanni G, Orlandi A, Bagni C, et al. New insights into the metastatic behavior after breast cancer surgery, according to well-established clinicopathological variables and molecular subtypes. *PLoS One*. 2017;12(9):e0184680-e.
23. Kennecke H, Yerushalmi R, Woods R, Cheang M, Voduc D, Speers C, et al. Metastatic behavior of breast cancer subtypes. *J Clin Oncol*. 2010;28(20):3271-7.
24. Sareyeldin RM, Gupta I, Al-Hashimi I, Al-Thawadi HA, Al Farsi HF, Vranic S, et al. Gene Expression and miRNAs Profiling: Function and Regulation in Human Epidermal Growth Factor Receptor 2 (HER2)-Positive Breast Cancer. *Cancers (Basel)*. 2019;11(5):646.
25. Wu Q, Li J, Zhu S, Wu J, Chen C, Liu Q, et al. Breast cancer subtypes predict the preferential site of distant metastases: a SEER based study. *Oncotarget*. 2017;8(17):27990.
26. Gabos Z, Sinha R, Hanson J, Chauhan N, Hugh J, Mackey JR, et al. Prognostic significance of human epidermal growth factor receptor positivity for the development of brain metastasis after newly diagnosed breast cancer. *J Clin Oncol*. 2006;24(36):5658-63.
27. Banerjee S, Reis-Filho JS, Ashley S, Steele D, Ashworth A, Lakhani SR, et al. Basal-like breast carcinomas: clinical outcome and response to chemotherapy. *J Clin Pathol*. 2006;59(7):729-35.
28. Milioli HH, Tishchenko I, Riveros C, Berretta R, Moscato P. Basal-like breast cancer: molecular profiles, clinical features and survival outcomes. *BMC Med Genomics*. 2017;10(1):19-.
29. Bertucci F, Finetti P, Cervera N, Esterni B, Hermitte F, Viens P, et al. How basal are triple-negative breast cancers? *Int J Cancer*. 2008;123(1):236-40.
30. Alluri P, Newman LA. Basal-like and triple-negative breast cancers: searching for positives among many negatives. *Surg Oncol Clin N Am*. 2014;23(3):567-77.
31. Foulkes WD, Smith IE, Reis-Filho JS. Triple-negative breast cancer. *N Engl J Med*. 2010;363(20):1938-48.
32. Criscitiello C, Azim H, Jr, Schouten P, Linn S, Sotiriou C. Understanding the biology of triple-negative breast cancer. *Ann Oncol*. 2012;23(suppl_6):vi13-vi8.
33. Chacón RD, Costanzo MV. Triple-negative breast cancer. *Breast Cancer Res*. 2010;12(2):S3.
34. Rakha EA, El-Sayed ME, Green AR, Lee AH, Robertson JF, Ellis IO. Prognostic markers in triple-negative breast cancer. *Cancer*. 2007;109(1):25-32.
35. Bauer K, Brown M, Cress R, Parise C, Caggiano V. Descriptive analysis of estrogen receptor (ER)-negative, progesterone receptor (PR)-negative, and HER2-negative invasive breast cancer, the so-called triple-negative phenotype: a population-based study from the California cancer Registry. *Cancer*. 2007;109(9):1721-8.

36. Siddharth S, Sharma D. Racial Disparity and Triple-Negative Breast Cancer in African-American Women: A Multifaceted Affair between Obesity, Biology, and Socioeconomic Determinants. *Cancers (Basel)*. 2018;10(12):514.
37. Foulkes W, Stefansson I, Chappuis P, Begin L, Goffin J, Wong N, et al. Germline BRCA1 mutations and a basal epithelial phenotype in breast cancer. *Journal of the National Cancer Institute*. 2003;95(19):1482-5.
38. Wang X, Qi Y, Kong X, Zhai J, Li Y, Song Y, et al. Immunological therapy: A novel thriving area for triple-negative breast cancer treatment. *Cancer Lett*. 2019;442:409-28.
39. Kassam F, Enright K, Dent R, Dranitsaris G, Myers J, Flynn C, et al. Survival outcomes for patients with metastatic triple-negative breast cancer: implications for clinical practice and trial design. *Clin Breast Cancer*. 2009;9(1):29-33.
40. Chue BM-F, La Course BD. Case report of long-term survival with metastatic triple-negative breast carcinoma: Treatment possibilities for metastatic disease. *Medicine (Baltimore)*. 2019;98(16):e15302-e.
41. Kumar P, Aggarwal R. An overview of triple-negative breast cancer. *Arch Gynecol Obstet*. 2016;293(2):247-69.
42. Tomao F, Papa A, Zaccarelli E, Rossi L, Caruso D, Minozzi M, et al. Triple-negative breast cancer: new perspectives for targeted therapies. *Onco Targets Ther*. 2015;8:177-93.
43. Bianchini G, Balko JM, Mayer IA, Sanders ME, Gianni L. Triple-negative breast cancer: challenges and opportunities of a heterogeneous disease. *Nature reviews Clinical oncology*. 2016;13(11):674-90.
44. Peer D, Karp JM, Hong S, Farokhzad OC, Margalit R, Langer R. Nanocarriers as an emerging platform for cancer therapy. *Nat Nanotechnol*. 2007;2(12):751.
45. Yagata H, Kajiura Y, Yamauchi H. Current strategy for triple-negative breast cancer: appropriate combination of surgery, radiation, and chemotherapy. *Breast Cancer*. 2011;18(3):165-73.
46. Haffty BG, Yang Q, Reiss M, Kearney T, Higgins SA, Weidhaas J, et al. Locoregional relapse and distant metastasis in conservatively managed triple negative early-stage breast cancer. *J Clin Oncol*. 2006;24(36):5652-7.
47. Nguyen PL, Taghian AG, Katz MS, Niemierko A, Abi Raad RF, Boon WL, et al. Breast cancer subtype approximated by estrogen receptor, progesterone receptor, and HER-2 is associated with local and distant recurrence after breast-conserving therapy. *J Clin Oncol*. 2008;26(14):2373-8.
48. Freedman GM, Anderson PR, Li T, Nicolaou N. Locoregional recurrence of triple-negative breast cancer after breast-conserving surgery and radiation. *Cancer*. 2009;115(5):946-51.
49. O'Rorke M, Murray L, Brand J, Bhoo-Pathy N. The value of adjuvant radiotherapy on survival and recurrence in triple-negative breast cancer: A systematic review and meta-analysis of 5507 patients. *Cancer Treat Rev*. 2016;47:12-21.
50. Yao Y, Chu Y, Xu B, Hu Q, Song Q. Radiotherapy after surgery has significant survival benefits for patients with triple-negative breast cancer. *Cancer Med*. 2019;8(2):554-63.
51. Group EBCTC. Comparisons between different polychemotherapy regimens for early breast cancer: meta-analyses of long-term outcome among 100 000 women in 123 randomised trials. *Lancet*. 2012;379(9814):432-44.

52. Nedeljković M, Damjanović A. Mechanisms of Chemotherapy Resistance in Triple-Negative Breast Cancer - How We Can Rise to the Challenge. *Cells*. 2019;8(9):957.
53. Echeverria GV, Ge Z, Seth S, Zhang X, Jeter-Jones S, Zhou X, et al. Resistance to neoadjuvant chemotherapy in triple-negative breast cancer mediated by a reversible drug-tolerant state. *Sci Transl Med*. 2019;11(488):eaav0936.
54. Cardoso F, Harbeck N, Fallowfield L, Kyriakides S, Senkus E. Locally recurrent or metastatic breast cancer: ESMO Clinical Practice Guidelines for diagnosis, treatment and follow-up. *Ann Oncol*. 2012;23(suppl_7):vii11-vii9.
55. Anampa J, Makower D, Sparano JA. Progress in adjuvant chemotherapy for breast cancer: an overview. *BMC Med Genomics*. 2015;13:195-.
56. Peto R, Davies C, Godwin J, Gray R, Pan H, Clarke M, et al. Early Breast Cancer Trialists' Collaborative G: Comparisons between different polychemotherapy regimens for early breast cancer: meta-analyses of long-term outcome among 100,000 women in 123 randomised trials. *Lancet*. 2012;379(9814):432-44.
57. Cortazar P, Zhang L, Untch M, Mehta K, Costantino JP, Wolmark N, et al. Pathological complete response and long-term clinical benefit in breast cancer: the CTNeoBC pooled analysis. *Lancet*. 2014;384(9938):164-72.
58. Von Minckwitz G, Untch M, Blohmer J-U, Costa SD, Eidtmann H, Fasching PA, et al. Definition and impact of pathologic complete response on prognosis after neoadjuvant chemotherapy in various intrinsic breast cancer subtypes. *J Clin Oncol*. 2012;30(15):1796-804.
59. Masuda N, Lee S-J, Ohtani S, Im Y-H, Lee E-S, Yokota I, et al. Adjuvant capecitabine for breast cancer after preoperative chemotherapy. *N Engl J Med*. 2017;376(22):2147-59.
60. Sikov WM, Berry DA, Perou CM, Singh B, Cirrincione CT, Tolaney SM, et al. Impact of the addition of carboplatin and/or bevacizumab to neoadjuvant once-per-week paclitaxel followed by dose-dense doxorubicin and cyclophosphamide on pathologic complete response rates in stage II to III triple-negative breast cancer: CALGB 40603 (Alliance). *J Clin Oncol*. 2015;33(1):13.
61. von Minckwitz G, Schneeweiss A, Loibl S, Salat C, Denkert C, Rezai M, et al. Neoadjuvant carboplatin in patients with triple-negative and HER2-positive early breast cancer (GeparSixto; GBG 66): a randomised phase 2 trial. *Lancet Oncol*. 2014;15(7):747-56.
62. Liu M, Mo QG, Wei CY, Qin QH, Huang Z, He J. Platinum-based chemotherapy in triple-negative breast cancer: A meta-analysis. *Oncol Lett*. 2013;5(3):983-91.
63. Coates AS, Winer EP, Goldhirsch A, Gelber RD, Gnant M, Piccart-Gebhart M, et al. Tailoring therapies - improving the management of early breast cancer: St Gallen International Expert Consensus on the Primary Therapy of Early Breast Cancer 2015. *Ann Oncol*. 2015;26(8):1533-46.
64. Zeichner SB, Terawaki H, Gogineni K. A review of systemic treatment in metastatic triple-negative breast cancer. *Breast Cancer (Auckl)*. 2016;10:BCBCR. S32783.
65. Senapati S, Mahanta AK, Kumar S, Maiti P. Controlled drug delivery vehicles for cancer treatment and their performance. *Signal Transduct Target Ther*. 2018;3(1):7.
66. Chidambaram M, Manavalan R, Kathiresan K. Nanotherapeutics to overcome conventional cancer chemotherapy limitations. *J Pharm Pharm Sci*. 2011;14(1):67-77.

67. O'Reilly EA, Gubbins L, Sharma S, Tully R, Guang MHZ, Weiner-Gorzel K, et al. The fate of chemoresistance in triple negative breast cancer (TNBC). *BBA Clin.* 2015;3:257-75.
68. Balko JM, Giltane JM, Wang K, Schwarz LJ, Young CD, Cook RS, et al. Molecular profiling of the residual disease of triple-negative breast cancers after neoadjuvant chemotherapy identifies actionable therapeutic targets. *Cancer Discov.* 2014;4(2):232-45.
69. Chalakur-Ramireddy NK, Pakala SB. Combined drug therapeutic strategies for the effective treatment of Triple Negative Breast Cancer. *Biosci Rep.* 2018;38(1):BSR20171357.
70. Shao F, Sun H, Deng C-X. Potential therapeutic targets of triple-negative breast cancer based on its intrinsic subtype. *Oncotarget.* 2017;8(42):73329-44.
71. Jamdade VS, Sethi N, Mundhe NA, Kumar P, Lahkar M, Sinha N. Therapeutic targets of triple-negative breast cancer: a review. *Br J Pharmacol.* 2015;172(17):4228-37.
72. Stergiopoulos SG. Emerging pathways in treating human epidermal growth factor receptor-2-negative breast cancer. *New Horiz Transl Med.* 2015;2(2):27-38.
73. Nakhjavani M, Hardingham JE, Palethorpe HM, Price TJ, Townsend AR. Druggable Molecular Targets for the Treatment of Triple Negative Breast Cancer. *J Breast Cancer.* 2019;22(3):341-61.
74. Hwang I, Ki D. Receptor-mediated T cell absorption of antigen presenting cell-derived molecules. *Front Biosci (Landmark Ed).* 2011;16:411.
75. Gregório AC, Lacerda M, Figueiredo P, Simões S, Dias S, Moreira JN. Therapeutic Implications of the Molecular and Immune Landscape of Triple-Negative Breast Cancer. *Pathol Oncol Res.* 2018;24(4):701-16.
76. Lee A, Djamgoz MB. Triple negative breast cancer: emerging therapeutic modalities and novel combination therapies. *Cancer Treat Rev.* 2018;62:110-22.
77. Audeh MW. Novel treatment strategies in triple-negative breast cancer: specific role of poly (adenosine diphosphate-ribose) polymerase inhibition. *Pharmacogenomics Pers Med.* 2014;7:307.
78. Li X, Heyer W-D. Homologous recombination in DNA repair and DNA damage tolerance. *Cell Res.* 2008;18(1):99-113.
79. Farmer H, McCabe N, Lord CJ, Tutt AN, Johnson DA, Richardson TB, et al. Targeting the DNA repair defect in BRCA mutant cells as a therapeutic strategy. *Nature.* 2005;434(7035):917.
80. Calabrese CR, Almassy R, Barton S, Batey MA, Calvert AH, Canan-Koch S, et al. Anticancer chemosensitization and radiosensitization by the novel poly (ADP-ribose) polymerase-1 inhibitor AG14361. *Journal of the National Cancer Institute.* 2004;96(1):56-67.
81. Nielsen TO, Hsu FD, Jensen K, Cheang M, Karaca G, Hu Z, et al. Immunohistochemical and clinical characterization of the basal-like subtype of invasive breast carcinoma. *Clin Cancer Res.* 2004;10(16):5367-74.
82. Yarden Y, Sliwkowski MX. Untangling the ErbB signalling network. *Nat Rev Mol Cell Biol.* 2001;2(2):127.
83. Rimawi MF, Shetty PB, Weiss HL, Schiff R, Osborne CK, Chamness GC, et al. Epidermal growth factor receptor expression in breast cancer association with biologic phenotype and clinical outcomes. *Cancer.* 2010;116(5):1234-42.

84. Brand TM, Iida M, Wheeler DL. Molecular mechanisms of resistance to the EGFR monoclonal antibody cetuximab. *Cancer Biol Ther.* 2011;11(9):777-92.
85. Cossu-Rocca P, Orrù S, Muroi MR, Sanges F, Sotgiu G, Ena S, et al. Analysis of PIK3CA mutations and activation pathways in triple negative breast cancer. *PLoS One.* 2015;10(11):e0141763.
86. Khan MA, Jain VK, Rizwanullah M, Ahmad J, Jain K. PI3K/AKT/mTOR pathway inhibitors in triple-negative breast cancer: a review on drug discovery and future challenges. *Drug Discov Today.* 2019;24(11):2181-91.
87. Costa R, Han H, Gradishar W. Targeting the PI3K/AKT/mTOR pathway in triple-negative breast cancer: a review. *Breast Cancer Res Treat.* 2018;169(3):397-406.
88. Chakrabarty A, Sánchez V, Kuba MG, Rinehart C, Arteaga CL. Feedback upregulation of HER3 (ErbB3) expression and activity attenuates antitumor effect of PI3K inhibitors. *Proceedings of the National Academy of Sciences of the United States of America.* 2012;109(8):2718-23.
89. Xu S, Li S, Guo Z, Luo J, Ellis MJ, Ma CX. Combined targeting of mTOR and AKT is an effective strategy for basal-like breast cancer in patient-derived xenograft models. *Mol Cancer Ther.* 2013;12(8):1665-75.
90. Sikandar B, Qureshi M, Naseem S, Khan S, Mirza T. Increased tumour infiltration of CD4+ and CD8+ T-lymphocytes in patients with triple negative breast cancer suggests susceptibility to immune therapy. *Asian Pac J Cancer Prev.* 2017;18(7):1827-32.
91. Budczies J, Bockmayr M, Denkert C, Klauschen F, Lennerz JK, Györfy B, et al. Classical pathology and mutational load of breast cancer—integration of two worlds. *J Pathol Clin Res.* 2015;1(4):225-38.
92. Pandya PH, Murray ME, Pollok KE, Renbarger JL. The Immune System in Cancer Pathogenesis: Potential Therapeutic Approaches. *J Immunol Res.* 2016;2016:4273943-.
93. Murphy K, Travers P, Walport M. Principles of innate and adaptive immunity. In: Murphy K, Weaver C, editors. *Janeway's Immunobiology 2007.* p. 1-38.
94. Parkin J, Cohen B. An overview of the immune system. *Lancet.* 2001;357(9270):1777-89.
95. Dranoff G. Cytokines in cancer pathogenesis and cancer therapy. *Nat Rev Cancer.* 2004;4(1):11.
96. Mortier A, Van Damme J, Proost P. Overview of the mechanisms regulating chemokine activity and availability. *Immunol Lett.* 2012;145(1):2-9.
97. Leleux J, Roy K. Micro and nanoparticle-based delivery systems for vaccine immunotherapy: an immunological and materials perspective. *Adv Healthc Mater.* 2013;2(1):72-94.
98. Delves PJ, Martin SJ, Burton DR, Roitt IM. *Roitt's Essential Immunology:* Wiley; 2017.
99. Punt J, Stranford S, Jones P, Owen J. *Kuby immunology:* Macmillan Higher Education; 2018.
100. Akira S, Hemmi H. Recognition of pathogen-associated molecular patterns by TLR family. *Immunol Lett.* 2003;85(2):85-95.
101. Sun JC, Lanier LL. Natural killer cells remember: an evolutionary bridge between innate and adaptive immunity? *Eur J Cancer.* 2009;39(8):2059-64.

102. Kolev M, Towner L, Donev R. Complement in Cancer and Cancer Immunotherapy. *Arch Immunol Ther Exp (Warsz)*. 2011;59(6):407-19.
103. Raphael I, Nalawade S, Eagar T, Forsthuber T. T cell subsets and their signature cytokines in autoimmune and inflammatory diseases. *Cytokine*. 2015;74(1):5-17.
104. Zhu J, Paul WE. CD4 T cells: fates, functions, and faults. *Blood*. 2008;112(5):1557-69.
105. Schenten D, Medzhitov R. The control of adaptive immune responses by the innate immune system. *Adv Immunol*. 109: Elsevier; 2011. p. 87-124.
106. Wculek SK, Cueto FJ, Mujal AM, Melero I, Krummel MF, Sancho D. Dendritic cells in cancer immunology and immunotherapy. *Nature reviews Immunology*. 2019.
107. Schlitzer A, McGovern N, Ginhoux F, editors. Dendritic cells and monocyte-derived cells: Two complementary and integrated functional systems. *Semin Cell Dev Biol*; 2015: Elsevier.
108. Pulendran B, Ahmed R. Translating innate immunity into immunological memory: implications for vaccine development. *Cell*. 2006;124(4):849-63.
109. Guermonprez P, Valladeau J, Zitvogel L, Théry C, Amigorena S. Antigen presentation and T cell stimulation by dendritic cells. *Annu Rev Immunol*. 2002;20(1):621-67.
110. Adams JL, Smothers J, Srinivasan R, Hoos A. Big opportunities for small molecules in immuno-oncology. *Nat Rev Drug Discov*. 2015;14(9):603-22.
111. Vesely MD, Kershaw MH, Schreiber RD, Smyth MJ. Natural innate and adaptive immunity to cancer. *Annu Rev Immunol*. 2011;29:235-71.
112. Finn OJ. Cancer immunology. *N Engl J Med*. 2008;358(25):2704-15.
113. Watts C. The exogenous pathway for antigen presentation on major histocompatibility complex class II and CD1 molecules. *Nat Immunol*. 2004;5(7):685-92.
114. Amigorena S, Savina A. Intracellular mechanisms of antigen cross presentation in dendritic cells. *Curr Opin Immunol*. 2010;22(1):109-17.
115. Vyas JM, Van der Veen AG, Ploegh HL. The known unknowns of antigen processing and presentation. *Nature reviews Immunology*. 2008;8(8):607-18.
116. Arens R, Schoenberger SP. Plasticity in programming of effector and memory CD8+ T-cell formation. *Immunol Rev*. 2010;235(1):190-205.
117. Hung K, Hayashi R, Lafond-Walker A, Lowenstein C, Pardoll D, Levitsky H. The central role of CD4+ T cells in the antitumor immune response. *J Exp Med*. 1998;188(12):2357-68.
118. Luckheeram RV, Zhou R, Verma AD, Xia B. CD4+ T cells: differentiation and functions. *Clin Dev Immunol*. 2012;2012.
119. Chaplin DD. Overview of the immune response. *J Allergy Clin Immunol Pract*. 2010;125(2, Supplement 2):S3-S23.
120. Swann JB, Smyth MJ. Immune surveillance of tumors. *J Clin Invest*. 2007;117(5):1137-46.
121. Dunn GP, Old LJ, Schreiber RD. The three Es of cancer immunoediting. *Annu Rev Immunol*. 2004;22:329-60.
122. Schreiber RD, Old LJ, Smyth MJ. Cancer immunoediting: integrating immunity's roles in cancer suppression and promotion. *Science*. 2011;331(6024):1565-70.

123. Matsueda S, Graham DY. Immunotherapy in gastric cancer. *World J Gastroenterol.* 2014;20(7):1657.
124. Matos AI, Carreira B, Peres C, Moura LI, Conriot J, Fourniols T, et al. Nanotechnology is an important strategy for combinational innovative chemo-immunotherapies against colorectal cancer. *J Control Release.* 2019;307:108-38.
125. Wu T, Dai Y. Tumor microenvironment and therapeutic response. *Cancer Lett.* 2017;387:61-8.
126. Valkenburg KC, de Groot AE, Pienta KJ. Targeting the tumour stroma to improve cancer therapy. *Nature reviews Clinical oncology.* 2018;15(6):366-81.
127. Gluz O, Nitz U, Harbeck N, Ting E, Kates R, Herr A, et al. Triple-negative high-risk breast cancer derives particular benefit from dose intensification of adjuvant chemotherapy: results of WSG AM-01 trial. *Ann Oncol.* 2008;19(5):861-70.
128. Bussard KM, Mutkus L, Stumpf K, Gomez-Manzano C, Marini FC. Tumor-associated stromal cells as key contributors to the tumor microenvironment. *Breast Cancer Res.* 2016;18(1):84.
129. Chouaib S, Kieda C, Benlalam H, Noman MZ, Mami-Chouaib F, Ruegg C. Endothelial cells as key determinants of the tumor microenvironment: interaction with tumor cells, extracellular matrix and immune killer cells. *Crit Rev Immunol.* 2010;30(6).
130. Madar S, Goldstein I, Rotter V. 'Cancer associated fibroblasts'—more than meets the eye. *Trends Mol Med.* 2013;19(8):447-53.
131. Ribatti D. *Inflammation and Angiogenesis: Springer; 2017.*
132. Mahmoud SM, Paish EC, Powe DG, Macmillan RD, Grainge MJ, Lee AH, et al. Tumor-infiltrating CD8+ lymphocytes predict clinical outcome in breast cancer. *J Clin Oncol.* 2011;29(15):1949-55.
133. Seo A, Lee H, Kim E, Kim H, Jang M, Lee H, et al. Tumour-infiltrating CD8+ lymphocytes as an independent predictive factor for pathological complete response to primary systemic therapy in breast cancer. *Br J Cancer.* 2013;109(10):2705.
134. Stanton SE, Adams S, Disis ML. Variation in the incidence and magnitude of tumor-infiltrating lymphocytes in breast cancer subtypes: a systematic review. *JAMA Oncol.* 2016;2(10):1354-60.
135. Liu F, Lang R, Zhao J, Zhang X, Pringle GA, Fan Y, et al. CD8+ cytotoxic T cell and FOXP3+ regulatory T cell infiltration in relation to breast cancer survival and molecular subtypes. *Breast Cancer Res Treat.* 2011;130(2):645-55.
136. Miyan M, Schmidt-Mende J, Kiessling R, Poschke I, de Boniface J. Differential tumor infiltration by T-cells characterizes intrinsic molecular subtypes in breast cancer. *J Transl Med.* 2016;14(1):227.
137. Allen M, Louise Jones J. Jekyll and Hyde: the role of the microenvironment on the progression of cancer. *J Pathol.* 2011;223(2):163-77.
138. Jang J-E, Hajdu CH, Liot C, Miller G, Dustin ML, Bar-Sagi D. Crosstalk between Regulatory T Cells and Tumor-Associated Dendritic Cells Negates Anti-tumor Immunity in Pancreatic Cancer. *Cell Rep.* 2017;20(3):558-71.
139. Mantovani A, Locati M. Tumor-associated macrophages as a paradigm of macrophage plasticity, diversity, and polarization: lessons and open questions. *Arterioscler Thromb Vasc Biol.* 2013;33(7):1478-83.

140. Wynn TA, Chawla A, Pollard JW. Macrophage biology in development, homeostasis and disease. *Nature*. 2013;496(7446):445-55.
141. Laoui D, Movahedi K, Van Overmeire E, Van den Bossche J, Schouppe E, Mommer C, et al. Tumor-associated macrophages in breast cancer: distinct subsets, distinct functions. *Int J Dev Biol*. 2011;55(7-8-9):861-7.
142. Hollmén M, Karaman S, Schwager S, Lisibach A, Christiansen AJ, Maksimow M, et al. G-CSF regulates macrophage phenotype and associates with poor overall survival in human triple-negative breast cancer. *Oncoimmunology*. 2016;5(3):e1115177.
143. Swierczak A, Mouchemore KA, Hamilton JA, Anderson RL. Neutrophils: important contributors to tumor progression and metastasis. *Cancer Metastasis Rev*. 2015;34(4):735-51.
144. Galdiero MR, Bonavita E, Barajon I, Garlanda C, Mantovani A, Jaillon S. Tumor associated macrophages and neutrophils in cancer. *Immunobiology*. 2013;218(11):1402-10.
145. Coffelt SB, Wellenstein MD, de Visser KE. Neutrophils in cancer: neutral no more. *Nat Rev Cancer*. 2016;16(7):431-46.
146. Rosser E, Mauri C. Regulatory B cells: origin, phenotype, and function. *Immunity*. 2015;42(4):607-12.
147. Sarvaria A, Madrigal JA, Saudemont A. B cell regulation in cancer and anti-tumor immunity. *Cell Mol Immunol*. 2017;14(8):662-74.
148. Olkhanud PB, Damdinsuren B, Bodogai M, Gress RE, Sen R, Wejksza K, et al. Tumor-evoked regulatory B cells promote breast cancer metastasis by converting resting CD4+ T cells to T-regulatory cells. *Cancer research*. 2011;71(10):3505-15.
149. Ishigami E, Sakakibara M, Sakakibara J, Masuda T, Fujimoto H, Hayama S, et al. Coexistence of regulatory B cells and regulatory T cells in tumor-infiltrating lymphocyte aggregates is a prognostic factor in patients with breast cancer. *Breast Cancer*. 2019;26(2):180-9.
150. Markowitz J, Wesolowski R, Papenfuss T, Brooks TR, Carson WE, 3rd. Myeloid-derived suppressor cells in breast cancer. *Breast Cancer Res Treat*. 2013;140(1):13-21.
151. Kumar S, Wilkes DW, Samuel N, Blanco MA, Nayak A, Alicea-Torres K, et al. Δ Np63-driven recruitment of myeloid-derived suppressor cells promotes metastasis in triple-negative breast cancer. *J Clin Invest*. 2018;128(11):5095-109.
152. Sato K, Uto T, Fukaya T, Takagi H. Regulatory Dendritic Cells. In: Yoshimura A, editor. *Emerging Concepts Targeting Immune Checkpoints in Cancer and Autoimmunity*. Cham: Springer International Publishing; 2017. p. 47-71.
153. Schmidt SV, Nino-Castro AC, Schultze JL. Regulatory dendritic cells: there is more than just immune activation. *Front Immunol*. 2012;3:274-.
154. Spranger S, Dai D, Horton B, Gajewski TF. Tumor-residing B_{atf3} dendritic cells are required for effector T cell trafficking and adoptive T cell therapy. *Cancer Cell*. 2017;31(5):711-23. e4.
155. Merad M, Sathe P, Helft J, Miller J, Mortha A. The dendritic cell lineage: ontogeny and function of dendritic cells and their subsets in the steady state and the inflamed setting. *Annu Rev Immunol*. 2013;31:563-604.
156. Böttcher JP, Reis e Sousa C. The role of type 1 conventional dendritic cells in cancer immunity. *Trends Cancer*. 2018;4(11):784-92.

157. Broz Miranda L, Binnewies M, Boldajipour B, Nelson Amanda E, Pollack Joshua L, Erle David J, et al. Dissecting the Tumor Myeloid Compartment Reveals Rare Activating Antigen-Presenting Cells Critical for T Cell Immunity. *Cancer Cell*. 2014;26(5):638-52.
158. Salmon H, Idoyaga J, Rahman A, Leboeuf M, Remark R, Jordan S, et al. Expansion and Activation of CD103(+) Dendritic Cell Progenitors at the Tumor Site Enhances Tumor Responses to Therapeutic PD-L1 and BRAF Inhibition. *Immunity*. 2016;44(4):924-38.
159. Sánchez-Paulete AR, Cueto FJ, Martínez-López M, Labiano S, Morales-Kastresana A, Rodríguez-Ruiz ME, et al. Cancer immunotherapy with immunomodulatory anti-CD137 and anti-PD-1 monoclonal antibodies requires BATF3-dependent dendritic cells. *Cancer Discov*. 2016;6(1):71-9.
160. Tussiwand R, Lee W-L, Murphy TL, Mashayekhi M, Wumesh K, Albring JC, et al. Compensatory dendritic cell development mediated by BATF-IRF interactions. *Nature*. 2012;490(7421):502.
161. Desch AN, Randolph GJ, Murphy K, Gautier EL, Kedl RM, Lahoud MH, et al. CD103+ pulmonary dendritic cells preferentially acquire and present apoptotic cell-associated antigen. *J Exp Med*. 2011;208(9):1789-97.
162. Desch AN, Gibbings SL, Clambey ET, Janssen WJ, Slansky JE, Kedl RM, et al. Dendritic cell subsets require cis-activation for cytotoxic CD8 T-cell induction. *Nat Commun*. 2014;5:4674.
163. Jakubzick C, Helft J, Kaplan TJ, Randolph GJ. Optimization of methods to study pulmonary dendritic cell migration reveals distinct capacities of DC subsets to acquire soluble versus particulate antigen. *J Immunol Methods*. 2008;337(2):121-31.
164. Zhang W, Wang L, Liu Y, Chen X, Liu Q, Jia J, et al. Immune responses to vaccines involving a combined antigen-nanoparticle mixture and nanoparticle-encapsulated antigen formulation. *Biomaterials*. 2014.
165. Gascard P, Tlsty TD. Carcinoma-associated fibroblasts: orchestrating the composition of malignancy. *Genes Dev*. 2016;30(9):1002-19.
166. Bottcher J, Bonavita E, Chakravarty P, Blees H, Cabeza-Cabrero M, Sammicheli S, et al. NK Cells Stimulate Recruitment of cDC1 into the Tumor Microenvironment Promoting Cancer Immune Control. *Cell*. 2018;172(5):1022-37.e14.
167. Ameres SL, Martinez J, Schroeder R. Molecular basis for target RNA recognition and cleavage by human RISC. *Cell*. 2007;130(1):101-12.
168. Buck MB, Knabbe C. TGF-beta signaling in breast cancer. *Ann N Y Acad Sci*. 2006;1089(1):119-26.
169. Xu J, Lamouille S, Derynck R. TGF-beta-induced epithelial to mesenchymal transition. *Cell Res*. 2009;19(2):156-72.
170. Casadevall A. Passive antibody therapies: progress and continuing challenges. *Clin Immunol*. 1999;93(1):5-15.
171. Bierie B, Moses HL. TGF-beta and cancer. *Cytokine Growth Factor Rev*. 2006;17(1):29-40.
172. Massagué J. TGF-beta in cancer. *Cell*. 2008;134(2):215-30.
173. Derynck R, Akhurst RJ, Balmain A. TGF-beta signaling in tumor suppression and cancer progression. *Nat Genet*. 2001;29(2):117-29.

174. Rubtsov YP, Rudensky AY. TGF β signalling in control of T-cell-mediated self-reactivity. *Nature reviews Immunology*. 2007;7(6):443-53.
175. Banerji S, Cibulskis K, Rangel-Escareno C, Brown KK, Carter SL, Frederick AM, et al. Sequence analysis of mutations and translocations across breast cancer subtypes. *Nature*. 2012;486(7403):405-9.
176. McArthur HL, Page DB. Immunotherapy for the treatment of breast cancer: checkpoint blockade, cancer vaccines, and future directions in combination immunotherapy. *Clin Adv Hematol Oncol*. 2016;14(11):922-33.
177. Galluzzi L, Vacchelli E, Bravo-San Pedro J-M, Buqué A, Senovilla L, Baracco EE, et al. Classification of current anticancer immunotherapies. *Oncotarget*. 2014;5(24):12472.
178. Page DB, Bourla AB, Daniyan A, Naidoo J, Smith E, Smith M, et al. Tumor immunology and cancer immunotherapy: summary of the 2014 SITC primer. *J Immunother Cancer*. 2015;3(25).
179. Le Du F, Eckhardt BL, Lim B, Litton JK, Moulder S, Meric-Bernstam F, et al. Is the future of personalized therapy in triple-negative breast cancer based on molecular subtype? *Oncotarget*. 2015;6(15):12890.
180. Coventry BJ. Therapeutic vaccination immunomodulation: forming the basis of all cancer immunotherapy. *Ther Adv Vaccines Immunother*. 2019;7:2515135519862234.
181. Lipson EJ, Forde P, Hammers H, Emens L, Taube J, Topalian S. Antagonists of PD-1 and PD-L1 in Cancer Treatment. *Seminars in oncology*. 2015;42(4):587-600.
182. Emens LA, Ascierto PA, Darcy PK, Demaria S, Eggermont AM, Redmond WL, et al. Cancer immunotherapy: opportunities and challenges in the rapidly evolving clinical landscape. *Eur J Cancer*. 2017;81:116-29.
183. Rudd CE, Taylor A, Schneider H. CD28 and CTLA-4 coreceptor expression and signal transduction. *Immunol Rev*. 2009;229(1):12-26.
184. Peggs KS, Quezada SA, Chambers CA, Korman AJ, Allison JP. Blockade of CTLA-4 on both effector and regulatory T cell compartments contributes to the antitumor activity of anti-CTLA-4 antibodies. *J Exp Med*. 2009;206(8):1717-25.
185. Wing K, Onishi Y, Prieto-Martin P, Yamaguchi T, Miyara M, Fehervari Z, et al. CTLA-4 control over Foxp3+ regulatory T cell function. *Science*. 2008;322(5899):271-5.
186. Faghfuri E, Faramarzi MA, Nikfar S, Abdollahi M. Nivolumab and pembrolizumab as immune-modulating monoclonal antibodies targeting the PD-1 receptor to treat melanoma. *Expert Rev Anticancer Ther*. 2015;15(9):981-93.
187. Hodi FS, O'Day SJ, McDermott DF, Weber RW, Sosman JA, Haanen JB, et al. Improved survival with ipilimumab in patients with metastatic melanoma. *N Engl J Med*. 2010;363(8):711-23.
188. Ai M, Curran MA. Immune checkpoint combinations from mouse to man. *Cancer Immunol Immunother*. 2015;64(7):885-92.
189. Bajwa R, Cheema A, Khan T, Amirpour A, Paul A, Chaughtai S, et al. Adverse Effects of Immune Checkpoint Inhibitors (Programmed Death-1 Inhibitors and Cytotoxic T-Lymphocyte-Associated Protein-4 Inhibitors): Results of a Retrospective Study. *J Clin Med Res*. 2019;11(4):225.
190. Page DB, Postow MA, Callahan MK, Allison JP, Wolchok JD. Immune modulation in cancer with antibodies. *Annu Rev Med*. 2014;65:185-202.

191. Hargadon KM, Johnson CE, Williams CJ. Immune checkpoint blockade therapy for cancer: an overview of FDA-approved immune checkpoint inhibitors. *Int Immunopharmacol.* 2018;62:29-39.
192. Heimes A-S, Schmidt M. Atezolizumab for the treatment of triple-negative breast cancer. *Expert Opin Investig Drugs.* 2019;28(1):1-5.
193. Brahmer JR, Tykodi SS, Chow LQ, Hwu W-J, Topalian SL, Hwu P, et al. Safety and activity of anti-PD-L1 antibody in patients with advanced cancer. *N Engl J Med.* 2012;366(26):2455-65.
194. Herbst RS, Soria J-C, Kowanetz M, Fine GD, Hamid O, Gordon MS, et al. Predictive correlates of response to the anti-PD-L1 antibody MPDL3280A in cancer patients. *Nature.* 2014;515(7528):563.
195. Swoboda A, Nanda R. Immune Checkpoint Blockade for Breast Cancer. *Cancer treatment and research.* 2018;173:155-65.
196. Polk A, Svane I, Andersson M, Nielsen D. Checkpoint inhibitors in breast cancer - Current status. *Cancer Treat Rev.* 2018;63:122-34.
197. Weinberg AD, Morris NP, Kovacsovics-Bankowski M, Urba WJ, Curti BD. Science gone translational: the OX40 agonist story. *Immunol Rev.* 2011;244(1):218-31.
198. Gramaglia I, Jember A, Pippig SD, Weinberg AD, Killeen N, Croft M. The OX40 costimulatory receptor determines the development of CD4 memory by regulating primary clonal expansion. *J Immunol.* 2000;165(6):3043-50.
199. Arch RH, Thompson CB. 4-1BB and Ox40 are members of a tumor necrosis factor (TNF)-nerve growth factor receptor subfamily that bind TNF receptor-associated factors and activate nuclear factor κB. *Mol Cell Biol.* 1998;18(1):558-65.
200. Vetto JT, Lum S, Morris A, Sicotte M, Davis J, Lemon M, et al. Presence of the T-cell activation marker OX-40 on tumor infiltrating lymphocytes and draining lymph node cells from patients with melanoma and head and neck cancers. *Am J Surg.* 1997;174(3):258-65.
201. Spranger S, Koblish HK, Horton B, Scherle PA, Newton R, Gajewski TF. Mechanism of tumor rejection with doublets of CTLA-4, PD-1/PD-L1, or IDO blockade involves restored IL-2 production and proliferation of CD8+ T cells directly within the tumor microenvironment. *J Immunother Cancer.* 2014;2(1):3.
202. Gajewski TF. The next hurdle in cancer immunotherapy: Overcoming the non-T-cell-inflamed tumor microenvironment. *Seminars in oncology.* 2015;42(4):663-71.
203. Minn AJ, Wherry EJ. Combination cancer therapies with immune checkpoint blockade: convergence on interferon signaling. *Cell.* 2016;165(2):272-5.
204. Adams S, Schmid P, Rugo H, Winer E, Loirat D, Awada A, et al. Pembrolizumab monotherapy for previously treated metastatic triple-negative breast cancer: cohort A of the phase II KEYNOTE-086 study. *Ann Oncol.* 2018;30(3):397-404.
205. Dirix L, Takacs I, Jerusalem G, Nikolinakos P, Arkenau H, Forero-Torres A, et al. Avelumab, an anti-PD-L1 antibody, in patients with locally advanced or metastatic breast cancer: a phase 1b JAVELIN Solid Tumor study. *Breast Cancer Res Treat.* 2018;167(3):671-86.
206. Schmid P, Cruz C, Braiteh FS, Eder JP, Tolaney S, Kuter I, et al. Abstract 2986: Atezolizumab in metastatic TNBC (mTNBC): Long-term clinical outcomes and biomarker analyses. *Cancer research.* 2017;77(13 Supplement):2986-.
207. Adams S, Loi S, Toppmeyer D, Cescon DW, De Laurentiis M, Nanda R, et al. Phase 2 study of pembrolizumab as first-line therapy for PD-L1-positive metastatic

- triple-negative breast cancer (mTNBC): preliminary data from KEYNOTE-086 cohort B. *Journal of Clinical Oncology*. 2017;35.
208. Wolchok JD, Chiarion-Sileni V, Gonzalez R, Rutkowski P, Grob J-J, Cowey CL, et al. Overall survival with combined nivolumab and ipilimumab in advanced melanoma. *N Engl J Med*. 2017;377(14):1345-56.
 209. Ott PA, Hu Z, Keskin DB, Shukla SA, Sun J, Bozym DJ, et al. An immunogenic personal neoantigen vaccine for patients with melanoma. *Nature*. 2017;547(7662):217.
 210. Sahin U, Derhovanessian E, Miller M, Kloke BP, Simon P, Lower M, et al. Personalized RNA mutanome vaccines mobilize poly-specific therapeutic immunity against cancer. *Nature*. 2017;547(7662):222-6.
 211. Conniot J, Scomparin A, Peres C, Yeini E, Pozzi S, Matos AI, et al. Immunization with mannosylated nanovaccines and inhibition of the immune-suppressing microenvironment sensitizes melanoma to immune checkpoint modulators. *Nat Nanotechnol*. 2019;14(9):891-901.
 212. Markman JL, Shiao SL. Impact of the immune system and immunotherapy in colorectal cancer. *J Gastrointest Oncol*. 2015;6(2):208.
 213. Couzin-Frankel J. Cancer immunotherapy. *Science*. 2013;342(6165):1432-3.
 214. Koerner J, Horvath D, Groettrup M. Harnessing Dendritic Cells for Poly (D, L-lactide-co-glycolide) Microspheres (PLGA MS)—Mediated Anti-tumor Therapy. *Front Immunol*. 2019;10.
 215. Silva JM, Videira M, Gaspar R, Pr eat V, Florindo HF. Immune system targeting by biodegradable nanoparticles for cancer vaccines. *J Control Release*. 2013;168(2):179-99.
 216. Krishnamachari Y, Geary SM, Lemke CD, Salem AK. Nanoparticle delivery systems in cancer vaccines. *Pharm Res*. 2011;28(2):215-36.
 217. Sarmiento B, das Neves J. Chitosan-based systems for biopharmaceuticals: delivery, targeting and polymer therapeutics: John Wiley & Sons; 2012.
 218. Coffman RL, Sher A, Seder RA. Vaccine adjuvants: putting innate immunity to work. *Immunity*. 2010;33(4):492-503.
 219. Palucka K, Banchereau J. Dendritic-cell-based therapeutic cancer vaccines. *Immunity*. 2013;39(1):38-48.
 220. Facciotti F, Cavallari M, Ang nieux C, Garcia-Alles LF, Signorino-Gelo F, Angman L, et al. Fine tuning by human CD1e of lipid-specific immune responses. *Proceedings of the National Academy of Sciences of the United States of America*. 2011;108(34):14228-33.
 221. Pashov AD, Monzavi-Karbassi B, Kieber-Emmons T. Glycan mediated immune responses to tumor cells. *Hum Vaccin*. 2011;7(sup1):156-65.
 222. Matera L. The choice of the antigen in the dendritic cell-based vaccine therapy for prostate cancer. *Cancer Treat Rev*. 2010;36(2):131-41.
 223. Mainardes RM, Silva LP. Drug delivery systems: past, present, and future. *Curr Drug Targets*. 2004;5(5):449-55.
 224. Srinivasan R, Wolchok JD. Tumor antigens for cancer immunotherapy: therapeutic potential of xenogeneic DNA vaccines. *J Transl Med*. 2004;2(1):12.
 225. Finn OJ. Human tumor antigens, immunosurveillance, and cancer vaccines. *Immunol Res*. 2006;36(1-3):73-82.

226. Florescu A, Amir E, Bouganim N, Clemons M. Immune therapy for breast cancer in 2010—hype or hope? *Curr Oncol*. 2011;18(1):e9-e18.
227. Tuohy VK, Jaini R, Johnson JM, Loya MG, Wilk D, Downs-Kelly E, et al. Targeted Vaccination against Human α -Lactalbumin for Immunotherapy and Primary Immunoprevention of Triple Negative Breast Cancer. *Cancers (Basel)*. 2016;8(6):56.
228. Chang A. Immunotherapy for Solid Malignancies, An Issue of Surgical Oncology Clinics of North America, Ebook: Elsevier; 2019.
229. Tuohy VK. Retired self-proteins as vaccine targets for primary immunoprevention of adult-onset cancers. *Expert Rev Vaccines*. 2014;13(12):1447-62.
230. Jaini R, Kesaraju P, Johnson JM, Altuntas CZ, Jane-Wit D, Tuohy VK. An autoimmune-mediated strategy for prophylactic breast cancer vaccination. *Nat Med*. 2010;16(7):799-803.
231. Nestle FO, Farkas A, Conrad C. Dendritic-cell-based therapeutic vaccination against cancer. *Curr Opin Immunol*. 2005;17(2):163-9.
232. Petrovsky N, Heinzl S, Honda Y, Lyons AB. New-age vaccine adjuvants: friend or foe? A major unsolved challenge in adjuvant development is how to achieve a potent adjuvant effect while avoiding reactogenicity or toxicity. *BioPharm Int*. 2007.
233. Tritto E, Mosca F, De Gregorio E. Mechanism of action of licensed vaccine adjuvants. *Vaccine*. 2009;27(25):3331-4.
234. O'Hagan DT, De Gregorio E. The path to a successful vaccine adjuvant—'the long and winding road'. *Drug Discov Today*. 2009;14(11):541-51.
235. Common ingredients in U.S. licensed vaccines: U.S. Food and Drug Administration (FDA); 2014 [updated 01/05/2014; cited 15/05/2014]. Available from: <http://www.fda.gov/BiologicsBloodVaccines/SafetyAvailability/VaccineSafety/ucm187810.htm>.
236. Baylor NW, Egan W, Richman P. Aluminum salts in vaccines - US perspective. *Vaccine*. 2002;20:S18-S23.
237. Petrovsky N, Heinzl S, Honda Y, Lyons AB. New-age vaccine adjuvants: friend or foe? A major unsolved challenge in adjuvant development is how to achieve a potent adjuvant effect while avoiding reactogenicity or toxicity. *BioPharm Int*. 2007;20(8):S24-S33.
238. Weeratna RD, McCluskie MJ. Recent Advances in Vaccine Adjuvants. In: Miller AA, Miller PF, editors. *Emerging Trends in Antibacterial Discovery: Answering the Call to Arms*: Caister Academic Press; 2011. p. 303.
239. Chen X, Kim P, Farinelli B, Doukas A, Yun S-H, Gelfand JA, et al. A novel laser vaccine adjuvant increases the motility of antigen presenting cells. *PLoS One*. 2010;5(10):e13776.
240. Morel S, Didierlaurent A, Bourguignon P, Delhaye S, Baras B, Jacob V, et al. Adjuvant System AS03 containing α -tocopherol modulates innate immune response and leads to improved adaptive immunity. *Vaccine*. 2011;29(13):2461-73.
241. Didierlaurent AM, Morel S, Lockman L, Giannini SL, Bisteau M, Carlsen H, et al. AS04, an Aluminum Salt- and TLR4 Agonist-Based Adjuvant System, Induces a Transient Localized Innate Immune Response Leading to Enhanced Adaptive Immunity. *J Immunol*. 2009;183(10):6186-97.

242. Del Giudice G, Fragapane E, Bugarini R, Hora M, Henriksson T, Palla E, et al. Vaccines with the MF59 Adjuvant Do Not Stimulate Antibody Responses against Squalene. *Clin Vaccine Immunol.* 2006;13(9):1010-3.
243. Montomoli E, Piccirella S, Khadang B, Mennitto E, Camerini R, De Rosa A. Current adjuvants and new perspectives in vaccine formulation. *Expert Rev Vaccines.* 2011;10(7):1053-61.
244. Van Duin D, Medzhitov R, Shaw AC. Triggering TLR signaling in vaccination. *Trends Immunol.* 2006;27(1):49-55.
245. Krieg AM. Therapeutic potential of Toll-like receptor 9 activation. *Nat Rev Drug Discov.* 2006;5(6):471-84.
246. Weeratna RD, Makinen SR, McCluskie MJ, Davis HL. TLR agonists as vaccine adjuvants: comparison of CpG ODN and Resiquimod (R-848). *Vaccine.* 2005;23(45):5263-70.
247. Iwasaki A, Medzhitov R. Toll-like receptor control of the adaptive immune responses. *Nat Immunol.* 2004;5(10):987-95.
248. Medzhitov R. Toll-like receptors and innate immunity. *Nature reviews Immunology.* 2001;1(2):135-45.
249. Kawai T, Akira S. TLR signaling. *Cell Death Differ.* 2006;13(5):816.
250. De Temmerman M-L, Rejman J, Demeester J, Irvine DJ, Gander B, De Smedt SC. Particulate vaccines: on the quest for optimal delivery and immune response. *Drug Discov Today.* 2011;16(13):569-82.
251. Peek LJ, Middaugh CR, Berkland C. Nanotechnology in vaccine delivery. *Advanced drug delivery reviews.* 2008;60(8):915-28.
252. Park Y-M, Lee SJ, Kim YS, Lee MH, Cha GS, Jung ID, et al. Nanoparticle-Based Vaccine Delivery for Cancer Immunotherapy. *Immune Netw.* 2013;13(5):177-83.
253. Gregory AE, Williamson D, Titball R. Vaccine delivery using nanoparticles. *Front Cell Infect Microbiol.* 2013;3:13.
254. Akagi T, Baba M, Akashi M. Biodegradable Nanoparticles as Vaccine Adjuvants and Delivery Systems: Regulation of Immune Responses by Nanoparticle-Based Vaccine. In: Kunugi S, Yamaoka T, editors. *Polymers in Nanomedicine.* Berlin, Heidelberg: Springer Berlin Heidelberg; 2012. p. 31-64.
255. Bachmann MF, Jennings GT. Vaccine delivery: a matter of size, geometry, kinetics and molecular patterns. *Nature reviews Immunology.* 2010;10(11):787-96.
256. Panyam J, Labhasetwar V. Biodegradable nanoparticles for drug and gene delivery to cells and tissue. *Advanced drug delivery reviews.* 2003;55(3):329-47.
257. Ikada Y, Tsuji H. Biodegradable polyesters for medical and ecological applications. *Macromol Rapid Commun.* 2000;21(3):117-32.
258. Giarelli E. Cancer vaccines: a new frontier in prevention and treatment. *Oncology (Williston Park).* 2007;21(11 Suppl Nurse Ed):11-7; discussion 8.
259. Perz JF, Armstrong GL, Farrington LA, Hutin YJ, Bell BP. The contributions of hepatitis B virus and hepatitis C virus infections to cirrhosis and primary liver cancer worldwide. *J Hepatol.* 2006;45(4):529-38.
260. Schiffman M, Castle PE, Jeronimo J, Rodriguez AC, Wacholder S. Human papillomavirus and cervical cancer. *Lancet.* 2007;370(9590):890-907.
261. Cheever MA, Higano CS. PROVENGE (Sipuleucel-T) in prostate cancer: the first FDA-approved therapeutic cancer vaccine. *Clin Cancer Res.* 2011;17(11):3520-6.

262. Quintero IB, Araujo CL, Pulkka AE, Wirkkala RS, Herrala AM, Eskelinen E-L, et al. Prostatic acid phosphatase is not a prostate specific target. *Cancer research*. 2007;67(14):6549-54.
263. Vikas P, Borchering N, Zhang W. The clinical promise of immunotherapy in triple-negative breast cancer. *Cancer Manag Res*. 2018;10:6823.
264. Palucka K, Banchereau J. Cancer immunotherapy via dendritic cells. *Nat Rev Cancer*. 2012;12(4):265.
265. Banchereau J, Pacesny S, Blanco P, Bennett L, Pascual V, Fay J, et al. Dendritic cells: controllers of the immune system and a new promise for immunotherapy. *Ann N Y Acad Sci*. 2003;987(1):180-7.
266. Banchereau J, Palucka AK. Dendritic cells as therapeutic vaccines against cancer. *Nature reviews Immunology*. 2005;5(4):296-306.
267. Hillaireau H, Couvreur P. Nanocarriers' entry into the cell: relevance to drug delivery. *Cell Mol Life Sci*. 2009;66(17):2873-96.
268. Merad M, Manz MG. Dendritic cell homeostasis. *Blood*. 2009;113(15):3418-27.
269. Kadowaki N. Dendritic Cells - A Conductor of T Cell Differentiation. *Allergol Int*. 2007;56(3):193-9.
270. Martín-Fontecha A, Sebastiani S, Höpken UE, Uguccioni M, Lipp M, Lanzavecchia A, et al. Regulation of dendritic cell migration to the draining lymph node: impact on T lymphocyte traffic and priming. *J Exp Med*. 2003;198(4):615-21.
271. Takeuchi S, Furue M. Dendritic Cells - Ontogeny. *Allergol Int*. 2007;56(3):215-23.
272. Gogolák P, Réthi B, Hajas G, Rajnavölgyi É. Targeting dendritic cells for priming cellular immune responses. *J Mol Recognit*. 2003;16(5):299-317.
273. Gilboa E. The promise of cancer vaccines. *Nat Rev Cancer*. 2004;4(5):401-11.
274. Sallusto F, Geginat J, Lanzavecchia A. Central memory and effector memory T cell subsets: function, generation, and maintenance. *Annu Rev Immunol*. 2004;22:745-63.
275. Kim BY, Rutka JT, Chan WC. Nanomedicine. *N Engl J Med*. 2010;363(25):2434-43.
276. Ferrari M. Cancer nanotechnology: opportunities and challenges. *Nat Rev Cancer*. 2005;5(3):161-71.
277. Xu H, Li Z, Si J. Nanocarriers in gene therapy: a review. *J Biomed Nanotechnol*. 2014;10(12):3483-507.
278. Yang Y, Chawla A, Zhang J, Esa A, Jang HL, Khademhosseini A. Chapter 29 - Applications of Nanotechnology for Regenerative Medicine; Healing Tissues at the Nanoscale. In: Atala A, Lanza R, Mikos AG, Nerem R, editors. *Principles of Regenerative Medicine (Third Edition)*. Boston: Academic Press; 2019. p. 485-504.
279. Suri SS, Fenniri H, Singh B. Nanotechnology-based drug delivery systems. *J Occup Med Toxicol*. 2007;2(1):16.
280. Toy R, Bauer L, Hoimes C, Ghaghada KB, Karathanasis E. Targeted nanotechnology for cancer imaging. *Advanced drug delivery reviews*. 2014;76:79-97.
281. Zhang X, Guo Q, Cui D. Recent advances in nanotechnology applied to biosensors. *Sensors*. 2009;9(2):1033-53.

282. Ryu JH, Lee S, Son S, Kim SH, Leary JF, Choi K, et al. Theranostic nanoparticles for future personalized medicine. *J Control Release*. 2014;190:477-84.
283. Alexis F, Rhee J-W, Richie JP, Radovic-Moreno AF, Langer R, Farokhzad OC. New frontiers in nanotechnology for cancer treatment. *Urol Oncol*. 2008;26(1):74-85.
284. Conniot J, Silva JM, Fernandes JG, Silva LC, Gaspar R, Brocchini S, et al. Cancer immunotherapy: nanodelivery approaches for immune cell targeting and tracking. *Frontiers in chemistry*. 2014;2:105.
285. Joshi MD, Unger WJ, Storm G, Van Kooyk Y, Mastrobattista E. Targeting tumor antigens to dendritic cells using particulate carriers. *J Control Release*. 2012;161(1):25-37.
286. Wicki A, Witzigmann D, Balasubramanian V, Huwyler J. Nanomedicine in cancer therapy: challenges, opportunities, and clinical applications. *J Control Release*. 2015;200:138-57.
287. Zupancic E, Peres C, I Matos A, Lopes J, N Moreira J, S Gaspar R, et al. Translational Peptide-Associated Nanosystems: Promising Role as Cancer Vaccines. *Curr Top Med Chem*. 2016;16(3):291-313.
288. Peres C, Matos AI, Conniot J, Sainz V, Zupančič E, Silva JM, et al. Poly (lactic acid)-based particulate systems are promising tools for immune modulation. *Acta Biomater*. 2017;48:41-57.
289. Mishra B, Patel BB, Tiwari S. Colloidal nanocarriers: a review on formulation technology, types and applications toward targeted drug delivery. *Nanomedicine*. 2010;6(1):9-24.
290. Krishnamoorthy K, Mahalingam M. Selection of a suitable method for the preparation of polymeric nanoparticles: multi-criteria decision making approach. *Adv Pharm Bull*. 2015;5(1):57-67.
291. Rawat M, Singh D, Saraf S, Saraf S. Nanocarriers: Promising Vehicle for Bioactive Drugs. *Biol Pharm Bull*. 2006;29(9):1790-8.
292. Gelperina S, Kisich K, Iseman M, Heifets L. The potential advantages of nanoparticle drug delivery systems in chemotherapy of tuberculosis. *Am J Respir Crit Care Med*. 2005;172(12):1487-90.
293. Kumari A, Yadav SK, Yadav SC. Biodegradable polymeric nanoparticles based drug delivery systems. *Colloids Surf B Biointerfaces*. 2010;75(1):1-18.
294. Singh R, Lillard JW. Nanoparticle-based targeted drug delivery. *Exp Mol Pathol*. 2009;86(3):215-23.
295. Noble GT, Stefanick JF, Ashley JD, Kiziltepe T, Bilgicer B. Ligand-targeted liposome design: challenges and fundamental considerations. *Trends Biotechnol*. 2014;32(1):32-45.
296. Mitragotri S, Burke PA, Langer R. Overcoming the challenges in administering biopharmaceuticals: formulation and delivery strategies. *Nat Rev Drug Discov*. 2014;13(9):655-72.
297. Lee BK, Yun Y, Park K. PLA micro-and nano-particles. *Advanced drug delivery reviews*. 2016;107:176-91.
298. Gaspar R. *Therapeutic products: regulating drugs and medical devices*: Edward Elgar Publishing; 2010.
299. Abraham J. International Conference On Harmonisation Of Technical Requirements For Registration Of Pharmaceuticals For Human Use. In: Tietje C,

- Brouder A, editors. Handbook of transnational economic governance regimes. Leiden, The Netherlands: Brill Nijhoff; 2010. p. 1041-53.
300. Shakya AK, Madhyastha H. Polymeric Nanoparticles for Vaccine Delivery. In: Nayak B, Nanda A, Baht MA, editors. Integrating Biologically-Inspired Nanotechnology into Medical Practice: IGI Global; 2017. p. 32-49.
 301. Smith JD, Morton LD, Ulery BD. Nanoparticles as synthetic vaccines. *Curr Opin Biotechnol.* 2015;34:217-24.
 302. Torchilin V. Intracellular delivery of protein and peptide therapeutics. *Drug Discov Today Technol.* 2008;5(2-3):e95-e103.
 303. Demento SL, Cui W, Criscione JM, Stern E, Tulipan J, Kaech SM, et al. Role of sustained antigen release from nanoparticle vaccines in shaping the T cell memory phenotype. *Biomaterials.* 2012;33(19):4957-64.
 304. Oyewumi MO, Kumar A, Cui Z. Nano-microparticles as immune adjuvants: correlating particle sizes and the resultant immune responses. *Expert Rev Vaccines.* 2010;9(9):1095-107.
 305. Steinhagen F, Kinjo T, Bode C, Klinman DM. TLR-based immune adjuvants. *Vaccine.* 2011;29(17):3341-55.
 306. Pavot V, Berthet M, Rességuier J, Legaz S, Handké N, Gilbert SC, et al. Poly (lactic acid) and poly (lactic-co-glycolic acid) particles as versatile carrier platforms for vaccine delivery. *Nanomedicine (Lond).* 2014;9(17):2703-18.
 307. Sanchez A, Gupta RK, Alonso MJ, Siber GR, Langer R. Pulsed Controlled-Release System for Potential Use in Vaccine Delivery. *J Pharm Sci.* 1996;85(6):547-52.
 308. Beier R, Gebert A. Kinetics of particle uptake in the domes of Peyer's patches. *Am J Physiol Gastrointest Liver Physiol.* 1998;275(1):G130-G7.
 309. Cruz LJ, Tacke PJ, Fokkink R, Joosten B, Stuart MC, Albericio F, et al. Targeted PLGA nano- but not microparticles specifically deliver antigen to human dendritic cells via DC-SIGN in vitro. *J Control Release.* 2010;144(2):118-26.
 310. Thomas SN, Vokali E, Lund AW, Hubbell JA, Swartz MA. Targeting the tumor-draining lymph node with adjuvanted nanoparticles reshapes the anti-tumor immune response. *Biomaterials.* 2014;35(2):814-24.
 311. Reddy ST, Rehor A, Schmoekel HG, Hubbell JA, Swartz MA. In vivo targeting of dendritic cells in lymph nodes with poly(propylene sulfide) nanoparticles. *J Control Release.* 2006;112(1):26-34.
 312. Yan S, Gu W, Xu ZP. Re-considering how particle size and other properties of antigen–adjuvant complexes impact on the immune responses. *J Colloid Interface Sci.* 2013;395:1-10.
 313. Gamvrellis A, Leong D, Hanley J, Xiang S, Mottram P, Plebanski M. Vaccines that facilitate antigen entry into dendritic cells. *Immunol Cell Biol.* 2004;82(5):506-16.
 314. Sahay G, Alakhova DY, Kabanov AV. Endocytosis of nanomedicines. *J Control Release.* 2010;145(3):182-95.
 315. Ehrlich M, Boll W, van Oijen A, Hariharan R, Chandran K, Nibert ML, et al. Endocytosis by Random Initiation and Stabilization of Clathrin-Coated Pits. *Cell.* 2004;118(5):591-605.
 316. Wang Z, Tiruppathi C, Minshall RD, Malik AB. Size and Dynamics of Caveolae Studied Using Nanoparticles in Living Endothelial Cells. *ACS Nano.* 2009;3(12):4110-6.

317. Xiang SD, Scholzen A, Minigo G, David C, Apostolopoulos V, Mottram PL, et al. Pathogen recognition and development of particulate vaccines: does size matter? *Methods*. 2006;40(1):1-9.
318. Wilson N, El-Sukkari D, Belz G, Smith C, Steptoe R, Heath W, et al. Most lymphoid organ dendritic cell types are phenotypically and functionally immature. *Blood*. 2003;102(6):2187-94.
319. Gratton SE, Ropp PA, Pohlhaus PD, Luft JC, Madden VJ, Napier ME, et al. The effect of particle design on cellular internalization pathways. *Proceedings of the National Academy of Sciences of the United States of America*. 2008;105(33):11613-8.
320. Herd H, Daum N, Jones AT, Huwer H, Ghandehari H, Lehr C-M. Nanoparticle geometry and surface orientation influence mode of cellular uptake. *ACS Nano*. 2013;7(3):1961-73.
321. Alexis F, Pridgen E, Molnar LK, Farokhzad OC. Factors Affecting the Clearance and Biodistribution of Polymeric Nanoparticles. *Mol Pharm*. 2008;5(4):505-15.
322. Foged C, Brodin B, Frokjaer S, Sundblad A. Particle size and surface charge affect particle uptake by human dendritic cells in an in vitro model. *Int J Pharm*. 2005;298(2):315-22.
323. Vasir JK, Labhsetwar V. Quantification of the force of nanoparticle-cell membrane interactions and its influence on intracellular trafficking of nanoparticles. *Biomaterials*. 2008;29(31):4244-52.
324. Knudsen KB, Northeved H, Kumar Ek P, Permin A, Gjetting T, Andresen TL, et al. In vivo toxicity of cationic micelles and liposomes. *Nanomedicine* 2015;11(2):467-77.
325. Cho EC, Zhang Q, Xia Y. The effect of sedimentation and diffusion on cellular uptake of gold nanoparticles. *Nat Nanotechnol*. 2011;6(6):385-91.
326. Owens III DE, Peppas NA. Opsonization, biodistribution, and pharmacokinetics of polymeric nanoparticles. *Int J Pharm*. 2006;307(1):93-102.
327. Hatakeyama H, Akita H, Harashima H. A multifunctional envelope type nano device (MEND) for gene delivery to tumours based on the EPR effect: a strategy for overcoming the PEG dilemma. *Advanced drug delivery reviews*. 2011;63(3):152-60.
328. Sahay G, Alakhova DY, Kabanov AV. Endocytosis of nanomedicines. *Journal of controlled release*. 2010;145(3):182-95.
329. Lasprilla AJ, Martinez GA, Lunelli BH, Jardini AL. Poly-lactic acid synthesis for application in biomedical devices - A review. *Biotechnol Adv*. 2012;30(1):321-8.
330. Auras RA, Lim L-T, Selke SE, Tsuji H. *Poly (lactic acid): synthesis, structures, properties, processing, and applications*: John Wiley & Sons; 2011.
331. Lopes MS, Jardini A, Filho RM. *Poly (Lactic Acid) Production for Tissue Engineering Applications*. *Procedia Engineering*. 2012;42:1402-13.
332. Albertsson A-C, Varma IK. *Aliphatic Polyesters: Synthesis, Properties and Applications*. *Degradable Aliphatic Polyesters*. Berlin, Heidelberg: Springer Berlin Heidelberg; 2002. p. 1-40.
333. Lassalle V, Ferreira ML. *PLA Nano-and Microparticles for Drug Delivery: An Overview of the Methods of Preparation*. *Macromol Biosci*. 2007;7(6):767-83.

334. Athanasiou KA, Niederauer GG, Agrawal CM. Sterilization, toxicity, biocompatibility and clinical applications of polylactic acid/polyglycolic acid copolymers. *Biomaterials*. 1996;17(2):93-102.
335. Dixit S, Singh SR, Yilma AN, Agee II RD, Taha M, Dennis VA. Poly (lactic acid)–poly (ethylene glycol) nanoparticles provide sustained delivery of a< i> Chlamydia trachomatis</i> recombinant MOMP peptide and potentiate systemic adaptive immune responses in mice. *Nanomedicine*. 2014.
336. Baxendale A, van Hooff P, Durrant L, Spendlove I, Howdle S, Woods H, et al. Single shot tetanus vaccine manufactured by a supercritical fluid encapsulation technology. *Int J Pharm*. 2011;413(1):147-54.
337. Vila A, Sanchez A, Evora C, Soriano I, Vila Jato J, Alonso M. PEG-PLA nanoparticles as carriers for nasal vaccine delivery. *J Aerosol Med*. 2004;17(2):174-85.
338. Raghuvanshi RS, Katare YK, Lalwani K, Ali MM, Singh O, Panda AK. Improved immune response from biodegradable polymer particles entrapping tetanus toxoid by use of different immunization protocol and adjuvants. *Int J Pharm*. 2002;245(1):109-21.
339. Johansen P, Estevez F, Zurbriggen R, Merkle HP, Glück R, Corradin G, et al. Towards clinical testing of a single-administration tetanus vaccine based on PLA/PLGA microspheres. *Vaccine*. 2000;19(9):1047-54.
340. Anish C, Goswami DG, Kanchan V, Mathew S, Panda AK. The immunogenic characteristics associated with multivalent display of Vi polysaccharide antigen using biodegradable polymer particles. *Biomaterials*. 2012;33(28):6843-57.
341. Eyles JE, Sharp GJE, Diane Williamson E, Spiers ID, Oya Alpar H. Intra nasal administration of poly-lactic acid microsphere co-encapsulated Yersinia pestis subunits confers protection from pneumonic plague in the mouse. *Vaccine*. 1998;16(7):698-707.
342. Florindo H, Pandit S, Gonçalves L, Alpar H, Almeida A. New approach on the development of a mucosal vaccine against stranglers: Systemic and mucosal immune responses in a mouse model. *Vaccine*. 2009;27(8):1230-41.
343. Florindo HF, Pandit S, Gonçalves LM, Videira M, Alpar O, Almeida AJ. Antibody and cytokine-associated immune responses to S. equi antigens entrapped in PLA nanospheres. *Biomaterials*. 2009;30(28):5161-9.
344. McCartney S, Vermi W, Gilfillan S, Cella M, Murphy TL, Schreiber RD, et al. Distinct and complementary functions of MDA5 and TLR3 in poly(I:C)-mediated activation of mouse NK cells. *J Exp Med*. 2009;206(13):2967-76.
345. Jain AK, Goyal AK, Gupta PN, Khatri K, Mishra N, Mehta A, et al. Synthesis, characterization and evaluation of novel triblock copolymer based nanoparticles for vaccine delivery against hepatitis B. *J Control Release*. 2009;136(2):161-9.
346. Jain AK, Goyal AK, Mishra N, Vaidya B, Mangal S, Vyas SP. PEG–PLA–PEG block copolymeric nanoparticles for oral immunization against hepatitis B. *Int J Pharm*. 2010;387(1):253-62.
347. Lv S, Wang J, Dou S, Yang X, Ni X, Sun R, et al. Nanoparticles encapsulating hepatitis B virus cytosine-phosphate-guanosine induce therapeutic immunity against HBV infection. *Hepatology*. 2014;59(2):385-94.
348. Thomas C, Rawat A, Hope-Weeks L, Ahsan F. Aerosolized PLA and PLGA Nanoparticles Enhance Humoral, Mucosal and Cytokine Responses to Hepatitis B Vaccine. *Mol Pharm*. 2011;8(2):405-15.

349. Pandit S, Cevher E, Zariwala MG, Somavarapu S, Alpar HO. Enhancement of immune response of HBsAg loaded poly (L-lactic acid) microspheres against Hepatitis B through incorporation of alum and chitosan. *J Microencapsul.* 2007;24(6):539-52.
350. Chen X, Liu Y, Wang L, Liu Y, Zhang W, Fan B, et al. Enhanced Humoral and Cell-Mediated Immune Responses Generated by Cationic Polymer-Coated PLA Microspheres with Adsorbed HBsAg. *Mol Pharm.* 2014;11(6):1772-84.
351. Ataman-Önal Y, Munier S, Ganée A, Terrat C, Durand P-Y, Battail N, et al. Surfactant-free anionic PLA nanoparticles coated with HIV-1 p24 protein induced enhanced cellular and humoral immune responses in various animal models. *J Control Release.* 2006;112(2):175-85.
352. Aline F, Brand D, Pierre J, Roingard P, Séverine M, Verrier B, et al. Dendritic cells loaded with HIV-1 p24 proteins adsorbed on surfactant-free anionic PLA nanoparticles induce enhanced cellular immune responses against HIV-1 after vaccination. *Vaccine.* 2009;27(38):5284-91.
353. Guillon C, Mayol K, Terrat C, Compagnon C, Primard C, Charles M-H, et al. Formulation of HIV-1 Tat and p24 antigens by PLA nanoparticles or MF59 impacts the breadth, but not the magnitude, of serum and faecal antibody responses in rabbits. *Vaccine.* 2007;25(43):7491-501.
354. Lamalle-Bernard D, Munier S, Compagnon C, Charles M-H, Kalyanaraman VS, Delair T, et al. Co-adsorption of HIV-1 p24 and gp120 proteins to surfactant-free anionic PLA nanoparticles preserves antigenicity and immunogenicity. *J Control Release.* 2006;115(1):57-67.
355. Liard C, Munier S, Arias M, Joulin-Giet A, Bonduelle O, Duffy D, et al. Targeting of HIV-p24 particle-based vaccine into differential skin layers induces distinct arms of the immune responses. *Vaccine.* 2011;29(37):6379-91.
356. Pavot V, Rochereau N, Primard C, Genin C, Perouzel E, Lioux T, et al. Encapsulation of Nod1 and Nod2 receptor ligands into poly(lactic acid) nanoparticles potentiates their immune properties. *J Control Release.* 2013;167(1):60-7.
357. Thapa P, Zhang G, Xia C, Gelbard A, Overwijk WW, Liu C, et al. Nanoparticle formulated alpha-galactosylceramide activates NKT cells without inducing anergy. *Vaccine.* 2009;27(25):3484-8.
358. Climent N, Munier S, Piqué N, García F, Pavot V, Primard C, et al. Loading dendritic cells with PLA-p24 nanoparticles or MVA expressing HIV genes induces HIV-1-specific T cell responses. *Vaccine.* 2014;32(47):6266-76.
359. Pavot V, Climent N, Rochereau N, Garcia F, Genin C, Tiraby G, et al. Directing vaccine immune responses to mucosa by nanosized particulate carriers encapsulating NOD ligands. *Biomaterials.* 2016;75:327-39.
360. Chen W-L, Liu S-J, Leng C-H, Chen H-W, Chong P, Huang M-H. Disintegration and cancer immunotherapy efficacy of a squalane-in-water delivery system emulsified by bioresorbable poly(ethylene glycol)-block-poly(lactide). *Biomaterials.* 2014;35(5):1686-95.
361. Men Y, Gander B, Merkle H, Corradin G. Induction of sustained and elevated immune responses to weakly immunogenic synthetic malarial peptides by encapsulation in biodegradable polymer microspheres. *Vaccine.* 1996;14(15):1442-50.
362. Kissick HT, Sanda MG. The role of active vaccination in cancer immunotherapy: lessons from clinical trials. *Curr Opin Immunol.* 2015;35:15-22.

363. Dominguez AL, Lustgarten J. Targeting the tumor microenvironment with anti-neu/anti-CD40 conjugated nanoparticles for the induction of antitumor immune responses. *Vaccine*. 2010;28(5):1383-90.
364. Egilmez N, Jong Y, Sabel M, Jacob J, Mathiowitz E, Bankert R. In situ tumor vaccination with interleukin-12-encapsulated biodegradable microspheres: Induction of tumor regression and potent antitumor immunity. *Cancer research*. 2000;60(14):3832-7.
365. Afonso CA, Santhakumar V, Lough A, Batey RA. An expedient synthesis of cationic rhodamine fluorescent probes suitable for conjugation to amino acids and peptides. *Synthesis*. 2003;2003(17):2647-54.
366. Freichels H, Danhier F, Pr eat V, Lecomte P, J er ome C. Fluorescent Labeling of Degradable Poly(Lactide-Co-Glycolide) for Cellular Nanoparticles Tracking in Living Cells. *Int J Artif Organs*. 2011;34(2):152-60.
367. Ogawa Y, Yamamoto M, Okada H, YASHIKI T, SHIMAMOTO T. A new technique to efficiently entrap leuprolide acetate into microcapsules of polylactic acid or copoly (lactic/glycolic) acid. *Chem Pharm Bull*. 1988;36(3):1095-103.
368. Freichels H, Danhier F, Pr eat V, Lecomte P, J er ome C. Fluorescent labeling of degradable poly (lactide-co-glycolide) for cellular nanoparticles tracking in living cells. *The International journal of artificial organs*. 2011;34(2):152-60.
369. Inaba K, Inaba M, Romani N, Aya H, Deguchi M, Ikehara S, et al. Generation of large numbers of dendritic cells from mouse bone marrow cultures supplemented with granulocyte/macrophage colony-stimulating factor. *J Exp Med*. 1992;176(6):1693-702.
370. Greg rio AC, Fonseca NA, Moura V, Lacerda M, Figueiredo P, Sim oes S, et al. Inoculated cell density as a determinant factor of the growth dynamics and metastatic efficiency of a breast cancer murine model. *PLoS One*. 2016;11(11):e0165817.
371. Moon JJ, Chu HH, Hataye J, Pag an AJ, Pepper M, McLachlan JB, et al. Tracking epitope-specific T cells. *Nat Protoc*. 2009;4(4):565.
372. DuPre S, Hunter K, Jr. Murine mammary carcinoma 4T1 induces a leukemoid reaction with splenomegaly: association with tumor-derived growth factors. *Exp Mol Pathol*. 2007;82(1):12-24.
373. Mougel A, Terme M, Tanchot C. Therapeutic Cancer Vaccine and Combinations With Antiangiogenic Therapies and Immune Checkpoint Blockade. *Front Immunol*. 2019;10.
374. Fares CM, Van Allen EM, Drake CG, Alisson JP, Hu-Lieskovan S. Mechanisms of Resistance to Immune Checkpoint Blockade: Why Does Checkpoint Inhibitor Immunotherapy Not Work for All Patients? *Am Soc Clin Oncol Educ Book*. 2019(39):147-64.
375. Mao S, Sun W, Kissel T. Chitosan-based formulations for delivery of DNA and siRNA. *Advanced drug delivery reviews*. 2010;62(1):12-27.
376. Sahoo SK, Panyam J, Prabha S, Labhasetwar V. Residual polyvinyl alcohol associated with poly (D, L-lactide-co-glycolide) nanoparticles affects their physical properties and cellular uptake. *J Control Release*. 2002;82(1):105-14.
377. Nair B. Final report on the safety assessment of polyvinyl alcohol. *Int J Toxicol*. 1998;17(5_suppl):67-92.
378. DeMerlis C, Schoneker D. Review of the oral toxicity of polyvinyl alcohol (PVA). *Food Chem Toxicol*. 2003;41(3):319-26.

379. Aruffo A, Stamenkovic I, Melnick M, Underhill CB, Seed B. CD44 is the principal cell surface receptor for hyaluronate. *Cell*. 1990;61(7):1303-13.
380. Do Y, Nagarkatti PS, Nagarkatti M. Role of CD44 and hyaluronic acid (HA) in activation of alloreactive and antigen-specific T cells by bone marrow-derived dendritic cells. *J Immunother*. 2004;27(1):1-12.
381. Azzi J, Yin Q, Uehara M, Otori S, Tang L, Cai K, et al. Targeted delivery of immunomodulators to lymph nodes. *Cell Rep*. 2016;15(6):1202-13.
382. Banchereau J, Briere F, Caux C, Davoust J, Lebecque S, Liu Y-J, et al. Immunobiology of dendritic cells. *Annu Rev Immunol*. 2000;18(1):767-811.
383. Gautier G, Humbert M, Deauvieu F, Scuiller M, Hiscott J, Bates EE, et al. A type I interferon autocrine–paracrine loop is involved in Toll-like receptor-induced interleukin-12p70 secretion by dendritic cells. *J Exp Med*. 2005;201(9):1435-46.
384. Jongbloed SL, Kassianos AJ, McDonald KJ, Clark GJ, Ju X, Angel CE, et al. Human CD141+ (BDCA-3)+ dendritic cells (DCs) represent a unique myeloid DC subset that cross-presents necrotic cell antigens. *J Exp Med*. 2010;207(6):1247-60.
385. Watts C, West MA, Zaru R. TLR signalling regulated antigen presentation in dendritic cells. *Curr Opin Immunol*. 2010;22(1):124-30.
386. Hanahan D, Coussens LM. Accessories to the crime: functions of cells recruited to the tumor microenvironment. *Cancer Cell*. 2012;21(3):309-22.
387. De Koker S, Cui J, Vanparijs N, Albertazzi L, Grooten J, Caruso F, et al. Engineering Polymer Hydrogel Nanoparticles for Lymph Node-Targeted Delivery. *Angew Chem Int Ed Engl*. 2016;55(4):1334-9.
388. Lou Y, Liu C, Lizée G, Peng W, Xu C, Ye Y, et al. Antitumor activity mediated by CpG: the route of administration is critical. *J Immunother*. 2011;34(3):279-88.
389. Humbert M, Guery L, Brighthouse D, Lemeille S, Hugues S. Intratumoral CpG-B Promotes Antitumoral Neutrophil, cDC, and T-cell Cooperation without Reprogramming Tolerogenic pDC. *Cancer research*. 2018;78(12):3280-92.
390. Miller JC, Brown BD, Shay T, Gautier EL, Jovic V, Cohain A, et al. Deciphering the transcriptional network of the dendritic cell lineage. *Nature immunology*. 2012;13(9):888.
391. Bachem A, Güttler S, Hartung E, Ebstein F, Schaefer M, Tannert A, et al. Superior antigen cross-presentation and XCR1 expression define human CD11c+ CD141+ cells as homologues of mouse CD8+ dendritic cells. *J Exp Med*. 2010;207(6):1273-81.
392. Silva JM, Zupancic E, Vandermeulen G, Oliveira VG, Salgado A, Videira M, et al. In vivo delivery of peptides and Toll-like receptor ligands by mannose-functionalized polymeric nanoparticles induces prophylactic and therapeutic anti-tumor immune responses in a melanoma model. *J Control Release*. 2015;198:91-103.
393. Zupančič E, Curato C, Kim J-S, Yeini E, Porat Z, Viana AS, et al. Nanoparticulate vaccine inhibits tumor growth via improved T cell recruitment into melanoma and huHER2 breast cancer. *Nanomedicine*. 2018;14(3):835-47.
394. Sainz V, Moura LI, Peres C, Matos AI, Viana AS, Wagner AM, et al. α -Galactosylceramide and peptide-based nano-vaccine synergistically induced a strong tumor suppressive effect in melanoma. *Acta Biomater*. 2018;76:193-207.

395. Peleteiro M, Presas E, González-Aramundiz JV, Sánchez-Correa B, Simón-Vázquez R, Csaba N, et al. Polymeric Nanocapsules for Vaccine Delivery: Influence of the Polymeric Shell on the Interaction With the Immune System. *Front Immunol*. 2018;9(791).
396. Kim H, Griffith TS, Panyam J. Poly(D,L-lactide-co-glycolide) Nanoparticles as Delivery Platforms for TLR7/8 Agonist-Based Cancer Vaccine. *J Pharmacol Exp Ther*. 2019;370(3):715-24.
397. Luo M, Wang H, Wang Z, Cai H, Lu Z, Li Y, et al. A STING-activating nanovaccine for cancer immunotherapy. *Nat Nanotechnol*. 2017;12(7):648-54.
398. Rietscher R, Schroder M, Janke J, Czaplowska J, Gottschaldt M, Scherliess R, et al. Antigen delivery via hydrophilic PEG-b-PAGE-b-PLGA nanoparticles boosts vaccination induced T cell immunity. *European journal of pharmaceutics and biopharmaceutics : official journal of Arbeitsgemeinschaft fur Pharmazeutische Verfahrenstechnik eV*. 2016;102:20-31.
399. Aspeslagh S, Postel-Vinay S, Rusakiewicz S, Soria J-C, Zitvogel L, Marabelle A. Rationale for anti-OX40 cancer immunotherapy. *Eur J Cancer*. 2016;52:50-66.
400. Curti BD, Kovacsovics-Bankowski M, Morris N, Walker E, Chisholm L, Floyd K, et al. OX40 is a potent immune-stimulating target in late-stage cancer patients. *Cancer research*. 2013;73(24):7189-98.
401. Gabrilovich DI. Myeloid-Derived Suppressor Cells. *Cancer Immunol Res*. 2017;5(1):3-8.
402. Limagne E, Euvrard R, Thibaudin M, Rébé C, Derangère V, Chevriaux A, et al. Accumulation of MDSC and Th17 cells in patients with metastatic colorectal cancer predicts the efficacy of a FOLFOX–bevacizumab drug treatment regimen. *Cancer research*. 2016;76(18):5241-52.
403. Chesney JA, Mitchell RA, Yaddanapudi K. Myeloid-derived suppressor cells—a new therapeutic target to overcome resistance to cancer immunotherapy. *J Leukoc Biol*. 2017;102(3):727-40.
404. Gebhardt C, Sevko A, Jiang H, Lichtenberger R, Reith M, Tarnanidis K, et al. Myeloid cells and related chronic inflammatory factors as novel predictive markers in melanoma treatment with ipilimumab. *Clin Cancer Res*. 2015;21(24):5453-9.
405. Stiff A, Trikha P, Wesolowski R, Kendra K, Hsu V, Uppati S, et al. Myeloid-derived suppressor cells express Bruton's tyrosine kinase and can be depleted in tumor-bearing hosts by ibrutinib treatment. *Cancer research*. 2016;76(8):2125-36.
406. Natarajan G, Oghumu S, Terrazas C, Varikuti S, Byrd JC, Satoskar AR. A Tec kinase BTK inhibitor ibrutinib promotes maturation and activation of dendritic cells. *Oncoimmunology*. 2016;5(6):e1151592.
407. Saljoughian N, Varikuti S, Halsey G, Oghumu S, Satoskar A. Ibrutinib has a novel immunomodulatory effect by enhancing DC maturation both in vivo and in a model of inflammation. *J Immunol*. 2018;200(1).
408. Natarajan G, Oghumu S, Terrazas C, Varikuti S, Byrd JC, Satoskar AR. A Tec kinase BTK inhibitor ibrutinib promotes maturation and activation of dendritic cells. *Oncoimmunology*. 2016;5(6):e1151592-e.
409. Sagiv-Barfi I, Kohrt H, Czerwinski D, Ng P, Chang B, Levy R. Therapeutic antitumor immunity by checkpoint blockade is enhanced by ibrutinib, an inhibitor of both BTK and ITK. *Proceedings of the National Academy of Sciences of the United States of America*. 2015;112(9):E966-72.

410. Fiorcari S, Maffei R, Audrito V, Martinelli S, Ten Hacken E, Zucchini P, et al. Ibrutinib modifies the function of monocyte/macrophage population in chronic lymphocytic leukemia. *Oncotarget*. 2016;7(40):65968.
411. Da Roit F, Engelberts PJ, Taylor RP, Breij EC, Gritti G, Rambaldi A, et al. Ibrutinib interferes with the cell-mediated anti-tumor activities of therapeutic CD20 antibodies: implications for combination therapy. *Haematologica*. 2015;100(1):77-86.
412. Dubovsky JA, Beckwith KA, Natarajan G, Woyach JA, Jaglowski S, Zhong Y, et al. Ibrutinib is an irreversible molecular inhibitor of ITK driving a Th1-selective pressure in T lymphocytes. *Blood*. 2013;122(15):2539-49.
413. Wang ML, Blum KA, Martin P, Goy A, Auer R, Kahl BS, et al. Long-term follow-up of MCL patients treated with single-agent ibrutinib: updated safety and efficacy results. *Blood*. 2015;126(6):739-45.
414. O'Brien SM, Furman RR, Coutre SE, Flinn IW, Burger J, Blum K, et al. Single-agent ibrutinib in treatment-naïve and relapsed/refractory chronic lymphocytic leukemia: a 5-year experience. *Blood*. 2018;131(17):1910-9.
415. Burger JA, Tedeschi A, Barr PM, Robak T, Owen C, Ghia P, et al. Ibrutinib as Initial Therapy for Patients with Chronic Lymphocytic Leukemia. *N Engl J Med*. 2015;373(25):2425-37.
416. Fleming V, Hu X, Weber R, Nagibin V, Groth C, Altevogt P, et al. Targeting Myeloid-Derived Suppressor Cells to Bypass Tumor-Induced Immunosuppression. *Front Immunol*. 2018;9:398-.
417. Sagiv-Barfi I, Kohrt HE, Burckhardt L, Czerwinski DK, Levy R. Ibrutinib enhances the antitumor immune response induced by intratumoral injection of a TLR9 ligand in mouse lymphoma. *Blood*. 2015;125(13):2079-86.
418. Simon S, Labarriere N. PD-1 expression on tumor-specific T cells: Friend or foe for immunotherapy? *Oncoimmunology*. 2018;7(1):e1364828.
419. Guo Z, Wang X, Cheng D, Xia Z, Luan M, Zhang S. PD-1 blockade and OX40 triggering synergistically protects against tumor growth in a murine model of ovarian cancer. *PLoS One*. 2014;9(2):e89350.
420. Shrimali RK, Ahmad S, Verma V, Zeng P, Ananth S, Gaur P, et al. Concurrent PD-1 blockade negates the effects of OX40 agonist antibody in combination immunotherapy through inducing T-cell apoptosis. *Cancer Immunol Res*. 2017;5(9):755-66.
421. Messenheimer DJ, Jensen SM, Afentoulis ME, Wegmann KW, Feng Z, Friedman DJ, et al. Timing of PD-1 blockade is critical to effective combination immunotherapy with anti-OX40. *Clin Cancer Res*. 2017;23(20):6165-77.
422. Inozume T, Hanada K-i, Wang QJ, Ahmadzadeh M, Wunderlich JR, Rosenberg SA, et al. Selection of CD8+ PD-1+ lymphocytes in fresh human melanomas enriches for tumor-reactive T-cells. *J Immunother*. 2010;33(9):956.
423. Gros A, Robbins PF, Yao X, Li YF, Turcotte S, Tran E, et al. PD-1 identifies the patient-specific CD8+ tumor-reactive repertoire infiltrating human tumors. *J Clin Invest*. 2014;124(5):2246-59.
424. Simon S, Vignard V, Florenceau L, Dreno B, Khammari A, Lang F, et al. PD-1 expression conditions T cell avidity within an antigen-specific repertoire. *Oncoimmunology*. 2016;5(1):e1104448.
425. Peng M, Mo Y, Wang Y, Wu P, Zhang Y, Xiong F, et al. Neoantigen vaccine: an emerging tumor immunotherapy. *Mol Cancer*. 2019;18(1):128.

426. Kuai R, Ochyl LJ, Bahjat KS, Schwendeman A, Moon JJ. Designer vaccine nanodiscs for personalized cancer immunotherapy. *Nature materials*. 2017;16(4):489.
427. Lesterhuis WJ, de Vries IJM, Schreiber G, Lambeck AJ, Aarntzen EH, Jacobs JF, et al. Route of Administration Modulates the Induction of Dendritic Cell Vaccine–Induced Antigen-Specific T Cells in Advanced Melanoma Patients. *Clin Cancer Res*. 2011;17(17):5725-35.
428. Sultan H, Kumai T, Nagato T, Wu J, Salazar AM, Celis E. The route of administration dictates the immunogenicity of peptide-based cancer vaccines in mice. *Cancer Immunol Immunother*. 2019;68(3):455-66.
429. Mak IW, Evaniew N, Ghert M. Lost in translation: animal models and clinical trials in cancer treatment. *Am J Transl Res*. 2014;6(2):114.
430. Olson B, Li Y, Lin Y, Liu ET, Patnaik A. Mouse models for cancer immunotherapy research. *Cancer Discov*. 2018;8(11):1358-65.